SEDIMENTARY ENVIRONMENTS AND PROCESSES IN A SHALLOW, GULF COAST ESTUARY-LAVACA BAY, TEXAS

A Thesis

by

JASON LEE BRONIKOWSKI

Submitted to the Office of Graduate Studies of
Texas A&M University
in partial fulfillment of the requirements for the degree of

MASTER OF SCIENCE

August 2004

Major Subject: Oceanography

SEDIMENTARY ENVIRONMENTS AND PROCESSES IN A SHALLOW, GULF COAST ESTUARY-LAVACA BAY, TEXAS

A Thesis

by

JASON LEE BRONIKOWSKI

Submitted to Texas A&M University
in partial fulfillment of the requirements
for the degree of

MASTER OF SCIENCE

Approved as to style and content by:

Timothy Dellapenna (Chair of Committee)	Jay Rooker (Member)
William Sager (Member)	Wilford Gardner (Head of Department)

August 2004

Major Subject: Oceanography

ABSTRACT

Sedimentary Environments and Processes in a Shallow,

Gulf Coast Estuary-Lavaca Bay, Texas. (August 2004)

Jason Lee Bronikowski, B.S., Lake Superior State University

Chair of Advisory Committee: Dr. Timothy Dellapenna

Sedimentation rates in sediment cores from Lavaca Bay have been high within the last 1-2 decays within the central portion of the bay, with small fluctuations from river input. Lavaca Bay is a broad, flat, and shallow (<3 m) microtidal estuary within the upper Matagorda Bay system. Marine derived sediment enters the system from Matagorda Bay, while two major rivers (Lavaca & Navidad) supply the majority of terrestrially derived sediment. With continuous sediment supply the bay showed no bathymetric change until the introduction of the shipping channel. Processes that potentially lead to sediment transport and resuspension within the bay include wind driven wave resuspension, storm surges, wind driven blowouts, and river flooding. These processes were assessed using X-radiographs, grain size profiles, and ^{210}Pb and ^{137}Cs geochronology of sediment diver cores. In six cores the upper 10 cm of the seabed has been physically mixed, whereas the rest showed a continuous sediment accumulation rate between 0.84-1.22 cm/yr.

Sidescan sonar and subbottom chirp sonar data coupled with sedimentological core and grab samples were used to map the location and delineate the sedimentary facies within the estuarine system in depths >1 m. Five sedimentary facies were

identified in Lavaca Bay and adjacent bays, they are: 1) estuarine mud; 2) fluvial sand; 3) beach sand; 4) bay mouth sand; and 5) oyster biofacies. Of the five facies, Lavaca Bay consists primarily of estuarine mud (68%).

Pre-Hurricane and post-Hurricane Claudette cores were obtained to observe the impact to the sedimentary processes. The north and south Lavaca Bay were eroded by 10 cm and 2-3 cm, respectively. Cox Bay and Keller Bay saw a net deposition of 2-3 cm.

ACKNOWLEDGMENTS

I would like to thank Texas A&M University of Galveston and College Station, the Texas Department of Parks and Wildlife, and the Texas General Land Office for their financial and personnel support during my thesis. Special thanks to my advisor, Dr. Dellapenna, my committee members, Dr. Sager and Dr. Rooker, for their support and guidance. I offer an additional extended thanks to all graduate students and lab assistants that helped during the fieldwork and lab procedures. Immense appreciation goes to Sandy Drews who helped and made problems disappear.

I dedicate this thesis to my family and girlfriend for their moral and spiritual support and direction.

TABLE OF CONTENTS

Page

LIST OF FIGURES

FIGURE Page

LIST OF TABLES

INTRODUCTION

The major sedimentary sources for an estuarine system are terrestrial-derived sediment from fluvial systems, marine derived sediment, resuspension of the estuarine bay floor, and estuarine bank erosion. After long-term net accumulation from erosion and deposition, and burial of sediment below a level of physical and biological reworking through seabed accretion, the stratigraphy within a facies will form (Nittrouer and Sternberg, 1981; Dellapenna et al., 1998). These estuarine facies and sedimentations are affected by variable energy conditions (Nichols et al., 1991). The energies of estuarine that affect sedimentation are derived from tides, waves, and wind. Suspended sediment entering an estuarine system from rivers and creeks will undergo repeated cycles of erosion, transportation, resuspension and deposition by ebb and flood tidal currents, wave induced resuspension, and resuspension due to anthropengic activities such as dredging and trawling (Nichols, 1984). If the sediment deposition is in equilibrium with the physical energy and sediment sources, balancing sea level fluctuation and subsidence, then the estuary will be maintained. If this balance is not maintained, the estuary will either deepen or fill. Additionally, tropical storms and hurricanes can create intense intermittent episodic energy sources, which will disrupt the equilibrium of an estuary by flushing sediment out of the estuarine system. Most sediment is likely moved during short episodes of high energy rather than during normal conditions (Schubel, 1974; Nichols, 1993; Dellapenna et al., 1998). With these periodic

---

This thesis follows the style and format of Estuarine, Coastal and Shelf Science.

storms, the estuary will have an increase in wind, wave and tidal energies that will affect the erosion, deposition, suspension and distribution of sediment. For example, with an increase in deposition from seasonal flooding, an estuary may become choked with sediment, and if this happens repeatedly, may lead ultimately to filling the estuary. If a periodic storm such as a hurricane or tropical storm occurs, the sediment will be reworked, eroded, and transported or flushed out of the estuarine system. A single storm can erode and deposit more sediment in an estuary in a few hours than would occur during a decade or more under normal conditions (Hayes, 1978; Nichols, 1993; Dellapenna et al., 1998). Many hurricanes and tropical storms have impacted Lavaca Bay in the past 150 years. Core data from a previous study of Lavaca Bay (Santschi et al, 1999) shows that some of the ^{210}Pb profiles have a stair-step appearance, suggesting deep physical mixing. The most likely agents for deep mixing are hurricanes or tropical storms. Some of the cores do not show this deep mixing, because the core is either in a well sheltered location, behind a land barrier, and/or from bioturbation or anthropogenic impact, such as dredging.

Lavaca Bay is a shallow microtidal estuary situated in the northern part of the Matagorda Bay system, along the central coastline of Texas (Figure 1). The majority of terrestrial sediments come from the Lavaca and Navidad rivers, which enter Lavaca Bay by the Lavaca River. Marine sediments are derived from the Matagorda Bay system and enter through the mouth of Lavaca Bay. In addition, anthropogenic impacts from ALCOA, dredging, oyster, and shrimping have influenced the estuarine sedimentation. ALCOA is the largest manufacturer of aluminum. The aluminum derives from bauxite

ore. The bauxite ore dust is introduced into the estuarine system during the unloading of cargo ships. Oyster dredging and shrimping trawl doors scour the seafloor resulting in mixing, and displacement of the sediment. This scouring releases organic matter, nutrients and buried contaminants, such as mercury, back into the system. Dredging releases contaminants, but also produces spoil areas that can be used as a foundation for oyster habitat. In addition, dredging also modifies the natural flow of an estuary by redirecting the sediment and water flow around spoil areas and through dredged channels.

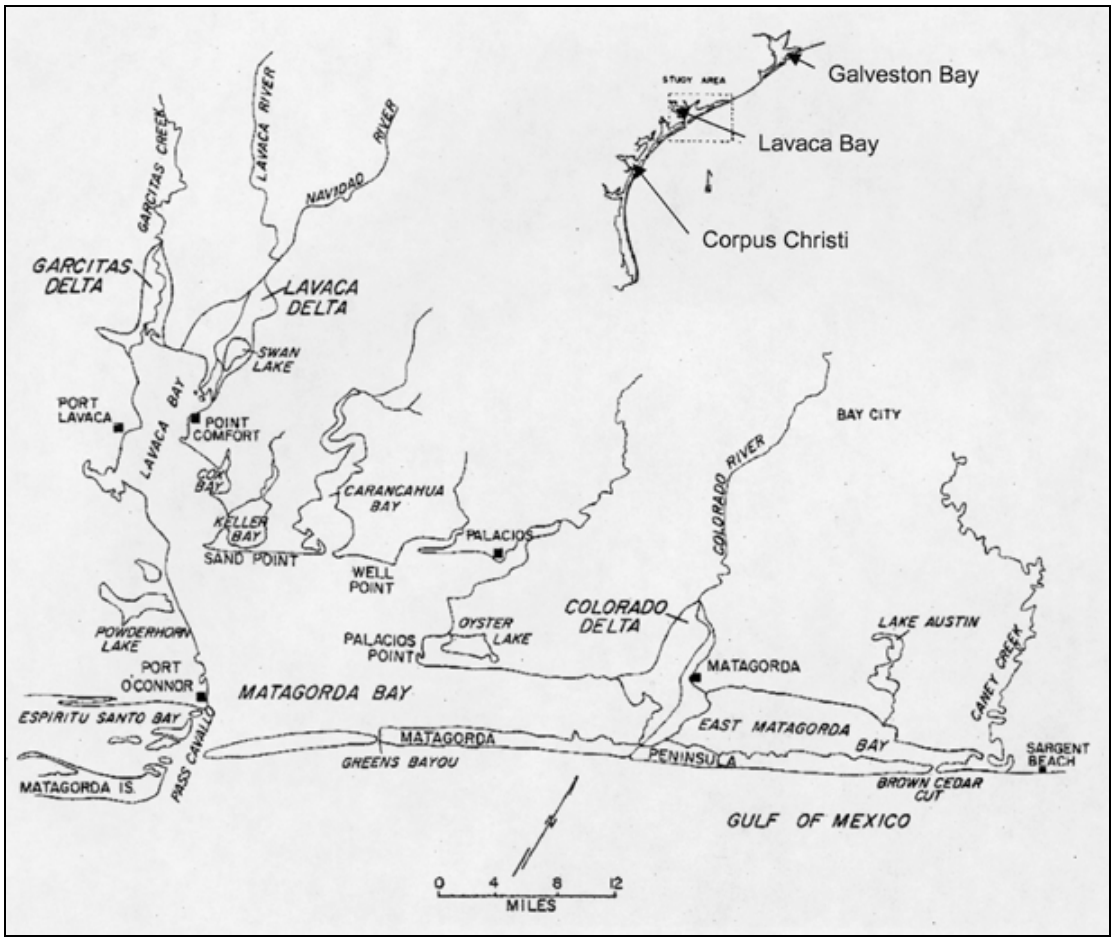

Figure 1. Location of Lavaca Bay, Texas (modified from Byrne, 1975).

The purpose of this thesis is to investigate the record of sedimentary processes that have occurred in Lavaca Bay. The main focus areas of this study are as follows:

1) To determine the distribution of sedimentary facies in Lavaca Bay and adjacent bays using sidescan sonar and chirp sonar data along with surficial sediment from cores and grab samples.

2) Assess the short-term and decadal sedimentary processes. Determine if frequent hurricanes and tropical storms induce deep seabed mixing and significant sediment transport.

3) Evaluate the impact of hurricanes on the sedimentary facies and the effects on different regions of Lavaca Bay.

BACKGROUND

Lavaca Bay is located northwest of Matagorda Bay on the central Texas coastline (Figure 1). It is approximately 20.6 km in length with a varying width of 3.6 to 10.3 km (Byrne, 1975). The average depth of the bay varies from 1.2 m in the northern bay to 2.8 m in the south, with a depth of 10.5 m in the ship channel (Figure 2). Lavaca Bay has a subhumid climate with average annual precipitation range from 91.4 to 101.6 cm (Carr, 1967; Byrne, 1975), and rainfall increases during June through September, coinciding with hurricanes (Hayes, 1965; Byrne, 1975). Two major rivers, Lavaca and Navidad, combine and empty the majority of freshwater and sediment into the northeast corner of the bay; minor contributions also come from Keller Bay, Cox Bay, Garcitas delta and small intermittent streams and creeks. With continuous sediment entering into Lavaca Bay from these sources, the system has been in a state of unbalance equilibrium.

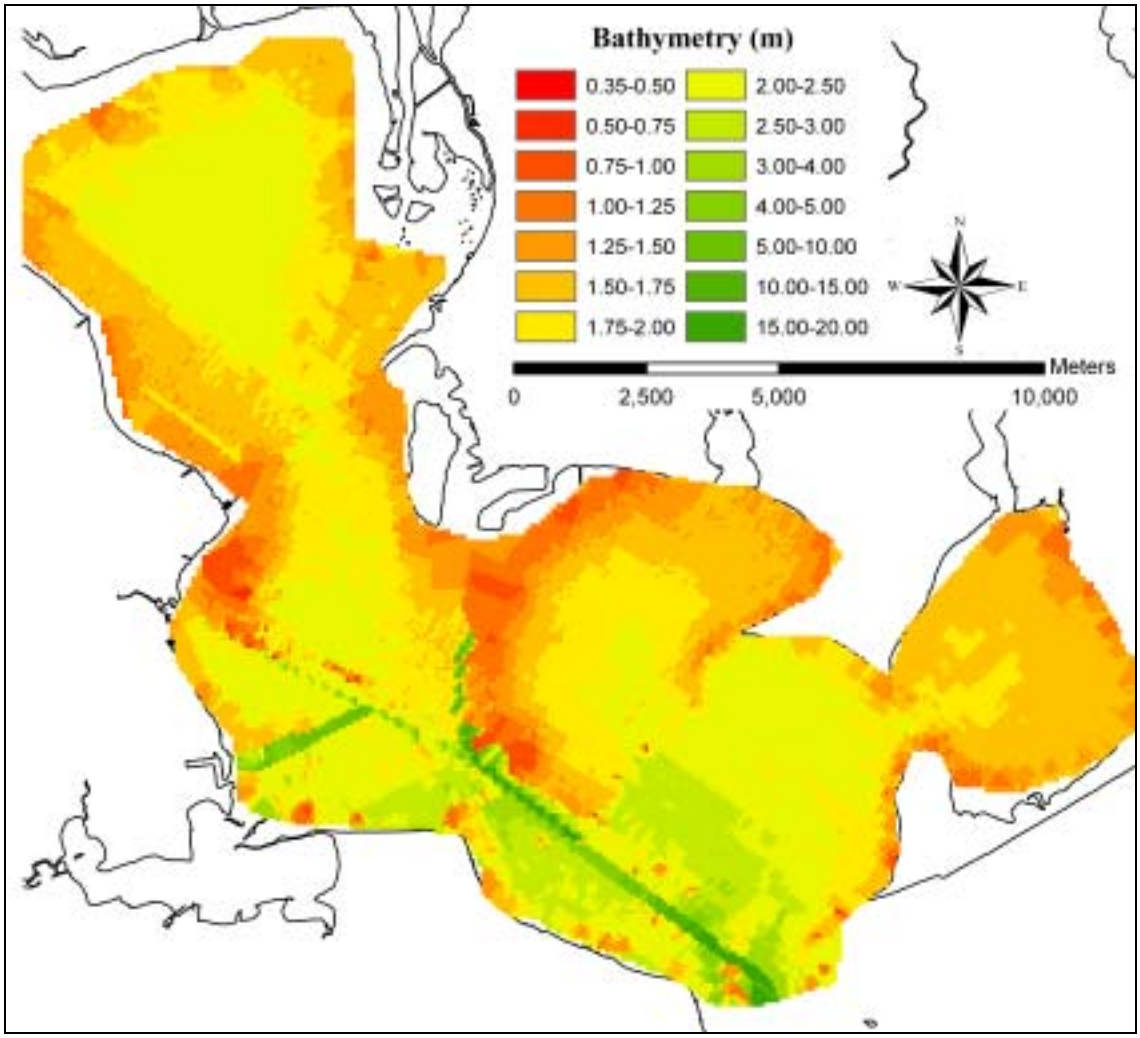

Figure 2. Bathymetric map shows Lavaca Bay to be a shallow and flat estuarine system. Data collected from December 2002 to April 2003 with a single beam Echo Sounder.

Hurricanes that strike the Texas coast occur approximately once every 1.5 years and only make landfall a few times a century in the same area (Byrne, 1975). The Matagorda Bay area has experienced many direct and indirect hurricanes and tropical storms since the late 19th century. Hurricane and tropical storm data were obtained from the National Oceanic and Atmospheric Administration (NOAA) and Weather Research Center of Houston Texas (WRC) websites. The category and year of hurricanes that

made landfall near Matagorda Bay area are; C2-3 of 1854, C2-3 of 1869, C1 of 1871, C1 of 1874, C4 of 1875, C4-5 of 1886, C1 of 1891, C1 of 1921, C1 of 1929, C3 of 1942, C3-4 of 1945, C2 of 1949, C4 of 1961 (Carla), C1 of 1971 (Fern), and C1 of 2003 (Claudette). Tropical storms hit Matagorda Bay area in 1880, 1901, 1933, 1938, 1964 (Abby), 1979 (Elena), 1998 (Charley), and 2002 (Fay).

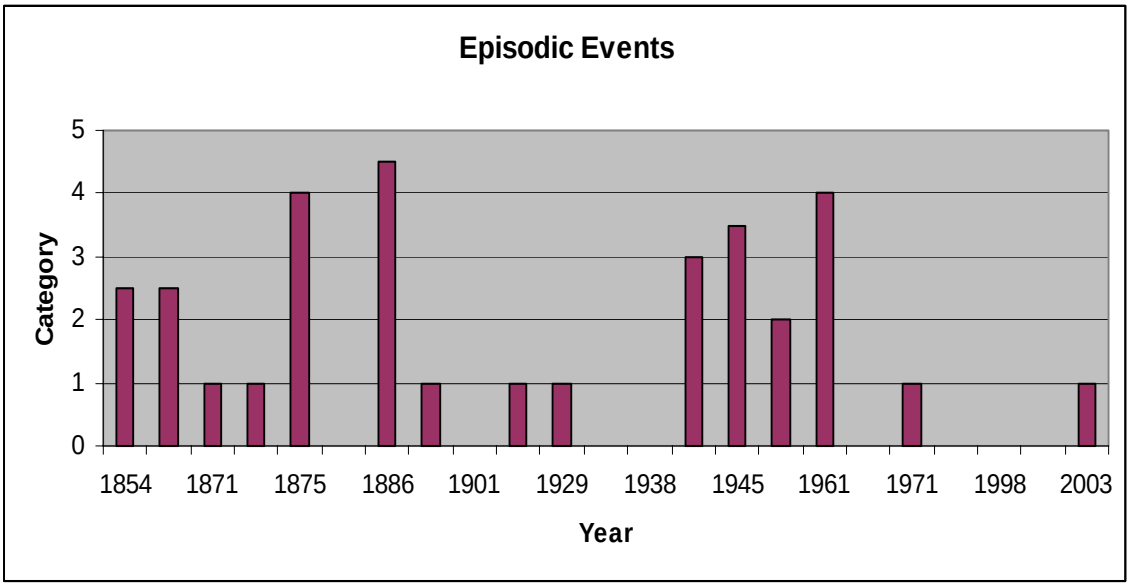

Figure 3. Major hurricanes that impacted Matagorda Bay within the past 150 years.

Although there have been many geological studies on the impacts of hurricanes on coastal systems, most studies have examined the erosion of oceanfront beaches and property (Hayes, 1967) along the Texas coast, (McGowen, & Scott, 1975), (Davis, 1972), (Morton, et al., 1995) and also the South Carolina coast (Collins, et al., 1999). Of the non-beach erosion studies, the majority have focused on coastal marshes, lacustrine and offshore environments rather than estuarine systems. However, studies on hurricane

impacts within estuaries have received some attention. For example, Rejmanek et al. (1988) studied the affects of hurricane induced-sediment distribution and deposition in four coastal marshes in the Mississippi River deltaic plain and concluded that minor hurricanes can transport sediments as far as 7 km inland from the source. Also sea level rises as a hurricane inundates a low-lying area causing widespread erosion and deposition (Hayes, 1967). According to McGowen and Scott (1975), hurricanes and tropical storms have played a major role in the modification of lagoonal and bay systems, causing a retreat of Southern Texas lagoons as much as 9.1 m.

Resuspension of fine sediment during episodic events was studied by Nichols (1984). He found that fine grain sediment undergoes a cycle of erosion, resuspension, transportation and deposition that is most intense during short episodes of high energy, such as a hurricane, rather than during normal conditions. All sediment undergoes some level of physical and biological reworking prior to permanent accumulation (Nittrouer & Sternberg, 1981; and Dellapenna, 2003). The estuary entrance zone allows for fine sediment to move landward or escape the estuarine system seaward during storms (Nichols, 1984). Fine grain fluvial sediments temporarily accumulate in the upper estuary, are scoured, then are transported and accumulate farther seaward (Nichols, 1993). Sediment response sequence during an episodic event are, 1) “Initial Response”; near bottom suspended sediment load increases 5 to 10 fold due to storm surge currents and wave resuspension, 2) “Shock”; river flooding; turbidity maximum shifts seaward at high river inflow, 3) “Rebound”; turbidity maximum shifts landward, with the lower salinity layer transporting sediment landward, and 4) “Recovery”; subsiding river inflow

and fair meteorological conditions, the estuary becomes reestablished to normal conditions (Nichols, 1993).

A study by Larm (1998) examined the impact of Hurricane Carla (category 4) within Cox Bay by using hydrodynamic and wave models. The advance circulation (ADCIRC) and simulating wave nearshore (SWAN) models were used to study sediment resuspension within Cox Bay, and were extrapolated to Lavaca Bay. They showed the overall erosion was primarily 0-5 cm, this increased to 20 cm along shoals and the shoreline. The calculated erosion increases were due to scouring from increase water levels and currents. Depositions were only calculated to occur within the active ship channel and behind barriers, such as islands, spits or peninsulas. Although the Hurricane Carla calculations showed sediment erosion of approximately 5 cm throughout the bay, a smaller episodic event could potentially have a greater effect on the bay.

Estuarine circulation is a form of gravity circulation where the water column is stratified with dense seawater coming in from the ocean along the bottom, while lower density freshwater entering from the fluvial portion of the system and exists as a layer above the seawater. Since Lavaca Bay is a shallow estuary, the water column is well mixed throughout the year, except during seasonal and episodic flooding when it can become partially stratified. Salinity data collected for 1 year shows fluctuations from 20 ppt to 3.5 ppt at a depth of $\leq$ 0.5 m (Gill, unpublished) (Table 1).

Table 1. Salinity concentration for Lavaca Bay

Sample Date	Sample Depth (m)	North Salinity (ppt)	Central1 Salinity (ppt)	Central2 Salinity (ppt)	South Salinity (ppt)
8/14/2002	0.5	17.6	19.3	16.2	11.4
9/21/2002	0.5	3.5	8.4	8.8	12.1
10/22/2002	0.2	13.5	15.9	16.7	19.5
12/5/2002	0.5	12.4	13.7	14	18.2
1/20/2003	0.2	5.7	11.5	6.8	14
2/21/2003	0.3	16.6	18.8	19.8	22.2
4/1/2003	0.5	16.7	20.4	20.2	21.6
5/21/2003	0.3	11.2	21.5	18.2	20.6
6/25/2003	0.5	19.2	22.6	24.1	24.1
8/5/2003	0.5	11.3	18.5	17.1	20

The null point is located where the net landward excursion of seawater ends. This is also the point where the freshwater layer decouples from the riverbed and begins to move seaward above marine layer (Nichols, 1984). The null point migrates up and down the bay and river with the tidal cycle. The null point will also migrate up a fluvial system during low discharge and migrate into an estuary during high discharge. At the null point there is a separation of flow causing fluvially derived suspended load to be entrained in the water column, above the marine layer, down stream of the null point. Because the fluvial water mass decouples from the seabed down stream of the null point, the bedload cannot migrate seaward pass the null point. As a result, coarser sediment deposits form upstream of the null point. During flooding, the null point and bedload deposits migrate down into the bay.

A turbidity maximum exists at and below the null point because as freshwater and seawater meet, the salinity neutralizes the negative charges, which exist on the suspended sediment particles in the freshwater. This neutralization of charges allows

flocculation to occur and the flocs to sink and rapidly deposit and are trapped down stream of the null point. The increase of fine grain sediment within the central portion of the bay probably results from this process.

The use of radioactive isotope series to evaluate the rate of sediment accumulation has become a geochronological tool to study the depositional history. ^{210}Pb and ^{137}Cs geochronology can be used to identify the rate of deposition, and whether there has been any kind of disturbance or hiatus in the record, on the decadal to centennial time-scale. ^{210}Pb geochronology allows insight into sediment accumulation along with the processes that affect accumulation (Nittrouer et al, 1979). ^{210}Pb is a member of the ^{238}U natural radioactive series, and is supplied to seawater of an estuarine system from runoff, atmospheric precipitation, and decay of ^{226}Ra precursor in the water column (Nittrouer et al., 1979). Fine-grained particles act as carriers for ^{210}Pb rather than coarse-grained particles (Ravichandran et al., 1995), due to the high surface area to low volume ratio. Sediment core profiles of fine-grained sediment can be used to establish the geochronologic record of the seabed (Nittrouer et al., 1979; Nichols, 1993; Ravichandran et al., 1995, Dellapenna et al., 1998; Rejmanek et al., 1998; Santschi et al., 1999). ^{137}Cs is an anthropogenic impulse tracer that was introduced into the environment by atmospheric atomic bomb testing that started in 1954 and reached peaks in 1961 and 1963, but ceased with the test ban treaty of 1963 (Dellapenna et al., 1998; Santschi et al., 1999; Bentley, 2002). Since ^{137}Cs is readily sorbed onto fine grained sediments, continuously accumulating sediment would be expected to incorporate ^{137}Cs in a vertical profile corresponding to that of atmospheric fallout (Chmura & Kosters,

1994; Pennington et al., 1973). Thus, in an ideal situation, the peak ^{137}Cs activity depth would indicate the 1961-63 Hurricane Carla layer. Comparing the maximum depth of ^{137}Cs to the accretion rates from ^{210}Pb profiles help correlated time and depth of seabed mixing. Using ^{210}Pb, ^{240}Pu, ^{239}Pu, and ^{137}Cs tracer profiles, Santschi et al (1999) estimated sedimentation rates in Lavaca bay to be approximately 2 cm/yr at near shore sites. This decreased towards the center of the bay.

Two tropical storms (1998-Charley & 2002-Fay) and Hurricane Claudette (2003) made landfall around Lavaca Bay causing an increase of energy and enhanced sediment movement. With these recent storms there may have been a change in erosion and deposition that would lead to different rates of sedimentation. The sediment reworking from these episodic events should potentially lead to different sedimentation rates and mixing depths for different locations within the bay. The majority of Santschi et al (1999) cores were isolated around the ALCOA facility, consequently cores sedimentation rates would have been influenced by anthropogenic impacts. The sediment distribution and facies delineation were identified with geophysical equipment of water depth of 1 m or greater, except for the ALCOA site.

Sidescan uses multiple transducers to produce an acoustic sonar beam that is reflected off varying density contrasts and received by the sidescan. The digital image is similar to an aerial photograph with high reflectivity or backscatter represented by lighter tones for coarser-grained material such as oyster, shell fragments or hardbottom, and low backscatter is represented by darker tones for finer-grain sediment. Subbottom Chirp profiler uses a single transducer to produce a low to high acoustic frequency pulse

to penetrate into the subsurface sediment, and two receivers receive the acoustic pulse. Chirp shows subbottom profiles of reflective density layers or the stratigraphy of the subsurface sediment.

METHODS

In order to investigate the effects hurricanes have on the sedimentological record, geophysical and sedimentological data were collected in Lavaca Bay aboard the Texas A&M University Galveston research vessel the R/V *Cavalla* over a nine month period from December 2002 to August 2003. The survey was partitioned within the field because of physical obstruction that inhibited the navigation of the vessel and also within the laboratory, because the processing computer could not handle the quantity of data essential to create a single mosaic. Geophysical data were collected with a Edgetech 272 Analog Survey Sidescan towfish at 500 kHz frequency, a Edgetech FSSB Full Spectrum SB-216S Chirp subbottom Profiler at 2-16 kHz frequency, and a Hydrotrac Precision Survey Echo Sounder. Data were processed with Coda Octopus GeoSurvey, Midas X-Star, and Hypack Coastal Oceanographic softwares. Sedimentological data were collected with diver cores and surfical sediment grab sampling. The sediment samples were subjected to grain size, water content, and X-radiograph analyses, as well as ^{137}Cs and ^{210}Pb radiochemical analysis by gamma ray and alpha particle spectrometry.

Geophysical Data

Sidescan Sonar Data

Lavaca Bay is approximately 174.5 km^2, survey lines were run with an acoustic range of 100 m per line and the lines were spaced every 250 m, providing 39.3%

coverage for all navigatable portions of the bay, which were conducted from December 2002 to April of 2003. This line spacing allowed for the identification of large oyster reefs or oyster patches to be less time consuming. Additional sidescan sonar lines were ran in August 2003 to provide 100% coverage where larger oyster reefs were present. Also, these additional lines were collected to identify the impact of Hurricane Claudette. In total, 257 survey lines were run, with 68.78 km^2 of the bay imaged within the mosaic. The sidescan towfish was towed at speeds of 3 to 5 knots; with an approximate layback of 17.4 m behind the vessel and suspended approximately 0.6 m depth from a homemade PVC (polyvinyl chloride) floatation catamaran to help minimize bayfloor snags. Sidescan and GPS coordinate data (UTM Zone 14 projection) were recorded digitally onto 4.7 GB DVD-RAM single-sided rewritable disks on Coda Octopus acquisition and processing software. A 500 kHz frequency obtained a high resolution image of the bayfloor and allowed for identification of areas of dense oyster shells. Post-processing data manipulation made slant range corrections, time varying gain (tvg) and also georeferenced each mosaic. Final mosaics were exported into ArcGIS software using approximately 1-1.5 ppm (pixel per meter) resolution.

Using a sidescan towfish in shallow water had its problems from deployment to data acquisition. In shallow water the sidescan data resolution decreases as the swath beam increases. Also signal interferences from surface noise associated with wave action and vessel turbulence (Roberts et al, 2000) gives a mispresentation of the bay floor texture. This was minimized by data acquisition on calm weather days and with the sidescan towfish floated an adequate distance behind the vessel.

Subbottom Chirp Data

Subbottom data were collected with Edgetech X-Star 2-16 kHz chirp profiler and Edgetech Midas Software, recorded on 4 mm data tapes, and later printed to an EPC model HSP-100 printer. With the chirp profiler towed behind and to the side of the vessel, approximately 76 cm below the water surface, this helped to limit the acoustical interferences. Using this system provided a high resolution image of the shallow subsurface beds with discrimination accuracy of approximately 5 cm. Post-processing data were performed using Midas X-star software.

Echo Sounder

A Hydrotrac Precision Survey Echo Sounder and a single beam transducer were used to obtain bathymetric data. Data were geoferenced from Hypack Coastal Oceanographic software and recorded digitally on a Gateway laptop. Hypack Coastal Oceanographic and ArcGIS software completed the post-processing of the data. Bathymetric data were also obtained from the first subbottom chirp acoustic reflector and combined with Hypack bathymetry in ArcGIS for a complete bathymetric map of Lavaca Bay. With this large data set, approximately 3.9 million points, only a fraction was used. The subbottom seismic data set had approximately 16,000 points and the Hypack data set had approximately 380,000 points. All of the data were corrected for tidal changes and transducer offsets. These data sets were joined together in ArcGIS and only 10% of this data were used to make a complete bathymetric map by interpolating the new data points using an inverse distance weighted technique, approximately 5,000

chirp data points and 30,000 hypack data points were used. Any errors in the bathymetry were due to four problems, they are: 1) uncorrected vibration motion of sensor head; 2) uncorrected heave and roll motion due to large waves; 3) no tie lines between survey lines; and 4) coverage was at 250 m line spacing.

Sedimentological Data

Core Sampling

Diver cores were collected in May and August of 2003 to analyze the sediment for geochronology, distribution and any sedimentological features. Eleven pre-hurricane cores were collected in May 2003 and four post-hurricane cores in August 2003. Divers collected the cores with 50-80 cm long by 15.24 cm diameter PVC pipes. The top core tubes were sealed with 15.24 cm diameter inner gripper plugs. The cores were then removed and the bases of the tubes were sealed as above with either gripper plugs or PVC caps for transportation back to the laboratory. In the laboratory, cores were extruded and sectioned at 1-cm intervals for the first 10 cm, every other centimeter for 10 to 50 cm, and every 5 cm thereafter. Sediment was removed and packed into plastic bags, homogenized, and then samples were extracted for each interval for water content, grain size analysis, ^{137}Cs and ^{210}Pb geochemistry.

Water Content

Samples were immediately placed into aluminum dishes after extrusion, weighed to the ten thousandth decimal place of a gram (g) and placed into ovens for at least 24

hrs. The samples were removed and weighed again to obtain water content. The porosities were calculated to obtain corrected depths for ^{210}Pb calculations.

Grain Size

Grain size distributions were determined for the cores following the Folk (1980) methodology. First, sediment samples weighing approximately 15 g were separated with Calgon (Sodium Metahexaphoshate Soap) causing deflocculation, followed with wet sieving the samples with deionized water into a 1000 ml graduated cylinder. Next the graduated cylinders were filled with deionized water and the sand content from the sieves were placed into an aluminum dish and weighed. Graduated cylinder samples were plunged for 20 seconds and left undisturbed for an additional 20 seconds, and then immediately a 20 ml pipette withdraws (4 phi) were taken at a depth of 10 cm. Approximately 2 hrs later, depending on air temperature, another 20 ml pipette withdraws (8 phi) were taken at a depth of 20 cm. All samples were dried, weighed and placed into a spreadsheet to determine fine to coarse grain distribution. Samples were plotted on a ternary diagram based on the classification by Shepard (1954).

^{137}Cs and ^{210}Pb Analysis

Samples for geochemical analyses were removed from homogeneous sample bags to determine the distribution of ^{137}Cs and ^{210}Pb. Sediment samples for ^{137}Cs analyses were wet packed and sealed with electrical tape in 60X15 mm Petri dish. The samples were counted on Canberra 2000 mm^2 planar coaxial detectors for 1-2 days per

sample. Gamma energy activities were measured for ^{137}Cs at the decay energy signal of 661.7 keV.

The excess activity of ^{210}Pb was measured by alpha spectroscopy following the methodology by Santschi et al. (1980, 1999). The method assumes that particle reworking is negligible over the corrected depth interval used to calculate sedimentation rates (Santschi et al., 1999). The formula used is from the Constant Initial Concentration (CIC) model, given in equation:

$$[^{210}Pb_{xs}(z)] = [^{210}Pb_{xs}(o)] \exp(-\alpha z)$$

$$\alpha = (\lambda/S)$$

where $^{210}Pb_{xs}(z)$ = corrected depth of excess ^{210}Pb activity in dpm/g, $^{210}Pb_{xs}(o)$ = initial corrected depth of excess ^{210}Pb activity in dpm/g, z = corrected depth in cm (or mass depth in g cm^{-2}), λ = decay constant of ^{210}Pb (= 0.031 yr^{-1}), and S = sedimentation rate in cm/yr (or sediment accumulation rate in g cm^{-2} yr^{-1}) (Santschi et al., 2001).

Sediment samples weighing approximately 15 g were dried for each selected depth, then pulverized and homogenized with a mortar and pestle. Approximately 0.5 g aliquots were placed into 100 ml Teflon beakers and leached with 15 ml of HCL and HNO_3, and 10 ml of HF. The samples were spiked with 500 µl of ^{209}Po and baked to near dryness on hotplates. Then 15 ml of HCL and HNO_3 were added to the samples and taken to near dryness again. The Teflon beakers were rinsed with 10 ml of HCL and baked to complete dryness. Samples were diluted with 50 ml of 1.5 N of HCL, and ascorbic acid was stirred in with a magnetic stir bars until the samples turned to clear color appearance. A 1-cm^2 silver planchet was placed opposite of the magnetic stir bar.

The beakers were covered with watch glasses and heated approximately to 80 degrees for 2.5 hrs. Silver plates were removed and counted for 1-2 days for alpha decay on Canberra Quad Alpha Spectrometer connected to S100 multi-channel analyzer to reach a counting error of ~ 2 % or less. Supported activities were estimated from total ^{210}Pb values deep in cores where excess activities have decayed to negligible values, and were subtracted from the total activity to determine excess activities (Dellapenna et al. 2003).

Surficial Sediment Samples

Approximately 38 grab samples were collected using a Ponar Grab Sampler. In addition, eleven 1-cm surficial samples came from the top of each dive core. The samples were packed and homogenized in plastic bags and grain size distribution was determined by Folk (1980) methodology. The surficial sediment samples were used to correlate fine and coarse grain size sediment to low and high backscatter within the sidescan sonar mosaics.

X-Radiography

Divers also collected 11 pre-hurricane and 4 post-hurricane X-radiograph core samples. A 10.5x2.5x70 cm Plexiglas tray was inserted in-situ along side the location of the dive cores. The trays were removed and capped with either Plexiglas or paper towels, then wrapped with duct tape and secured in a cooler for transportation to the laboratory. X-radiographs were taken with a portable X-radiograph Unit model PX-

15HF at 72 kV and 50 mAs for each plexglas tray. Fugi sheet negatives were developed and scanned with Microtek ScanMaker 9600XL into digital forms.

RESULTS

Bathymetric Map of Lavaca Bay

The bathymetric data shows Lavaca Bay to be a shallow estuary system with broad shoals <1 m deep along the margins of the bays. The centers of the bays are generally 2 m deep. The actively dredged ship channel is 12 m deep with the non-active channel filling in with sediment reaching a bay depth of 2 m (Figure 2). Adjacent to both the active and non-active ship channels are spoils areas that are usually <2 m deep, but some of these spoil areas are exposed above the waterline during low tide.

Since bathymetric data was only collected during the initial survey and not after Hurricane Claudette, no comparison could be made on the affects of hurricane impacts on bathymetry. The bathymetric map has some errors due to using two different techniques of collecting the data. Deeper parallel lines can be seen within Keller Bay due to these errors. A direct correlation exists between the bathymetry and sedimentary facies data. The facies location is controlled by the geomorphology of the bay system. The oyster biofacies generally occur on bathymetric highs, such as spoil areas. Distributions of the beach sand facies are located along shoals, which are located along the shoreline and alone side the active ship channels. One shoal extends from Rhodes point into South LB there the oyster reefs act like barriers, causing a decrease of energy allowing for coarser sediment to settle adjacent to these reefs.

Sidescan Sonar and Surficial Sediment Data

Based on acoustic backscatter signatures off different density bay floor features, the sidescan mosaic revealed distinct backscatter features (Figure 4); these features are: 1) basin-wide low backscatter (dark tones) background and 2) high backscatter (lighter tones) of various shapes, including 3) an area of 4.96 km^2 extending northward from Lavaca Bay's mouth; 4) a long, linear, high-relief deposit that runs parallel to the ship channel; 5) a long, linear shape cutting cross from the northeast area of Cox Bay to the southwest area of Lavaca Bay and it covers an area of 0.75 km^2; 6) a high-relief crescent-shape zone protruding from Rhodes Point; 7) isolated, high-relief, circular shapes approximately 25 m in diameter; and 8) shallow, linear and semi-circular depressions. These various shapes were determined to correlate to oyster reefs and a pipeline.

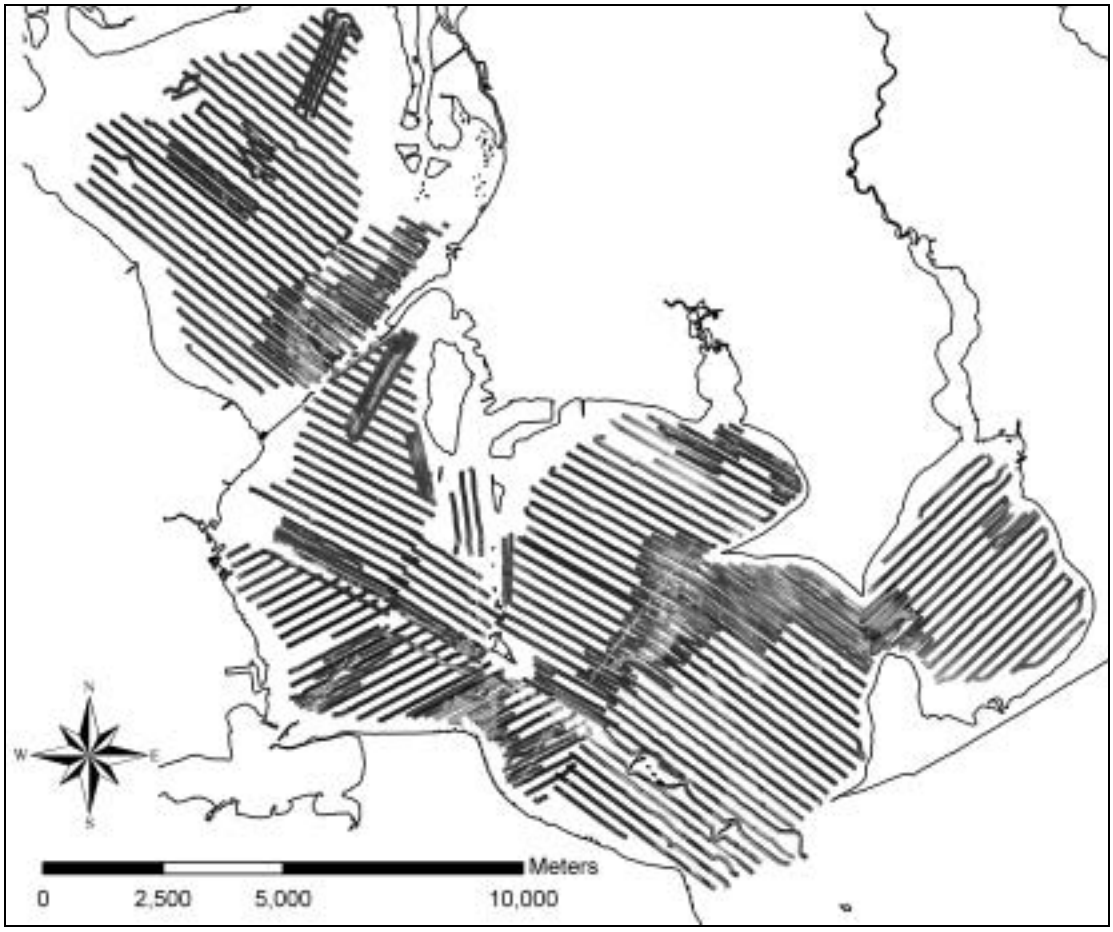

Figure 4. Entire sidescan sonar mosaic showing the distribution of high and low backscatters.

Sidescan sonar mosaics of low and high backscatter characteristics were used to analyze the seafloor characteristics. Comparing the sidescan sonar mosaics to surficial grainsize data (Figure 5 & 6) enabled a correlation between low and high backscatter to muddy and sandy substrates. Low backscatter correlated to fine grain sediment and the high backscatter to coarser sediment deposits at grab locations, and these were extrapolated to the entire bay floor. Identified in Lavaca Bay were ten dominant bottom type textures ranging from sand to clay (Figure 7). The dominant bottom types are: 1)

silty clay (28%); 2) sand silt clay (26%); 3) clayey sand (20%); 4) sand (10%); and 5) clay (10%).

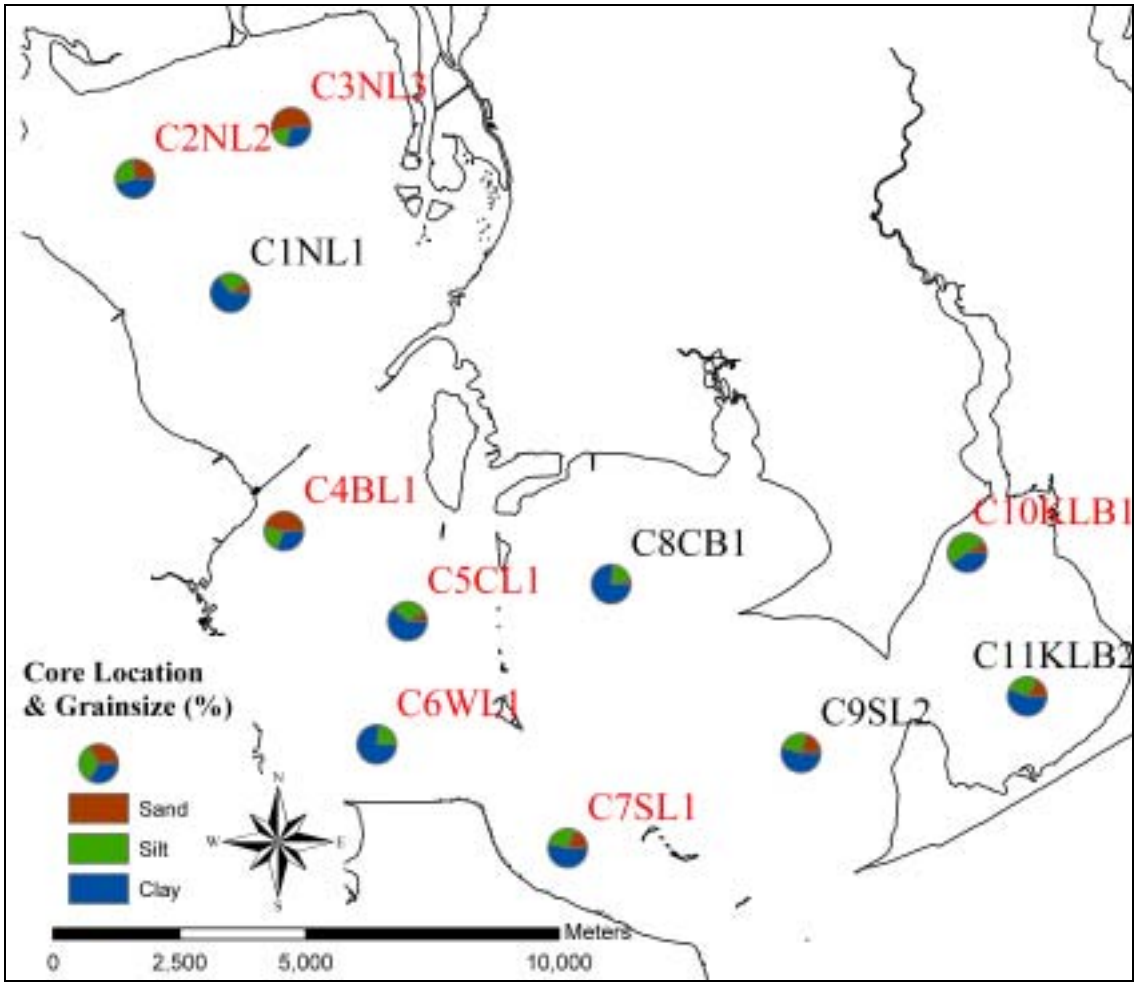

Figure 5. Diver cores' location and surficial grainsize data. The black number cores correspond to the location where pre-hurricane and post-hurricane Claudette cores were collected. The red number cores are where only pre-hurricane Claudette cores were taken.

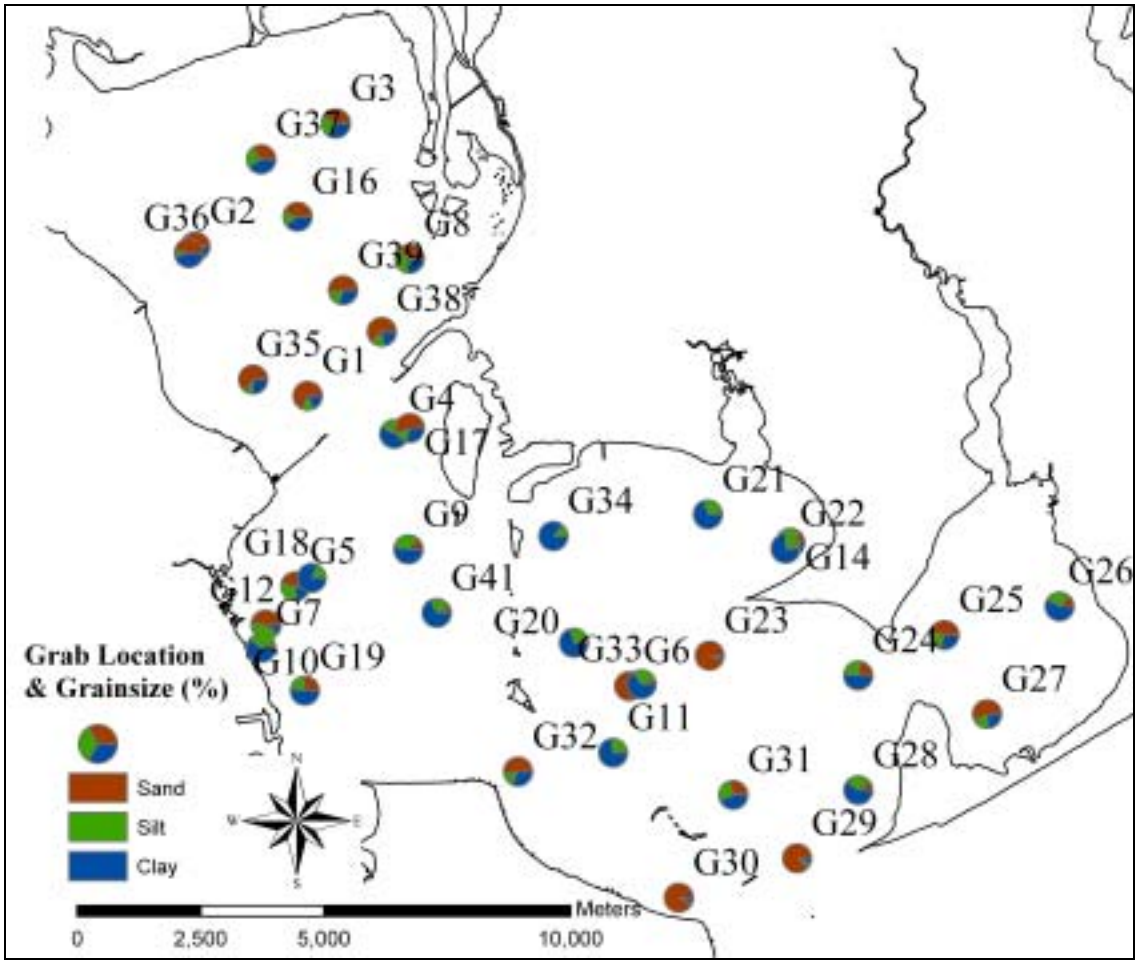

Figure 6. Locations of the 38 surficial grab samples.

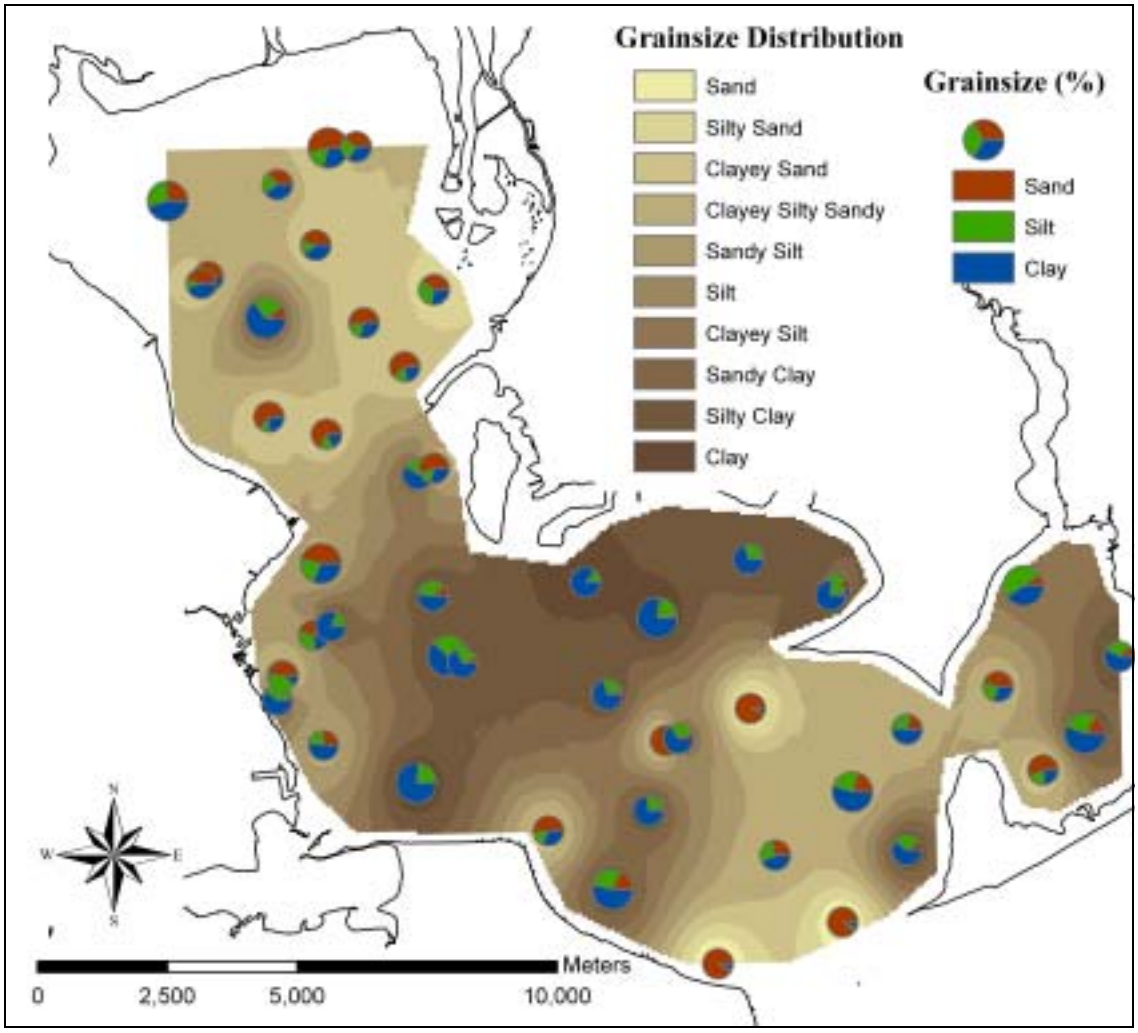

Figure 7. Grainsize map showing the distribution of textures throughout the bay. Delineation of bottom types is based on Shepard's Classification.

Based on these bottom types and seismic data, five sedimentary facies were identified as: 1) bay mouth sand facies; 2) estuary mud facies; 3) fluvial sand facies; 4) beach sand facies; 5) oyster biofacies (Figure 8). Within the post-hurricane lines were a noticeable decrease of high backscatter and increase of low backscatter, suggesting an increase of the mud facies. This was verified by the identification of an oozy mud layer.

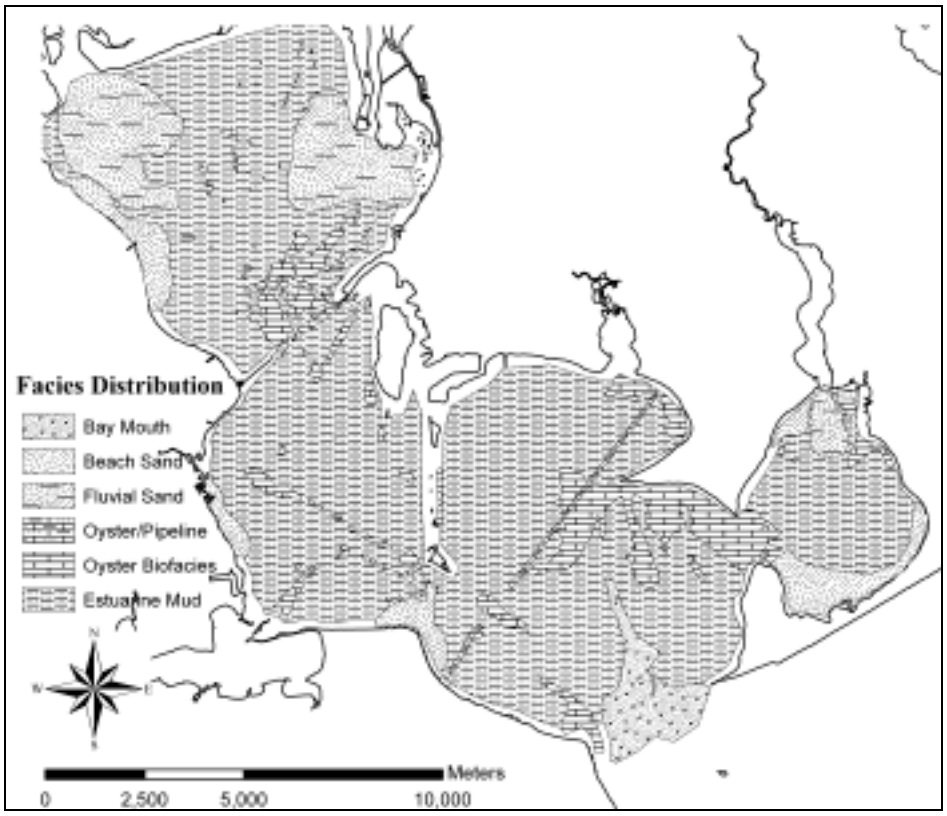

Figure 8. Facies map that was interpreted from sidescan sonar mosaic (Figure 4) and surface samples (Figure 7).

Anthropogenic impacts were only identified within individual sidescan sonar lines due to the scour marks size (Figure 9). Within the 100 m wide sidescan sonar lines were oyster scour marks with a width of 1.4 m and shrimp scour marks with a width of 1.4-2.1 m. The oyster scours were differentiated from the shrimp scours by their circular patterns over high backscatter, this suggests trawls over either oyster reefs or patchy oysters (Figure 9a). The shrimp scours were identified primarily within low backscatter that correlates to mud (Figure 9b-d), because of less damage to the shrimp net and shrimp prefer a muddy substrate.

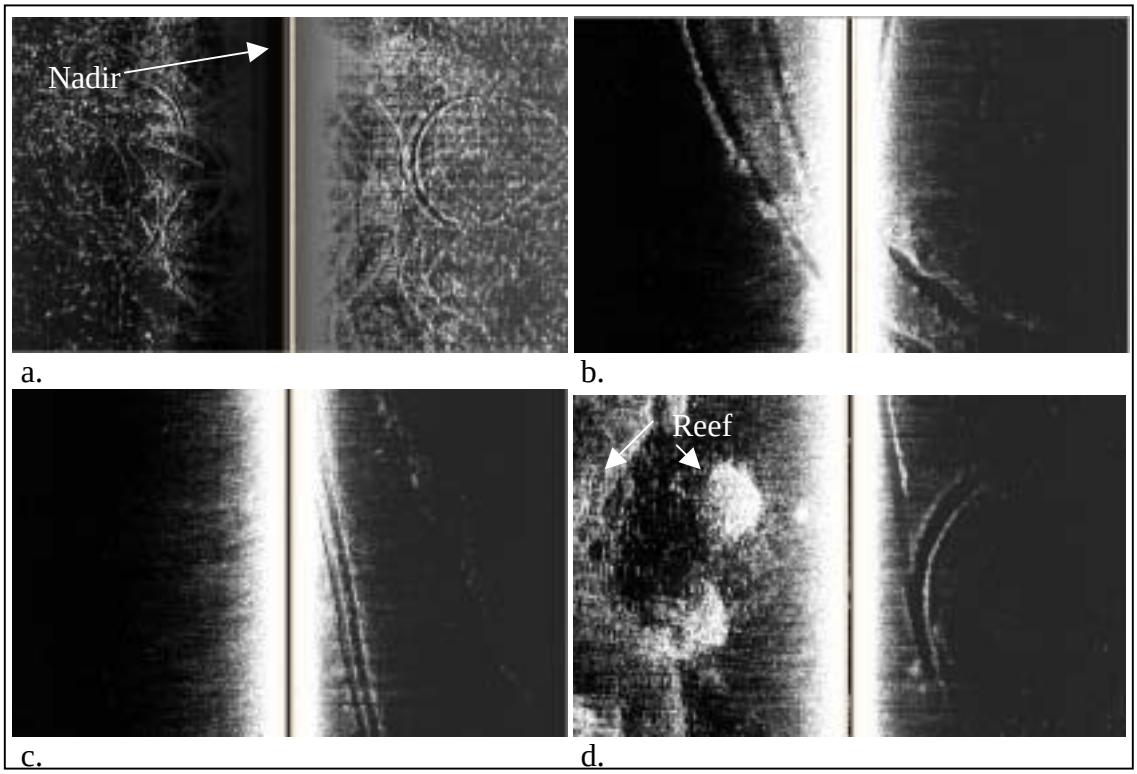

Figure 9. Anthropogenic impacts that were identified within Lavaca Bay. All individual lines are 100 m wide. (a) Oyster scour marks over a patchy oyster field (1.4 m wide). (b) & (c) Shrimp trawl marks (1.4-2.1 m wide) within the estuarine mud facies. (d) Similar shrimp trawls along side an oyster reef.

Northern LB (NLB)

The northern mosaic consists of the area north of the Lavaca Bridge and is dominated by low backscatter (Figure 10). The majority of grab samples contain clayey sand and clay silt sand for most of NLB. The center contains clayey mud, while sand is isolated near the shore face and shoal areas. Sandier sediment dominated the estuarine shoreline boundaries due to the higher increase of shoreline erosion. Within the Lavaca River mouth the grab samples show high mud content and directly north of the mouth was high sand content, suggesting sediment is being entrained to the north. Directly north of the Lavaca Bridge is a large area of high backscatter that correlates with clayey sand containing shell fragments. Ground truthing of the high backscatter were verified to be living oyster by Dr. Simmons and Mr. Harper by using an oyster dredge. The emergent reef size is uncertain due to intermixing of moderately high-to-high backscatter signals that correlated with the shelly sediment and oysters. In addition, small patches of high backscatter approximately 25 m in diameter were concentrated in the northeastern area, interpreted as oyster patches. These oyster patches were numerous and located sporadically throughout the northern part of Lavaca Bay.

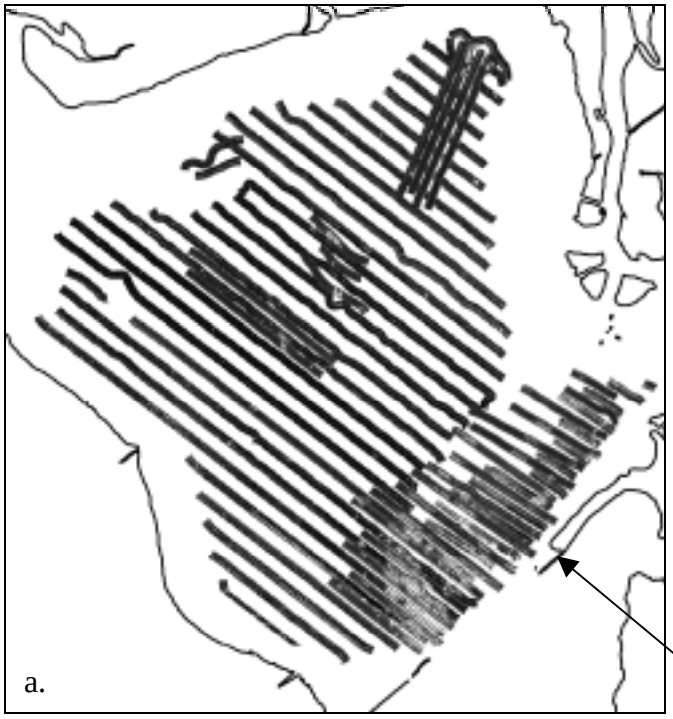

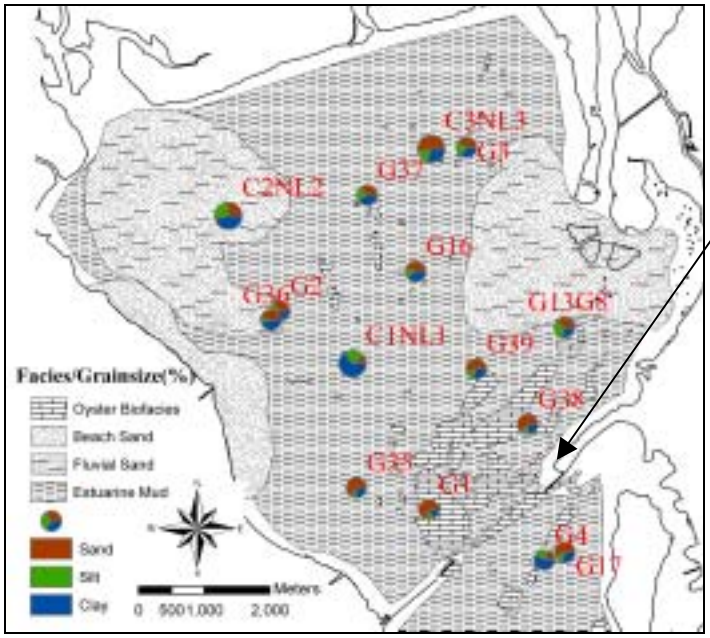

Lavaca Bridge

b.

Figure 10. North Lavaca Bay. (a) Sidescan mosaic (b) Interpretation map that shows the distribution of the oyster biofacies. High backscatter (lighter tones) represents coarser sediment, and low backscatter (darker tones) interpreted as finer sediment. The high backscatter in the southern portion adjacent to the Lavaca Bridge is due to large amounts of oysters and shells.

Central LB (CLB)

The Central LB is composed of mud, sand deposits, and oyster reefs (Figure 11). Directly south of the Lavaca Bridge is a low backscatter zone and an elongated high backscatter feature that covers an area approximately 3.0 km^2. Central LB contains five dredged ship channels. The dredged spoils that have been dumped adjacent to the ship channels now contain coarser sediments and oyster beds. These areas were verified by ground truthing efforts by Dr. Jim Simmons, Josh Harper and I. Dr. Simmons and Mr. Harper ground truthed the high backscatter areas with an oyster dredger and found an abundance of live oysters. I ground truthed the spoil areas with a grab sampler and found only coarse sediment such as sand and shell fragments. The majority of grab samples show sandy silt along the shore faces of the northern and western boundaries, but sediment textures decrease to silty clay in the center and southern areas. In the western area, the sidescan sonar mosaic revealed evidence of a sandy substrate or an oyster reef that extends from Gallinipper Point's shore face towards the active ship channel. The high backscatter near Gallinipper Point was identified by ground truthing to be abundant with oysters. The sand shoreline layer correlated to a medium-high backscatter, this was extrapolated from other known areas of medium-high backscatter that were identified as sand.

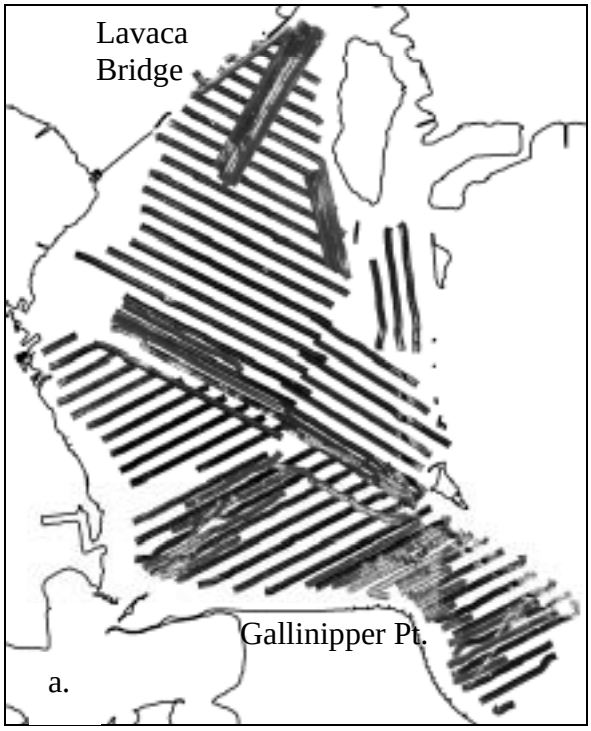

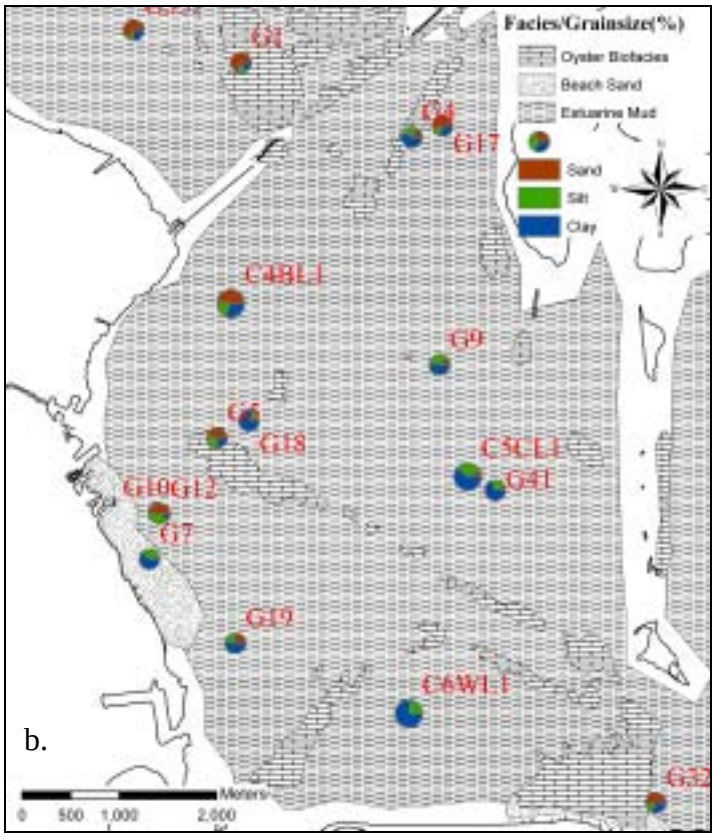

Figure 11. Central Lavaca Bay. (a) Sidescan mosaic (b) Interpretation map.

Cox Bay (CXB)

Cox Bay has an approximately equal area of low and high backscatter (Figure 12). Prominent high backscatter areas are located in the northern area near Cox Point, northeastern area just south of Cox Creek, and a third area of high backscatter feature cutting southwest to northeast through the southeast of the bay.

Grab samples of the northeastern area identified an oyster deposit coupled with a sandy clay bottom, which had a strong putrid odor. The northern area with its high intense backscatter was believed to be oyster reef system, but the grab sample at that location showed mostly clay. Post hurricane Claudette ground truthing and sidescan imaging identified a low backscatter and muddy sediment bottom type. The third prominent high backscatter feature ran northeast to southwest, and correlated with a gas pipeline on nautical charts.

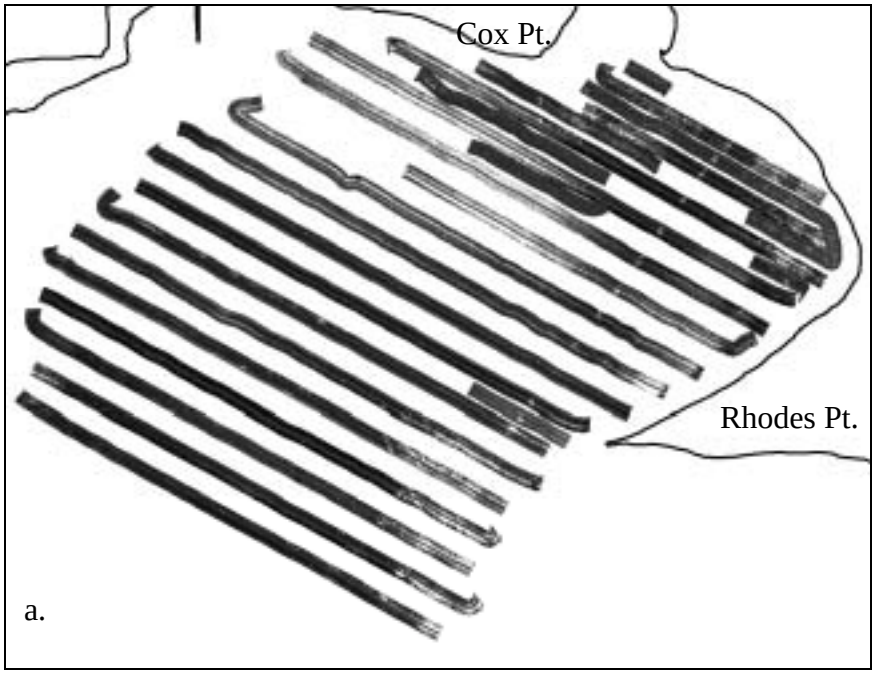

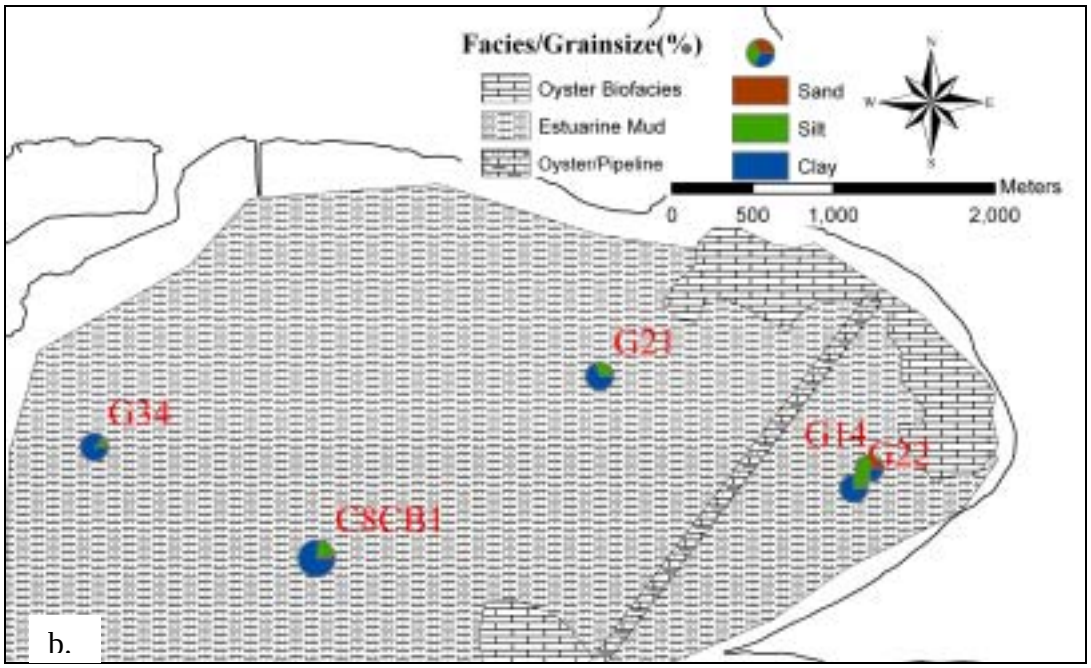

Figure 12. Cox Bay. (a) Sidescan mosaic (b) Interpretation map. The high backscatter southwest of Cox Point was verified after Hurricane Claudette to be part of the low backscatter. Post-hurricane sidescan lines are the low backscatter lines between the high backscatter lines.

Southern LB (SLB)

The southern area contained a clayey silty sandy substrate with two prominent features (Figure 13). The first feature is a large medium-high backscatter area that correlates with sandy grab samples. Two grab samples contained 90 to 100 percent sand. The sidescan mosaic shows this feature extending from the estuarine mouth towards Rhodes Point. The second feature was identified within the bathymetric data has a high relief area. Sidescan sonar mosaic identified this feature as a crescent shape that protrudes from Rhodes Point into the southern bay area and correlates with a sandy/shelly grab sample. It correlates well with an oyster reef. It covers an area approximately 5.25 km^2.

Keller Bay (KLB)

Five grab samples from Keller Bay show that the bay bottom consists primarily of mud. As a result the mosaic shows mainly low backscatter (Figure 14). This bay also contains oyster reefs located at the bay mouth opening and along the eastern shoreline. The mosaic also reveals limited high backscatter areas located along the shoreline of the spit deposit of Sandy Point. Grab samples taken at this location show an equal amount of clay, silt, and sand.

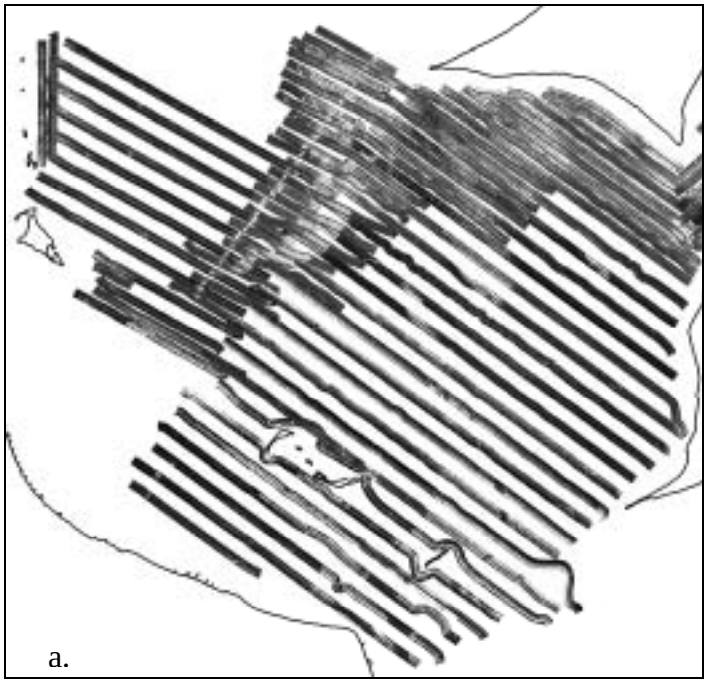

a.

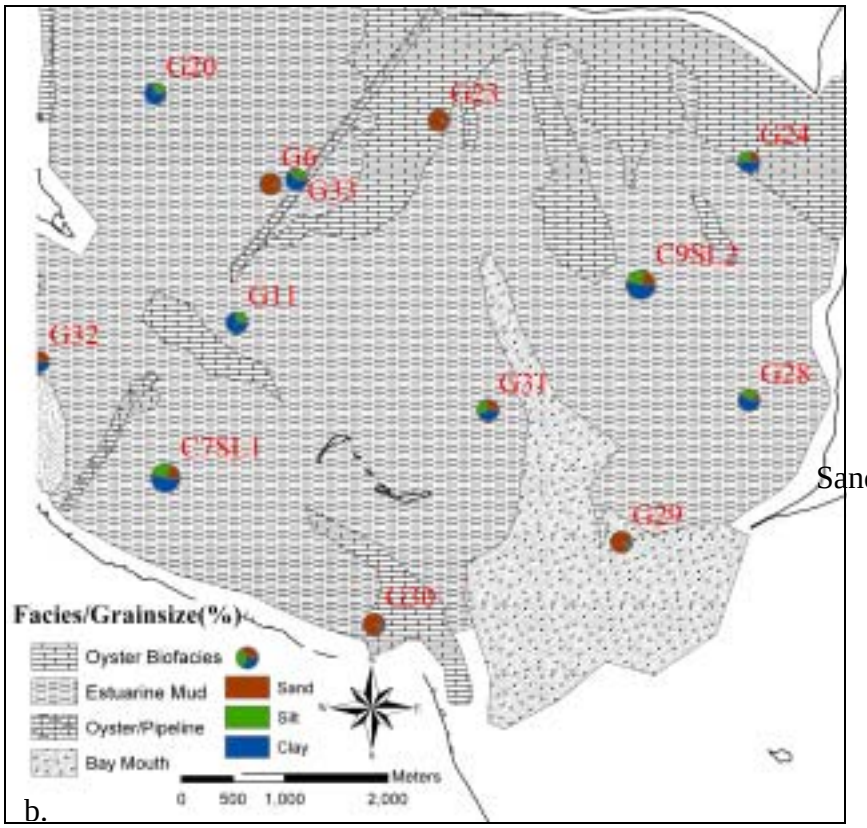

Sand Pt.

b.

Figure 13. South Lavaca Bay. (a) Sidescan mosaic (b) Interpretation map.

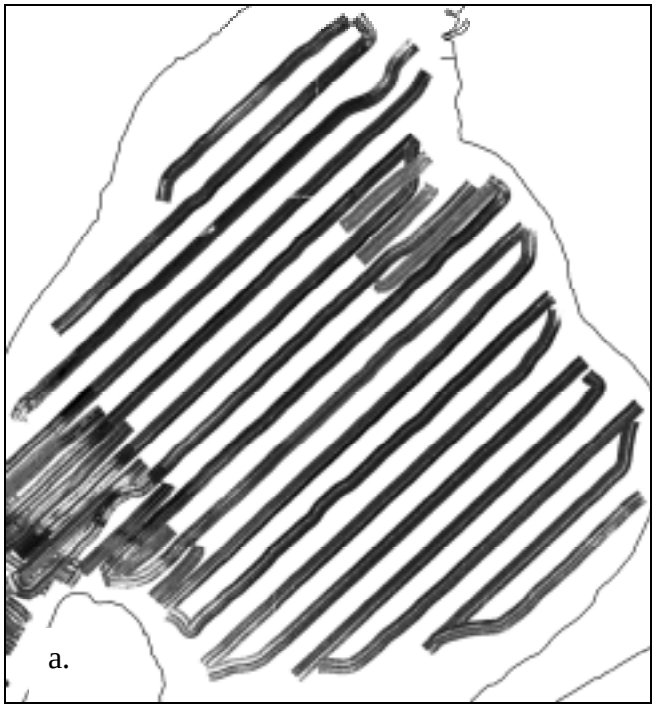

a.

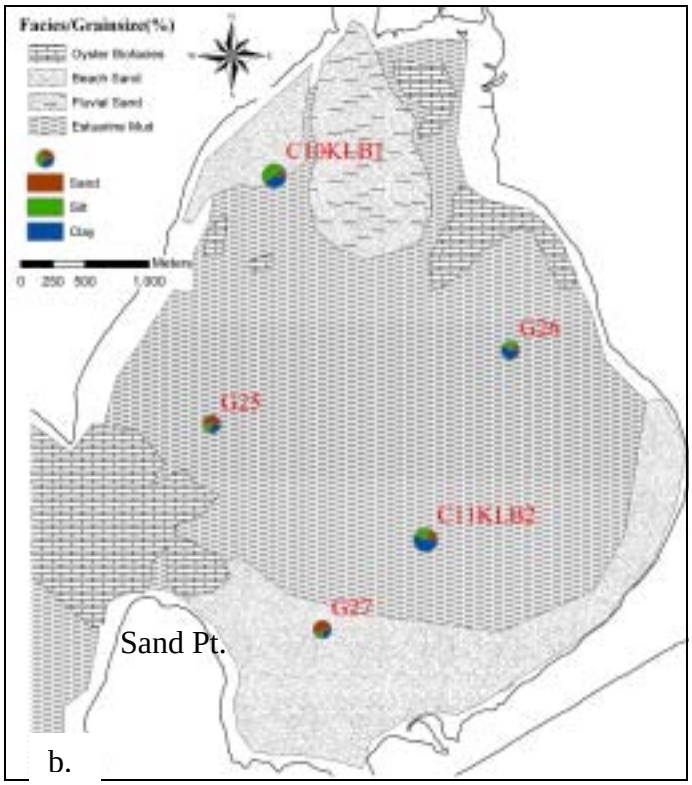

b.

Figure 10. Keller Bay. (a) Sidescan mosaic with high backscatter represents coarse sediment and low backscatter represents finer sediment. (b) Interpretation map.

Chirp Data

Subbottom profile data obtained from Lavaca Bay show stratigraphic layering of differing density down to the Pleistocene, approximately 22 m in depth (Figure 15) similar to Byrne (1975). Within south Lavaca Bay (SLB) a delta deposit was identified that extends northward approximately 1300 m from the bay mouth. The presences of landward dipping clinoforms suggest that it is a flood tidal delta deposit. Within the profile the stratigraphic layers of different density onlap the flood tidal delta, making the tidal delta older. In remote areas of the SLB the chirp penetration was limited because of high sand content and oyster shells.

Although these acoustic data contains a rich record of the geological history of Lavaca Bay since the Pleistocene/Holocene, this study will only focus on the upper few meters of this record. Some of the subbottom chirp profile data shows buried oyster reefs and the mud layer thickness above the buried oysters, also the height of the present oyster reef systems (Figure 16). Buried oyster reefs were dominantly noticeable in the NLB and SLB chirp profiles were located at a depth of 2 m. The buried reefs and the mud thickness were both interpreted and approximated from the subbottom profiles. Another dominant feature was the present ship channel, but penetration was limited due to the chirps depth and velocity, and gas buildup from dredging (Figure 17).

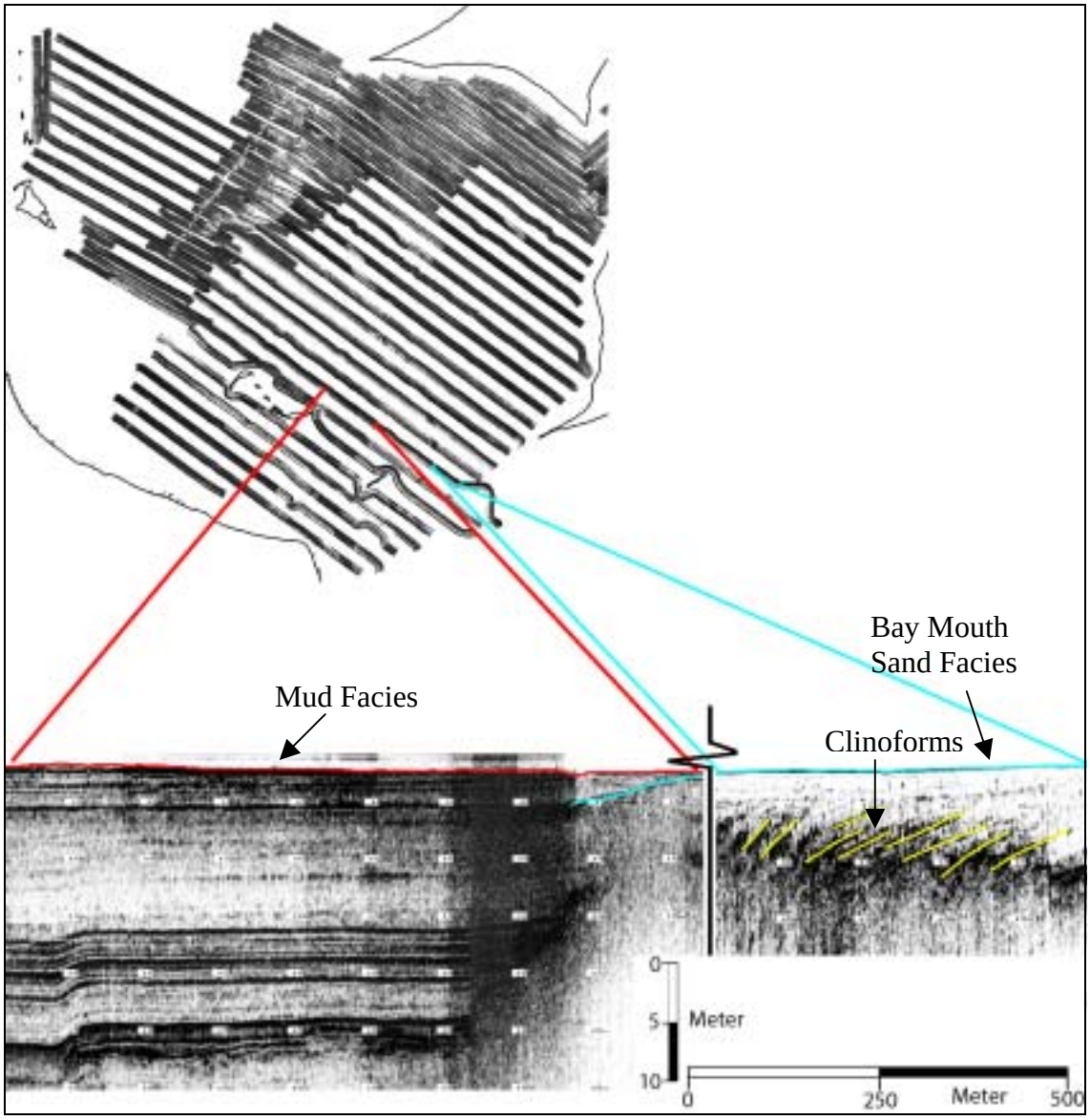

Figure 15. South Lavaca Bay sidescan mosaic and chirp profile showing tidal deltaic boundary. Red represents mud facies, blue represents relict flood tidal deltaic sand, and yellow represents landward dipping clinoforms.

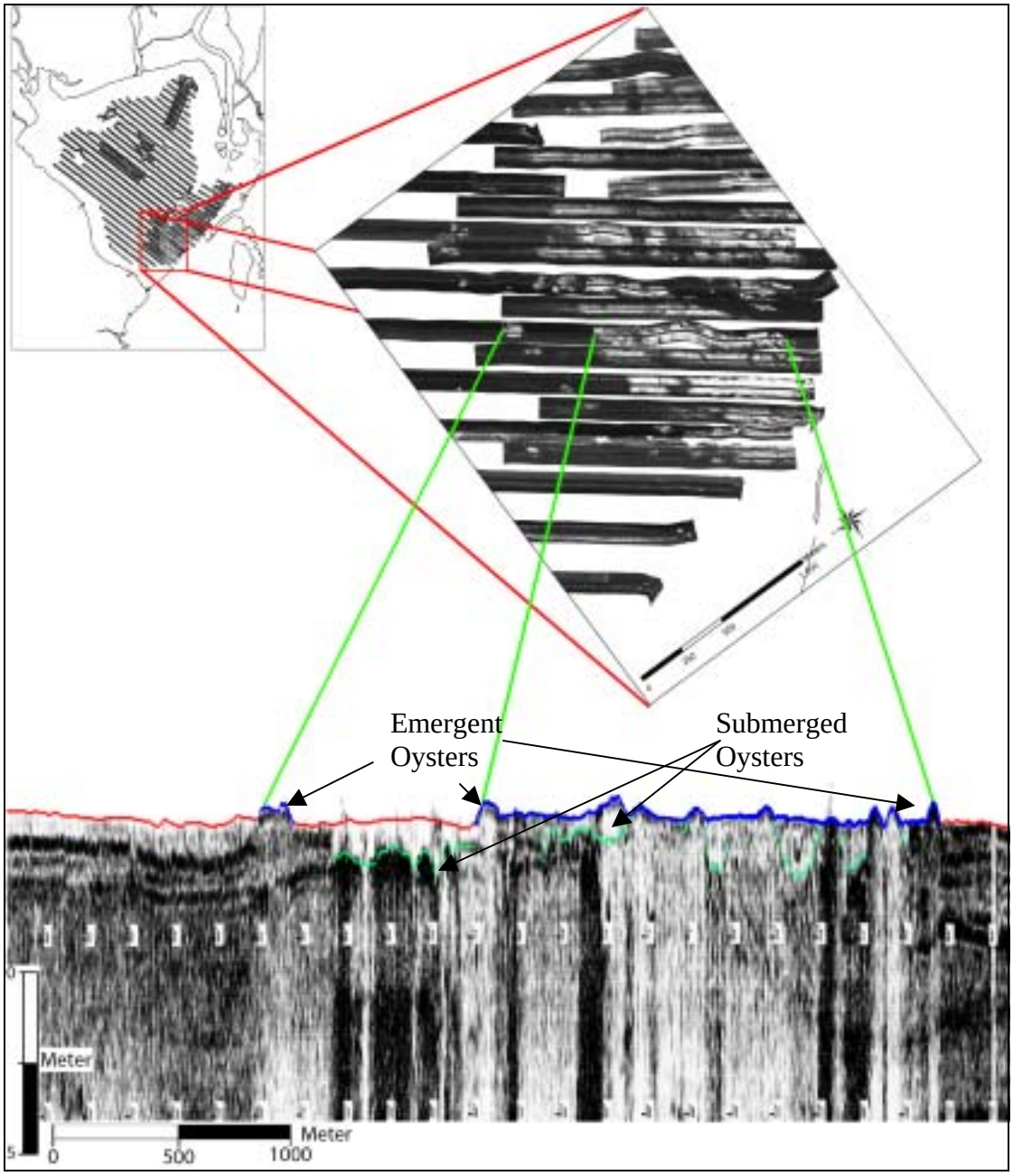

Figure 16. North Lavaca Bay sidescan sonar mosaic shows high backscatter that is interpreted as an oyster reef. Within the subbottom chirp profile (4x vertical exaggeration) red represents the mud; blue represents emergent oyster reefs, which were verified by ground truthing techniques and correlated to the sidescan sonar image. The green represents a density contrast difference. Beneath this green line are wipe out effects that are produced by high density material, and these were interpreted as submergent oyster reefs. The emergent oyster reef is approximately 0.5-0.75 m above the bay floor.

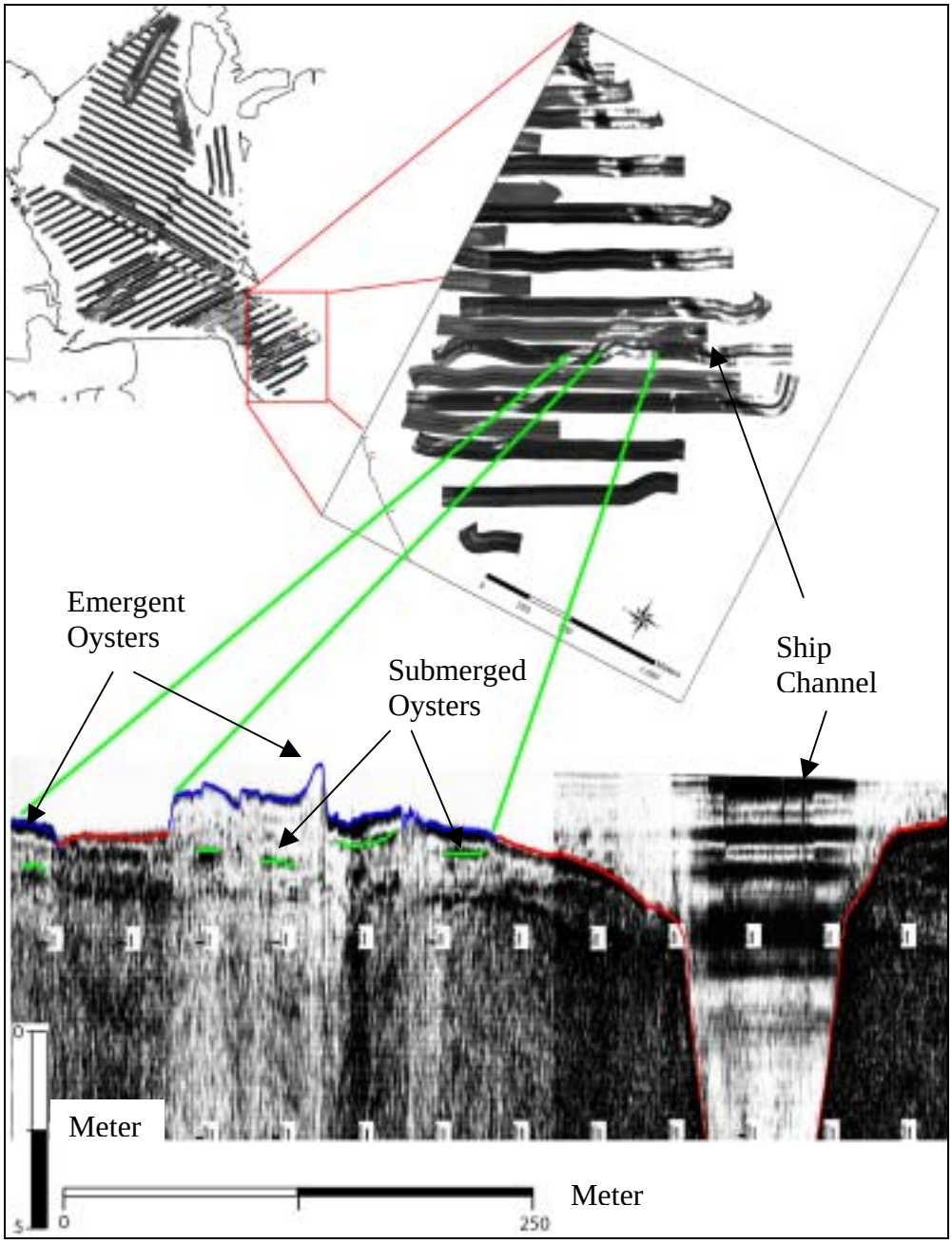

Figure 17. Central Lavaca Bay sidescan mosaic shows high backscatter (lighter tones) that was interpreted as an oyster reef. Within the subbottom chirp profile (3x vertical exaggeration) red represents the mud; blue represents emergent oyster reefs, which were verified by ground truthing techniques and correlated to the sidescan sonar image. The green represents a density contrast difference. Beneath this green line are wipe out effects that are produced by high density material, and these were interpreted as submergent oyster reefs. The emergent oyster reef is approximately 1.5 m above the bay floor.

Core and Geochemistry Data

Pre-hurricane Claudette diver cores were taken at eleven locations (Figure 5), and were analyzed for water content, grain size distribution, X-radiograph, excess ^{210}Pb profiles, and maximum depth of ^{137}Cs. The post-hurricane Claudette diver cores were taken at four previous sites, but were not analyzed for geochemistry. The post-hurricane cores; C12NL4, C13CB2, C14KLB3, and C15SL3; corresponds to the location of the pre-hurricane cores C1NL1, C8CB1, C9SL2, and C11KLB2, respectively. All cores ranged from depths of 35 to 90 cm. The data and profiles are given in appendixes A, B, and C.

Sedimentation rates in Lavaca, Keller and Cox Bays were determined for 11 cores by using ^{210}Pb and ^{137}Cs radioisotopes. Sedimentation rates were calculated by the CIC equation when the mixing or bioturbation layers were absent within the ^{210}Pb profiles. In the sediment of the Lavaca Bay estuary ^{210}Pb activities of the sediment ranged from 2.71-0.11 dpm/g. The maximum and minimum ^{210}Pb activities were calculated by the best-fit line, where the excess activity had an exponential decrease (Appendix C). Where the excess ^{210}Pb activities were uniformed, physical mixed layers were identified. These mix layers were present in cores C1NL1, C2NL2, C5CL1, C6WL1, C8CB1 and C11KLB2, and ranged in depth of 10-16 cm. Overall, ^{210}Pb sedimentation rates ranged from 0.20 to 1.29 cm/yr (Table 2). These ^{210}Pb rates were compared to the calculated ^{137}Cs rates. The sedimentation by of ^{137}Cs calculations were 0.29 to 1.65 cm/yr. The overall ^{137}Cs sedimentation rates agreed with the ^{210}Pb

sedimentation rates for six of the eight cores. These sedimentation rates fit within the range of the rates reported by Santschi et al. (1999) for the cores within the same vicinity.

Table 2. Comparison of radionuclide sedimentation rates

Core no.	Depth (m)	Sed. Rate, ^{137}Cs (cm/yr)	Sed. Rate, ^{210}Pb (cm/yr)
C1NL1	1.55	0.29	0.20
C2NL2	1.37	0.46	0.39
C3NL3	1.62	1.00	0.84
C5CL1	2.01	1.03	0.82
C6WL1	1.77	----	1.13
C7SL1	2.01	0.96	0.90
C8CB1	1.74	----	1.29
C9SL2	1.83	1.44	1.22
C10KLB1	1.46	1.65	0.65
C11KLB2	1.55	1.08	0.43

Northern LB

Three pre-hurricane (C1NL1, C2NL2, & C3NL3) and 1 post-hurricane (C12NL4) Claudette cores were collected in North Lavaca Bay (NLB), with the post-hurricane core taken at the same location as core C1NL1. Within the cores there were many coarsening upward sequences that were truncated by planar or way laminations, suggesting multiple short and high energy input (Appendix C). The average down core porosity decreased towards the northeastern corner of the bay due to an increase of sand content. The accretion rates were low south of the Garcitas delta, approximately 0.3 cm/yr, and increased to the northeast to 0.8 cm/yr. Within cores C1NL1 and C12NL4 there were similar grainsize and porosity profiles, but C12NL4 had an offset of 10 cm

closer to the bay floor, suggesting erosion after the passing of Hurricane Claudette (Figure 18).

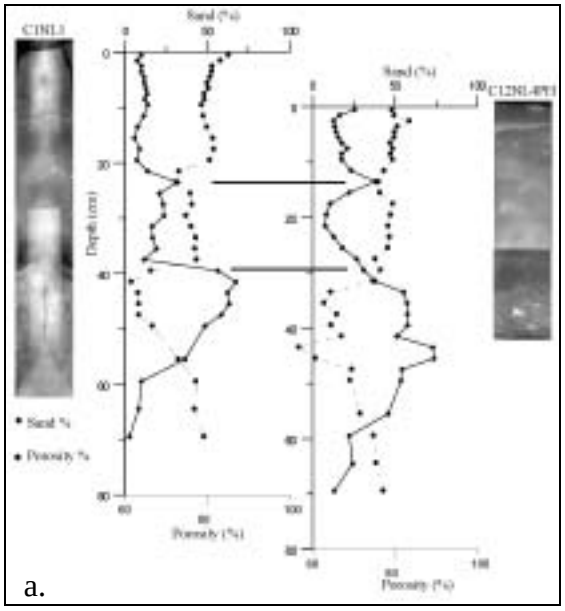

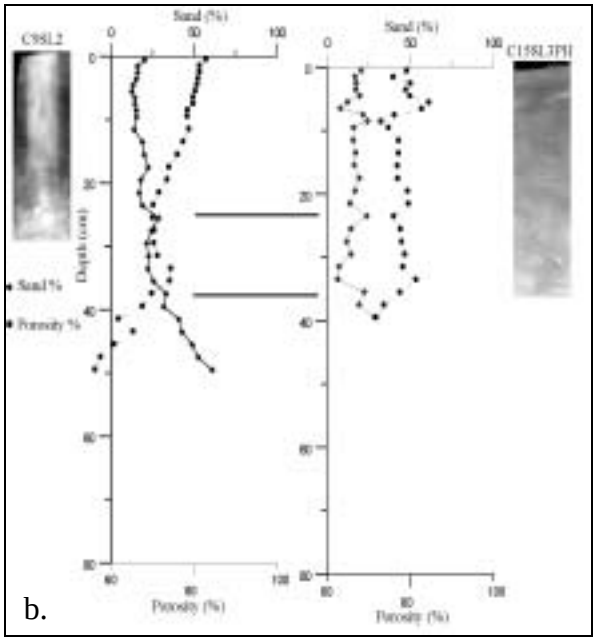

Figure 18. Pre-hurricane and post-hurricane Claudette grainsize and porosity profiles (Erosion of C1NL1, C9SL1). (a) C1NL1 and C12NL4 cores show net erosion of 10 cm. (b) C9SL1 and C15SL3 cores show net erosion of 2-3 cm.

Central LB

Three pre-hurricane (C4BL1, C5CL1, & C6WL1) cores were collected in Central Lavaca Bay (CLB). Core C4BL1 shows the extent of the toe of the shoreline. The other cores show a high mud content, approximately 90% to 100%, with interbedded sand lenses. Both of these cores show a 10-cm thick mixed layer with an accretion rate of approximately 1 cm/yr.

Cox Bay

One pre-hurricane (C8CB1) and 1 post-hurricane (C13CB2) Claudette cores were collected in Cox Bay (CXB). The grainsize data shows a fining upward sequence with the ^{210}Pb profile showing a stair-step appearance, suggesting episodes of sediment mixing. The only difference between the cores was the deposition of 2 cm of sediment (Figure 19).

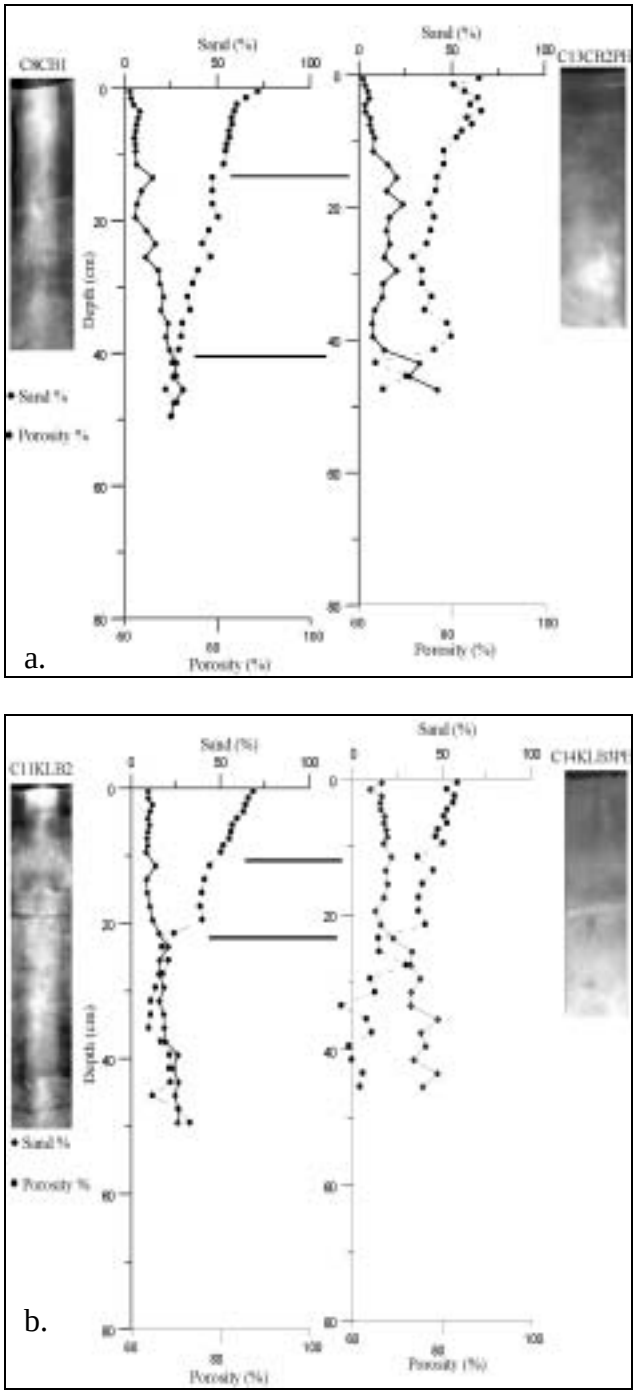

Figure 19. Pre-hurricane and post-hurricane Claudette grainsize and porosity data profiles (Deposition of C8CB1, C11KLB2). (a) C8CB1 and C13CB2 cores show net deposition of 2 cm. (b) C11KLB2 and C14KLB3 cores show net deposition of 2-3 cm.

Southern LB

Two pre-hurricane (C7SL1, & C9SL2) and 1 post-hurricane (C15SL3) Claudette cores were collected in South Lavaca Bay (SLB), with the post-hurricane core taken at the same location as core C9SL2. Both cores show a fining upward sequence with steady accumulation rates between 1 cm/yr and 1.2 cm/yr. Core C9SL2 shows maximum ^{137}Cs depth correlate with a dramatic increase of sand content and a dramatic decrease within the ^{210}Pb profile, suggesting an episodic event (Appendix C). The comparison of pre-hurricane and post-hurricane cores showed 2-cm of erosion.

Keller Bay

Two pre-hurricane (C10KLB1, & C11KLB2) and 1 post-hurricane (C14KLB3) Claudette cores were collected in Keller Bay (KLB), with the post-hurricane core sample was taken at the same location as core C11KLB2. Core C11KLB2 contains 10-cm thick mixed layer with a stair-step grainsize profile, suggesting a change in energy conditions. Laminations were also present where the sand content decreased. Core C10KLB1 had no mixed layer (Appendix C) but contains a fining upward sequence. The post-hurricane core had overall similar grainsize profiles as C11KLB2, but shifted down within the core, suggesting 2-cm of deposition.

DISCUSSION

Sedimentary Textures and Facies Distribution

Sidescan sonar mosaics, subbottom profiler, 50 surficial grab samples, and 15 cores were used to characterize and delineate the sedimentary facies and their distribution within Lavaca Bay. Lavaca Bay bottom consists of 42 % mud, 26 % sandy mud, 22 % muddy sand, and 10 % sand (Figure 5 & 6). According to Byrne (1975), Lavaca Bay consists of 3 recent sedimentary facies: fluvial-deltaic sand and muddy sand, bay margin sand and mud. During my study, 5 sedimentary facies have been identified; they are: 1) estuarine mud, 2) fluvial sand, 3) bay mouth sand, 4) beach sand, and 5) oyster biofacies (Figures 8, 10-14). The sand facies were found to be on dredge spoils banks adjacent to ship channels and adjacent to shorelines, and river and bay mouths. The mud facies and oyster biofacies were found throughout the bay system.

Estuarine Mud Facies

The mud facies is composed of fine grain siliclastic silts and clays with a color range from light to dark gray and light tan gray. Since Lavaca Bay is a low energy system, light gray sediment was identified throughout the system. The samples that are lighter tan-gray in color have high silt content, and are found around the shoreline margins. These sediments derive from both bluff erosion and suspended material from fluvial systems (Byrne, 1975). Darker gray samples have higher organic materials

content. The mud facies contains primarily of quartz and feldspar grains, montmorillonite clay and shell fragments with minor amounts of feldspars (Byrne, 1975). The mud facies within Lavaca Bay exists in deeper water depths (>1.5 m) or within the center bays and dredged ship channels. Only one exception was Cox Bay. This area contains a higher organic content within the muddy shoreline, and is proximal to where mud was being piped from dredging operations.

Beach Sand Facies

This facies contains light tan colored, fine-grain siliclastic sand. According to Byrne (1975), feldspars are the most dominant secondary mineral within the sand facies. This sand facies was restricted to the shoreline and areas where the depth is less than 1 m (Figure 6). During high energy storm surges the beach is eroded by waves breaking on the shoreline and bottom currents carrying the sediment. These storms will cause the sand facies to migrate into deeper portions of the bay.

Bay Mouth Sand Facies

This sand facies is a relict tidal delta that contains siliclastic sediment and shell fragments (Figure 13). This facies is located between at the mouth, and extends northward into Lavaca Bay. This facies is a reworked relict tidal delta deposit. Dredging of the ship channel has altered the geometry of this facies.

Oyster Biofacies

This facies contains both intertidal and subtidal oyster reefs. Oysters most maintain positive bathymetric reef to survive siliclastic burial from seasonal and episodic flooding. The distribution of the live emergent reefs is mainly controlled by the geomorphology of the bay, the presence of underlying submerged reefs and other hard substrate, such as sand and shoals. Within NLB (Figure 16) and CLB (Figure 17) there are large live reefs that are 1.5 m above the seafloor and between these reefs are smaller lower relief live reefs. Shelly shoals exist around the outer limits of the oyster reefs. Shells from the oyster reef are transported away from the reef system during high energy storms. The collection of small fragments of abrasive oyster shells suggests waves are reworking the shells. This facies is also distributed around dredge spoils and other bathymetric highs, including anthropogenic structures, such as electrical towers, bridge pilings and pipelines.

Fluvial Sand Facies

This facies was only identified within the cores and chirp data. The subbottom profiler identified a large wedge of high density material that is located south of the Lavaca-Navidad River. This was interpreted as the bayward extent of the Lavaca-Navidad bay-head delta (Figure 20). This facies is also located near each river or creek that enters Lavaca Bay and adjacent bays (Figure 10). According to Byrne (1975) and McGowen and Breton (1975) the Lavaca-Navidad delta has not changed significantly in the last 100 years, suggesting sediment migration into the estuary. Grab samples (Figure

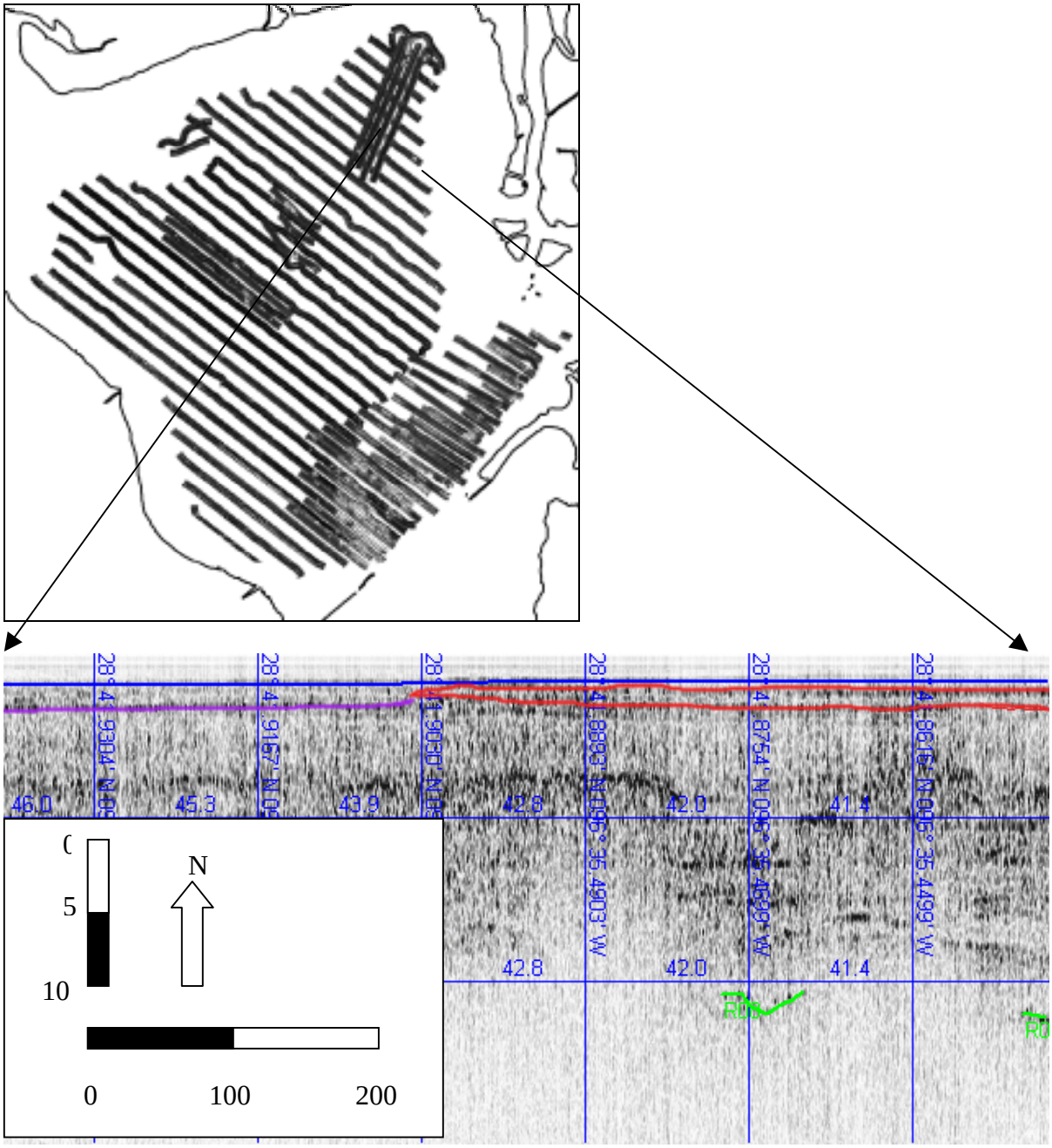

Figure 20. Lavaca-Navidad river delta.

5 & 6) show a distribution of fine grain sediment in front of the Lavaca-Navidad delta. Additionally, the core C3NL3 surficial sample and excess ^{210}Pb profile (Appendix C) show coarser grain sediment north of the delta suggesting that coarser sediment is being entrained north of the bay-head delta.

Sedimentary Processes

Estuarine Mud Facies

Lavaca Bay is a low energy system. Majority of fine grain sediments that supplies the mud facies enters into Lavaca Bay by the Lavaca-Navidad fluvial system and smaller rivers. High accumulation rates observed within the CLB and CXB excess ^{210}Pb profiles (Appendix C) are probably due to fine grain sediment input from localized dredging and river sediment influx. Study by Santschi et al., (1999) found similar rates of 1.6 to 2.2 cm/yr around Dredge Island. The channel dredging in the 1950's changed the hydrodynamics of this area. Santschi et al., (1999) suggest this is due to sediment infilling and equilibration of the area.

Since the deposition of the gray mud facies, the bay conditions have remained relatively constant (Byrne, 1975). The ^{210}Pb profiles (Appendix C) suggest that within this facies there are intervals with high accumulations, and higher accretion rates. These higher rates probably resulted from either high-energy storm or anthropogenic events. Physical mixing dominated areas with high mud content, while limited reworking and continuous deposition were limited to areas of coarser grain sediment.

Fluvial Sand Facies

The present Lavaca-Navidad delta has prograded 4.3 km into the present Lavaca Bay, but has prograded as far as 17.5 km in the past (Byrne, 1975). The fluctuations of the delta resulted from sea level shifting, but the present day delta progradation is believed to be the result of flooding during and after hurricanes. During flooding, the null point and bedload migrates down into the bay. As the flooding subsides, the null point migrates up the fluvial system, as the turbidity maximum is re-established to its original pre-flood position, fine grain sediment is deposited on top of the coarser material, rapidly burying it.

The fluvial sand facies was identified in the chirp records and the grainsize core profiles in the North LB (Appendix C), and are in line with the axis of the Garcitas and the Lavaca-Navidad delta. In core C2NL2, the sand layer was approximately 30 cm thick and at the depth of 40 cm, while core C1NL1 had a layer of 20 cm thick and at the same depth of 40 cm. This sand deposit is part of the deltaic sand lobe of either Garcitas or Lavaca-Navidad Deltas. According to the study by Byrne (1975) the Garcitas creek delta has not prograded into Lavaca Bay, and has only been a minor contributor of sediment, plant material and fresh water to the Lavaca-Navidad estuary. This suggests that the sand source originated from the Lavaca-Navidad River. This buried sand layer probably formed during the hurricanes of 1875 and 1886. These two hurricanes significantly altered the Texas coastline. Likely there was an intense storm surge followed by episodic flooding within the drainage basin. When the flooding occurred, the turbidity maximum and null point would have been driven from the tributaries into

Lavaca Bay, and allowing for the transport of bedload sands, which would have normally been deposited in the bayhead delta. The sand body is more pronounced further south in core C1NL1 than in C2NL2. Alternatively, C2NL2 had a larger sediment deposit that could have formed from increased shoreline erosion and sediment input from the Garcitas Delta. As the estuary circulation became re-established in its non-flooding configuration, trapping of sediment by the turbidity maximum would have rapidly buried the coarse grained flood deposits with fine grained estuarine mud and limiting the identification within the geophysical data.

Bay Mouth Sand Facies

The bay mouth sand facies is between Lavaca and Matagorda Bays. Chirp seismic profiles show that the estuarine mud facies onlaps the bay mouth sand facies (Figure 15), suggesting the sand facies is much older than the recent mud facies. Also the chirp record contains landward dipping clinoforms indicating this to be a relict tidal delta deposit rather than a relict bayhead delta. The chirp profiles show the subsurface distribution of this sand body to be a wedge shaped fan deposit that thickens with increase depth. But the sidescan sonar mosaic shows the areal distribution as asymmetrical (Figure 13). The surficial sand derives from the relict tidal delta deposit, and has been reworked by wave and tide energy as well as ship channel dredging on the western side of the flood tidal delta.

Beach Sand Facies

The beach sand facies is located along a relict barrier spit shoreline, which comprises Sand Point (Figure 10). Major erosional scarps were observed along the beach/water interface during the field survey. The major beach erosion and deposition of this sand facies occur during high-energy washover events, which result from hurricanes and storms, as well as lower energy tidal and wave driven erosional events. During hurricanes and tropical storms, storm surges occur, inundate low-lying areas, resulting in nearshore erosion and deposition (Hayes, 1978). In core C11KL2 of Keller Bay (Appendix C), the sand deposit probably resulted from overwash fans during a storm surge. A storm breached the Keller Bay/Lavaca Bay barrier spit. This process along occasional flooding of from Keller Creek appear to have helped transport some of the sediment to the western end of Keller Bay and contributed to the infilling of this bay. Large storms such as Carla, with a 3.4 m storm surge in the Matagorda area, cut the peninsula into numerous, small islands and the shoreline was cut back as much as 243.8 m (McGowen & Scott, 1975). These islands have since formed a new peninsula.

According to Hayes (1967), Hurricane Carla (1961) produced wave-cut cliffs as much as 3 to 4.5 m high. Hurricane Carla produced a storm surge of approximately 7 m that increase major beach erosion. With waves breaking onto the shoreline the coarser sediment was transported towards the bay center. A small increase of high backscatter can be seen within the sidescan sonar mosaic (Figures 6) and core C4BL1. Core C4BL1 (Appendix C) contain 38 cm of 75 % of sand, capped at the surface with 2-3 cm of mud. This sand layer is the southern extent of the toe of the beach.

Oyster Biofacies

The oyster biofacies is composed of oyster reefs and oyster shells (Figures 10-14). The distribution was found to coincide with bathymetric highs and submerged reefs. Oysters swim or float freely in the water during a larval stage, settling to a fixed substrate, such as oyster bed, shells, pilings, pipelines, bulkheads, etc., only after they reach a stage of considerable development (Moore & Danglade, 1914). During settlement and fixation a slight film of mud or slime is sufficient to stifle them (Moore & Danglade, 1914). The minor oyster patches located in the organic rich mud environment must have formed when the oyster larva attached to scattered shells lying on the sediment surface. When oysters are harvested the dead shell material is discarded over the side of the harvest boat and can become widely distributed. Data collected from Moore & Danglade (1914) confirmed the existents of an oyster reef in Cox Bay. They found the bottom to be generally hard and covered by a dense growth of from about 250 to 550 bushels of market oyster per acre, but the oysters were in a scattered cluster and of poor quality. Since the 1914 major anthropogenic changes, such as dredging, appear to have buried the oyster reef. Although the oyster biofacies were identified throughout Lavaca Bay, the majority biofacies were located in the North LB and South LB, with a total of 17.6 km^2 for both oyster reefs and oyster patches.

Bathymetry

Bathymetric data collected by NOAA's National Ocean Service (NOS) showed similar depths between 1849 and 1934, suggesting low sediment accretion (Figure 21). The years before 1958 and between 1958 to1992, there were many bathymetry changes, primarily within central and south Lavaca Bay. These areas contained as much as 0.9 m of sediment infill. A large amount of sediment infilling occurred during the dredging of the present ship channels. This could partially explain the pulse or stair-step appearance within the core C8CB1 from Cox Bay.

Variations in Sediment Accretions Between the Bays

North LB

The three cores that were collected and processed for geochemical analysis within North LB showed the lowest sediment accumulation rates of 0.20 cm/yr and 0.39 cm/yr. Cores C1NL1 and C2NL2 (Appendix C) contains similar depositional history. The ^{210}Pb activities showed a decrease at depths of 10 cm and 5 cm, respectively, this interval correlates to a grainsize increase within the grainsize profiles and a wavy lamination within the X-radiograph. This pulse of sediment may be associated with the flooding in 1971, associated with Hurricane Fern, which resulted in > 50 cm of rain (Davis, 1972). These low ^{210}Pb activities are probably due to a temporary increase in sediment supply. If the accumulation rate was re-calculated for the ^{210}Pb profile from

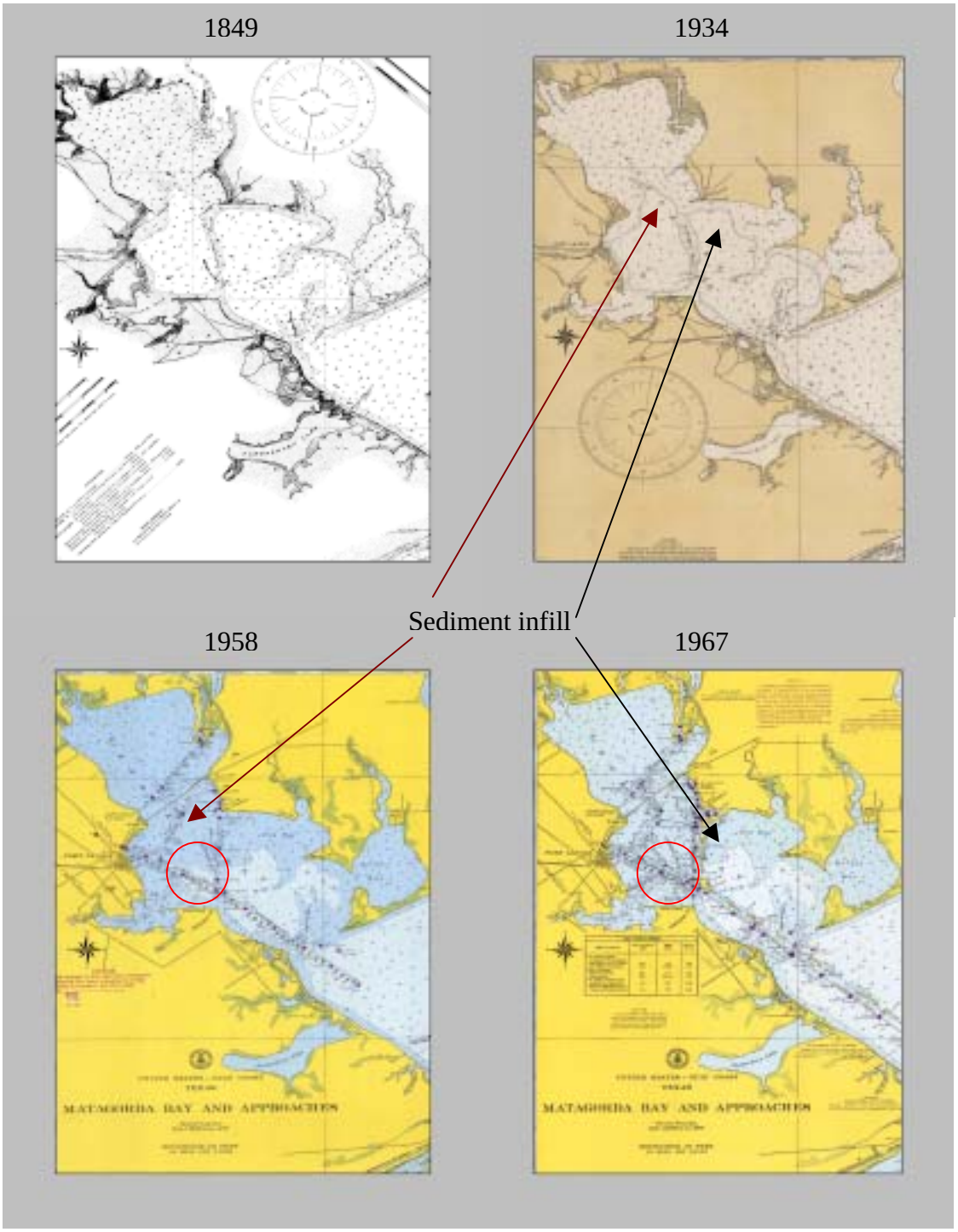

Figure 21. Historical bathymetric charts of Lavaca Bay, Texas. Increase of sedimentation rates are observed between the 1934 and 1967 charts within the central and southern Lavaca Bay. These increases are due to the dredging of the present ship channel.

the decrease activity peak, which is believed to have occurred in 1971, to the surface, the accretion rate would be 0.65 cm/yr. At this rate the Hurricane Fern layer should be located at a corrected depth (assuming no compaction) of 20 cm and not 12.1 cm, if it is assumed that the sedimentation rates were continuous since Hurricane Fern. The recent impact from Hurricane Claudette shows that a category 1 hurricane can erode 10 cm, suggesting that tropical storms can result in similar erosion of the baybed. Some of the sediment may have also been eroded during tropical storms of 1998 and 2002, but the amount of erosion is unknown.

Core C3NL3 contains lower ^{210}Pb activity with a constant slope profile. This suggests that Lavaca River has rapidly delivered sediment into the Northeast NLB. The accretion rate was 0.84 cm/yr. This high accretion rate is 3 to 4 times that of cores C1NL1 and C2NL2, which indicates this area should have filled in. Erosion and flushing of sediment that occurs during storm events likely explains why the bay has not filled in. This elevated ^{210}Pb profile accretion rate may be artificially elevated due to the high sand content.

Central LB

Core C4BL1 was not analyzed for geochemistry because it contained 75% sand. This core contains the relict beach sand facies that has recently been covered with mud. Physically mixed layer of 11 cm was identified within core C6WL1, which resulted from sediment transportation during higher energy or from an anthropogenic impact. Impacts from shrimping activity were observed within the sidescan sonar lines (Figure 9) and

these trawls produced 1.4-2.1 m wide scours. Shrimp trawls approximately 2 m wide could scour the upper sediment surface, producing the observed ^{210}Pb mixing. The ^{210}Pb accumulation rate was 1.13 cm/yr (Figure 21a). Within the central area, according to the NOS maps, the water depth has decreased due to sediment infill. In 1849 and 1934 the water depths were approximately 2.4-2.1 m, but in 1958 and 1967 the depth decreased to 1.8 m and 2.1 m, respectively (Figure 21). Today the depth is 1.5-1.8 m. Enhanced sedimentation due to dredging activity likely explains the high accretion rate.

Cox Bay

This bay is characterized by muddy sediment which was identified from the sidescan mosaic (Figure 12). Within core C8CB1 there is a fining upward sequence within the grainsize profile (Appendix C). The shape of the ^{210}Pb profile shows uniform mixing between the depths of 0-10 cm and 16-24 cm. The ^{210}Pb profile appears to not be affected by grainsize fluctuations. Based on ^{210}Pb profile the sediment accumulation rate is 1.29 cm/yr, however this rate could not be confirmed because the maximum ^{137}Cs depth was unknown (Figure 21a). During the seismic collecting processes there was a large amount of sediment being pumped into the Cox Bay area from a piping system associated with a dredging operation. The ^{210}Pb activity pulse correlates to episodes of dredging in the past few decades. According to Santschi et al., (1999) the elevated sedimentation rates within Cox Bay during the last 1-2 decades have been higher than previously.

South LB

This bay contains accretion rates that were estimated for cores C7SL1 and C9SL2 (Appendix C) located in the western and eastern portions; they are 0.90 cm/yr and 1.22 cm/yr, respectively. These ^{210}Pb accretion rates are consistent with the maximum ^{137}Cs depth. The grainsize profiles for the SLB suggest continuous sedimentation, however the high accretion could be elevated due to the dredging of the ship channel proximal to the coring site.

Keller Bay

Cores C10KLB1 and C11KLB2 show different ^{210}Pb accretion rates versus ^{137}Cs accumulation rate. The core C11KLB2 contains a fine grain sand layer that is capped by a 20 cm thick mud layer. This sandier layer probably resulted from Hurricane Carla's storm surge, which would leave an eroded shoreline and may have even deposited a small washover fan. The shoreline sediment is eroded by both a storm surge and waves that increased the shear stress on the baybed (Dellapenna et al., 1998), resulting in coarser sediment to be transported into the deeper portions of the bay. As the storm subsides and the bay returns to normal, fine grain sediment settles out of the water column which rapidly buries the coarser sediment.

Hurricane Impacts on Sedimentation

On July 15, 2003 Hurricane Claudette made landfall along Matagorda Peninsula, with sustained wind speeds of 65-85 knots (33-44 m/s), a 2 m storm surge, and the eye of the storm went up the axis of Lavaca Bay. With this increase in wind and current energy, is an increase of bed shear stress that leads to erosion and the potential for large-scale sediment transport within Lavaca Bay. Eleven cores were collected in May 2003, four of these core locations were re-sampled after Hurricane Claudette to assess the amount of either erosion or deposition due to the hurricane. As Figure 18 & 19 show, within the lower half of Lavaca Bay, core C15SL3 had +/- 2 cm of erosion compared to pre-Hurricane core C9SL2 collected at the same location; and C14KLB3 had +/- 2 cm of deposition, compared to pre-Hurricane Core C11KLB2. Within Cox Bay, C13CB2 shows +/- 2 cm of deposition compared with C8CB1 taken pre-Hurricane. In North Lavaca Bay C12NL4 shows ~10 cm of erosion compared with pre-Hurricane core C1NL1.

The numerical models (ADCIRC & SWAN) used by Larm and Edge (1998) predicted that the impact of Hurricane Carla on Cox Bay would have resulted in net erosion. This model did not consider new fluvial sediment input or re-deposition of old sediment during non-flooding periods. Calculations showed fine sediment erosion of a few centimeters for the entire Lavaca Bay, and deposition within the dredged-shipping channel, in Keller Bay and between Rhodes and Sand points. Their calculations were 0-2.4 cm of erosion within a water depth of 2.35 m for a category one hurricane within

Cox Bay. Our core data showed that instead of erosion of 0-2.4 cm, there was deposition of 2 cm (Figure 19), suggesting that sediment was deposited at the southern portion of Cox Bay. Flooding that occurred after the passing of the hurricane, brought sediment into the system from the drainage basin. Since Cox Bay is protected by Rhodes point it is expected that there should be less impact from the passing of hurricanes, due to the decrease of direct wind. Additionally, the post-hurricane Claudette sidescan lines showed a decrease in high backscatter to low backscatter, suggesting an increase of mud content. This, coupled with post-hurricane ground truthing, showed that the bay was primarily mud. Keller Bay data showed a similar amount of sediment deposition (2-3 cm), because it is protected by the Lavaca/Matagorda Peninsula and the bay also has a high sediment deposition during flooding events which derives from Keller Creek. The post X-radiograph for the southern SLB showed cross and wavy laminations, suggesting reworking of fine and coarse sediment by currents. The grainsize data showed erosion of 3 cm, since southern SLB does not have sediment input from a fluvial system it is believed the erosion is due to increase bi-directional currents that scour the seafloor during the recovery phase of the estuary.

When the Larm numerical model was extrapolated for all of Lavaca Bay, the models miscalculated the impact a category one hurricane verses a category four hurricane would have on sediment across the bay. Their model stated that there would be an increase of erosion during a category four hurricane, like Carla. In the NLB, there was only 0-5 cm of erosion, Larm's calculations, throughout the majority of the area.

Their calculations showed a category one hurricane would erode 0-5 cm, while a category four hurricane like Carla would erode 10.2 cm. Our data showed a net erosion of 10 cm from Hurricane Claudette, a category one hurricane, within the NLB area. Cox Bay is protected from direct meteorological forces by Rhodes point, while NLB is open and exposed to increased storm surge, wind, water currents, and terrestrial input, which would lead to an increase of erosion and sediment transportation. Other parts of the bay would have the same effects, but of the cores that were collected, only the NLB site showed intense erosion of the bay floor.

NLB was impacted by the hurricane more than the other bays because it is more exposed and also because it contains two large fluvial systems. The SLB is protected by Sand Point, and is less impacted than NLB. Cox and Keller were the least impacted, because they are sheltered and semi-enclosed systems. During wavy survey days, data were collected in Cox or Keller Bay, because the bays were calmer. Since Cox and Keller are protected from the increase of energy during hurricanes, it would require less time for sediment to settle out of the water column. Post-hurricane data were not obtained for the Central LB. Central LB would have had no protection from the increase of energy, and since CLB is exposed it probably had similar erosion as NLB.

CONCLUSIONS

The sidescan sonar, subbottom chirp and textural data found the bay to contain five sedimentary facies, they are: 1) estuarine mud (69.5%), 2) oyster biofacies (11.7%), 3) fluvial sand (10.0%), 4) beach sand (5.4%), and 5) bay mouth sand (3.4%). Most of the bay bottom consists primarily of estuarine mud, with shoals forming along the banks and becoming progressively sandier as the water depth decreases. Additionally, near the mouth of the bay there is an exposed relict flood tidal delta sand bed that contained shell fragments. Seismic data found there to be abundant oyster reef facies situated on bathymetric highs and ancient reef systems approximately two meters beneath the surficial sediment. Submerged reefs and geomorphology control the presence of the emergent reefs. The new oyster map delineated the oyster reefs from the mud deposits by representing light tones (high backscatter) and dark tones (low backscatter) respectively. The most noticeable change was the increase of low backscatter, interpreted as mud, within Cox Bay.

The sidescan sonar mosaic showed a difference between the pre-hurricane and post-hurricane survey lines that were obtained before and after the passing of Hurricane Claudette. Within the post-hurricane lines, there was an increase of low backscatter over previously high backscatter areas, suggesting that recent mud was deposited over an existing reef system. Within Cox Bay the pre-hurricane and post-hurricane sidescan lines showed the greatest difference. This difference probably resulted from either hurricane impacts or recent dredging. Surficial sediment grab and X-radiograph samples

were collected to verify the mosaic interpretation and the effects of Hurricane Claudette. Cores from sites C1NL1, and C9SL2 showed net erosion. This may have been due to increased currents, wave, tidal energies and fluvial sediment inputs from Hurricane Claudette. The NLB site was eroded by 10 cm while SLB was only eroded by 2-3 cm. The sites C8CB1 and C11KLB2 were areas of deposition of 2 cm and 2-3 cm, respectively. These cores also contain the record of other hurricane events with cores C1NL1 and C2NL2 containing the most complete record of hurricane impacts of the last century. Both of these cores contain thick sand lobes that probably resulted from the passing of hurricanes, such as the 1875 & 1886 hurricanes. These cores also contain a record of Hurricane Carla that correlated with the maximum ^{137}Cs depth.

Sedimentation rates were determined using ^{210}Pb and ^{137}Cs isotopes. When the maximum ^{137}Cs depths were present and the sand content within the cores were low, the comparison of the ^{210}Pb and ^{137}Cs rates were within 15% of each other. NLB contained the lowest accretion rates, while CLB and CXB were the highest. These higher rates could not be confirmed with the maximum ^{137}Cs depth, because ^{137}Cs was present at the base of the cores. Four cores showed little or no physical mixing in the surface interval, for the most part these were from sheltered locations. The six cores that exhibit physical mixing have a mixed layer of 10-15 cm. These cores were within the axis of the bay, in exposed locations. The physical mixing found within SLB, CLB, or CXB probably resulted from a combination of hurricane wind driven wave resuspension and anthropogenic impacts from shrimp trawling and oyster dredging.

REFERENCES

Bentley, S. J., Keen, T. R., Blain, C. A., & Vaughan, W. C., 2002. The origin and preservation of a major hurricane event in the northern Gulf of Mexico: Hurricane Camille, 1969. Marine Geology 186, 423-446.

Byrne, J. R., 1975. Holocene depositional history of Lavaca Bay, Central Texas Gulf Coast. Dissertation, The University of Texas, Austin.

Carr, J. T., Jr., 1967. The climate and physiography of Texas. Texas Water Development Board 53, 35.

Chmura, G. L., & Kosters, E. C., 1994. Storm deposition and ^{137}Cs accumulation in fine-grained marsh sediments of the Mississippi Delta plain. Estuarine, Coastal and Shelf Science 39, 33-44.

Collins, E. S., Scott, D. B., Gayes, P. T., 1999. Hurricane records on the South Carolina coast: Can they be detected in the sediment record? Quaternary International 56, 15-26.

Davis R. A., Jr., 1972. Beach changes, on the central Texas coast associated with Hurricane Fern, September, 1971. Contributions in Marine Science 16, 89-98.

Dellapenna, T. M., Kuehl, S. A., & Schaffner, L. C., 1998. Seabed mixing and particle residence times in biologically and physically dominated estuarine systems: A comparison of Lower Chesapeake Bay and the York River subestuary. Estuarine, Coastal and Shelf Science 46, 777-795.

Dellapenna, T. M., Kuehl, S. A., & Schaffner. L. C., 2003. Ephemeral deposition, seabed mixing and fine-scale strata formation in the York River estuary, Chesapeake Bay. Estuarine Coastal and Shelf Science 58, 621-643.

Folk, R. L., 1980. Petrology of sedimentary rocks, Hemphill Publishing Company, Austin, TX. pp.185.

Gill, G., Unpublished Data. One year of salinity concentrations for Lavaca Bay, Texas. Texas A&M University at Galveston, TX.

Hayes, M. O., 1965. Sedimentation on a semiarid, wave-dominated coast (South Texas) with emphasis on hurricane effects. Unpublished Dissertation, The University of Texas, Austin, pp. 350.

Hayes, M. O., 1967. Hurricanes as geological agents: Case studies of Hurricanes Carla, 1961, and Cindy, 1963. Bureau Economic Geology Report of Investigations 61, The University of Texas, Austin.

Hayes, M. O., 1978. Impacts of hurricanes on sedimentation in estuaries, bays, and lagoons. In: Wiley, M.L. (ed.), Estuarine Interactions, Academic Press, NY pp. 323-346.

Hjulstrom, F., 1939. Transportation of detritus by moving water. In: Trask, P.D. (ed.), Recent Marine Sediments, a Symposium. American Association of Petroleum Geologists, Tulsa, OK. pp. 5-31.

Larm, K., 1998. Study of sediment resuspension due to Hurricane Carla in Lavaca Bay, Texas. Thesis, Texas A&M University, College Station.

Larm, K., & Edge, B., 1998. Sediment resuspension in hurricane conditions. Environmental Coastal Regions 1, 417-426.

McGowen, J. H., & Scott, A. J., 1975. Hurricanes as geologic agents on the Texas coast. In: Cronin, L.E. (Ed.), Estuarine Resources II., Geological and Engineering, Academic Press, NY. pp. 23-46.

Moore, H. F., & Danglade, E., 1914. Condition and extent of the natural oyster beds and barren bottoms of Lavaca Bay, Texas. Department of Commerce, Bureau of Fisheries, Washington, D.C. pp 5-45

Morton, R. A., Gibeaut, J. C., & Paine, J. G., 1995. Meso-scale transfer of sand during and after storms: Implications for prediction of shoreline movement. Marine Geology 126, 161-179.

National Oceanic and Atmospheric Administration (NOAA), United States Department of Commerce, 2004, http://www.noaa.gov.

Nichols, M. M., 1984. Effects of fine sediment resuspension in estuaries. In: Mehta, A. (ed.), Estuarine Cohesive Sediment Dynamics., Lecture Notes on Coastal and Estuarine Studies, Springer-Verlag, Berlin. 5-42.

Nichols, M. M., Johnson, G. H., & Peebles, P. C., 1991. Modern sediments and facies model for a microtidal coastal plain estuary, the James Estuary, Virginia. Journal of Sedimentary Petrology 61, 883-899.

Nichols, M. M., 1993. Response of coastal plain estuaries to episodic events in the Chesapeake Bay region. Mehta (ed.), Nearshore and Estuarine Cohesive Sediment Transport, Coastal and Estuarine Studies, American Geophysical Union, Washington, D.C. pp 1-20.

Nittrouer, C. A., Sternberg, R. W., Carpenter, R., & Bennett, J. T., 1979. The use of Pb-210 geochronology as a sedimentological tool: Application to the Washington continental shelf. Marine Geology 31, 297-316.

Nittrouer, C. A., & Sternberg, R. W., 1981. The formation of sedimentary strata in an allochthonous shelf environment: The Washington continental shelf. Marine Geology 42, 201-232.

Pennington, W., Cambray, R. S., & Fisher, E. M., 1973. Observations on lake sediments using fallout ^{137}Cs as a tracer. Nature 242, 324-326.

Ravichandran, M., Baskaran, M., Santschi, P. H., & Bianchi, T. S., 1995. Geochronology of sediments in the Sabine-Neches estuary, Texas, U.S.A. Chemical Geology 125, 291-306.

Rejmanek, M., Sasser, C. E., & Peterson, G. W., 1988. Hurricane-induced sediment deposition in a gulf coast marsh. Estuarine, Coastal and Shelf Science 27, 217-222.

Roberts, H. H., Wilson, C., & Supan, J., 2000. Acoustic Surveying of Ultra-Shallow Water Bottoms (<2.0 m) for both Engineering, and Environments Applications. Offshore Technology Conference, TX. 12108.

Santschi, P. H., Li, Y. H., Bell, J. J., Trier, R. M., & Kawtaluk, K., 1980. Pu In Coastal Marine Environments. Earth and Planetary Science Letters 51**,** 248-265.

Santschi, P. H., Allison, M. A., Asbill, S., Perlet, B., Cappellino, S., Dobbs, C., & Mcshea, L., 1999. Sediment transport and Hg recovery in Lavaca Bay, as evaluated from radionuclide and Hg distributions. Environmental Science Technology 33, 378-391.

Schubel, J.R., 1974. Effects of tropical storm Agnes on the suspended solids of northern Chesapeake Bay. In: Gibbs, R. (ed.), Suspended Solids in Water., Plenum Marine Science, Plenum Press, NY, pp. 113-132.

Shepard. F. P., 1954. Nomenclature based on sand-silt-clay ratios. Journal of Sedimentary Petrology 24, 151-158.

Weather Research Center (WRC), 2001 Texas tropical storms & hurricanes. Http://www.wxresearch.org/family/thurlist.htm Houston, Texas.

APPENDIX A

GRAIN SIZE / POROSITY DATA

Grainsize and Porosity Data for Dive Cores taken in Lavaca, Keller and Cox Bay.

Lavaca Bay Sample C1NL1

(Latitude: 28d 40.524') (Longitude: 96d 36.929')

Core Depth	% Mud	% Sand	% Silt	% Clay	% Porosity
0-1 cm	90.15	9.85	25.20	64.94	85.1
1-2 cm	92.71	7.29	24.48	68.23	83.1
2-3 cm	89.97	10.03	26.52	63.46	81.1
3-4 cm	90.24	9.76	26.92	63.32	81.0
4-5 cm	88.48	11.52	27.02	61.46	80.6
5-6 cm	88.30	11.70	26.76	61.54	79.9
6-7 cm	87.34	12.66	24.38	62.96	80.2
7-8 cm	86.75	13.25	21.45	65.30	79.2
8-9 cm	88.03	11.97	23.45	64.58	79.2
9-10 cm	86.13	13.87	25.85	60.27	78.6
11-12 cm	88.68	11.32	24.67	64.01	79.0
13-14 cm	92.42	7.58	26.76	65.66	79.8
15-16 cm	94.24	5.76	23.39	70.85	81.3
17-18 cm	91.14	8.86	18.47	72.68	81.5
19-20 cm	92.85	7.15	19.88	72.97	80.5
21-22 cm	86.38	13.62	48.90	37.48	73.0
23-24 cm	68.04	31.96	16.29	51.76	72.4
25-26 cm	79.13	20.87	18.04	61.09	75.8
27-28 cm	76.89	23.11	16.56	60.33	76.2
29-30 cm	76.33	23.67	14.78	61.55	74.8
31-32 cm	83.55	16.45	20.36	63.19	76.0
33-34 cm	83.34	16.66	19.26	64.08	77.2
35-36 cm	80.91	19.09	15.14	65.77	76.9
37-38 cm	88.47	11.53	20.41	68.07	77.3
39-40 cm	43.63	56.37	10.46	33.17	66.3
41-42 cm	32.64	67.36	8.28	24.36	61.5
43-44 cm	37.79	62.21	10.46	27.32	63.1
45-46 cm	36.75	63.25	10.37	26.38	63.3
47-48 cm	41.54	58.46	12.39	29.15	63.3
49-50 cm	51.44	48.56	14.13	37.31	66.6
55-56 cm	63.61	36.39	14.57	49.04	72.9
59-60 cm	89.99	10.01	15.53	74.47	77.2
64-65 cm	91.70	8.30	16.85	74.86	76.8
69-70 cm	97.40	2.60	13.52	83.88	79.2

Lavaca Bay Sample C2NL2

(Latitude: 28d 41.770') (Longitude: 96d 38.062')

Core Depth	% Mud	% Sand	% Silt	% Clay	% Porosity
0-1 cm	74.20	25.80	28.56	45.65	80.3
1-2 cm	78.82	21.18	29.08	49.74	80.0
2-3 cm	81.21	18.79	32.22	48.99	79.8
3-4 cm	67.86	32.14	28.16	39.70	75.5
4-5 cm	71.95	28.05	44.91	27.04	74.3
5-6 cm	63.03	36.97	26.39	36.64	73.1
6-7 cm	59.67	40.33	25.56	34.11	71.9
7-8 cm	61.85	38.15	23.97	37.88	72.6
8-9 cm	63.50	36.50	24.45	39.05	72.7
9-10 cm	64.64	35.36	24.35	40.29	73.1
11-12 cm	68.77	31.23	23.80	44.97	74.2
13-14 cm	75.83	24.17	26.98	48.84	75.0
15-16 cm	72.94	27.06	27.38	45.56	72.8
17-18 cm	71.44	28.56	27.69	43.75	71.5
19-20 cm	70.80	29.20	25.64	45.16	71.7
21-22 cm	83.00	17.00	24.50	58.50	76.4
23-24 cm	86.43	13.57	26.58	59.85	76.7
25-26 cm	85.93	14.07	28.04	57.89	75.7
27-28 cm	84.84	15.16	30.09	54.75	74.6
29-30 cm	83.57	16.43	26.08	57.49	75.9
31-32 cm	79.88	20.12	26.73	53.15	75.5
33-34 cm	78.01	21.99	28.75	49.26	74.0
35-36 cm	70.52	29.48	28.98	41.54	72.0
37-38 cm	62.82	37.18	24.35	38.47	70.4
39-40 cm	62.42	37.58	23.70	38.72	69.9
41-42 cm	63.60	36.40	24.31	39.28	69.9
43-44 cm	63.68	36.32	24.40	39.28	70.1
45-46 cm	55.20	44.80	22.33	32.87	66.9
47-48 cm	54.48	45.52	21.84	32.64	66.9
49-50 cm	59.06	40.94	24.83	34.23	68.0
55-56 cm	41.51	58.49	21.23	20.28	59.2
59-60 cm	38.98	61.02	19.94	19.04	58.6
64-65 cm	45.20	54.80	21.15	24.05	59.3
69-70 cm	50.64	49.36	23.16	27.48	58.8

Lavaca Bay Sample C3NL3

(Latitude: 28d 42.291') (Longitude: 96d 36.151')

Core Depth	% Mud	% Sand	% Silt	% Clay	% Porosity
0-1 cm	46.72	53.28	17.21	29.51	73.4
1-2 cm	44.70	55.30	19.06	25.64	67.8
2-3 cm	41.98	58.02	19.37	22.61	63.8
3-4 cm	40.80	59.20	19.68	21.11	61.5
4-5 cm	42.03	57.97	19.29	22.75	61.7
5-6 cm	41.90	58.10	16.77	25.13	60.0
6-7 cm	43.61	56.39	18.11	25.51	64.0
7-8 cm	50.59	49.41	19.66	30.93	65.7
8-9 cm	48.20	51.80	18.60	29.59	67.8
9-10 cm	49.04	50.96	18.66	30.39	63.9
11-12 cm	55.17	44.83	19.75	35.42	68.8
13-14 cm	49.80	50.20	19.67	30.13	63.8
15-16 cm	47.80	52.20	18.24	29.56	64.4
17-18 cm	44.09	55.91	17.85	26.24	62.2
19-20 cm	43.72	56.28	16.89	26.83	62.7
21-22 cm	33.66	66.34	15.37	18.29	57.4
23-24 cm	33.64	66.36	14.22	19.42	56.1
25-26 cm	40.32	59.68	16.22	24.10	58.1
27-28 cm	40.45	59.55	15.02	25.43	62.9
29-30 cm	54.47	45.53	18.70	35.77	67.3
31-32 cm	59.73	40.27	18.12	41.61	67.6
33-34 cm	58.24	41.76	18.70	39.54	67.8
35-36 cm	55.88	44.12	19.65	36.22	66.1
37-38 cm	67.66	32.34	19.58	48.08	71.7
39-40 cm	60.33	39.67	22.62	37.71	66.9
41-42 cm	54.89	45.11	22.19	32.70	64.6
43-44 cm	56.47	43.53	21.73	34.74	65.6
45-46 cm	56.89	43.11	22.34	34.55	65.4
47-48 cm	58.78	41.22	22.12	36.66	65.1
49-50 cm	61.03	38.97	24.11	36.92	67.6
55-56 cm	65.54	34.46	23.53	42.02	69.2

Lavaca Bay Sample C4BL1

(Latitude: 28d 37.948') (Longitude: 96d 36.338')

Core Depth	% Mud	% Sand	% Silt	% Clay	% Porosity
0-1 cm	53.49	46.51	22.02	31.48	75.6
1-2 cm	31.34	68.66	14.45	16.88	64.0
2-3 cm	18.52	81.48	7.98	10.54	52.9
3-4 cm	12.02	87.98	5.15	6.87	43.8
4-5 cm	11.22	88.78	5.15	6.07	44.8
5-6 cm	7.74	92.26	4.50	3.24	40.8
6-7 cm	7.79	92.21	4.57	3.22	39.9
7-8 cm	13.12	86.88	7.30	5.82	40.6
8-9 cm	9.37	90.63	4.73	4.64	45.0
9-10 cm	11.51	88.49	4.34	7.17	45.9
11-12 cm	10.52	89.48	5.32	5.21	41.9
13-14 cm	10.93	89.07	5.01	5.91	42.4
15-16 cm	14.60	85.40	7.68	6.92	42.8
17-18 cm	11.71	88.29	6.17	5.54	42.5
19-20 cm	17.26	82.74	9.83	7.43	43.7
21-22 cm	14.47	85.53	7.03	7.44	43.0
23-24 cm	14.79	85.21	7.09	7.69	41.4
25-26 cm	11.92	88.08	5.50	6.42	41.4
27-28 cm	17.80	82.20	6.88	10.92	44.6
29-30 cm	18.13	81.87	7.19	10.94	46.5
31-32 cm	23.44	76.56	8.78	14.66	47.0
33-34 cm	19.65	80.35	7.77	11.88	42.9
35-36 cm	17.60	82.40	6.73	10.87	43.4
37-38 cm	17.09	82.91	6.76	10.32	42.6
39-40 cm	16.33	83.67	5.82	10.52	46.0
41-42 cm	17.57	82.43	6.27	11.30	48.1

Lavaca Bay Sample C5CL1

(Latitude: 28d 36.953') (Longitude: 96d 34.862')

Core Depth	% Mud	% Sand	% Silt	% Clay	% Porosity
0-1 cm	92.26	7.74	30.56	61.70	86.3
1-2 cm	94.10	5.90	33.88	60.21	84.8
2-3 cm	94.35	5.65	32.32	62.03	84.3
3-4 cm	94.23	5.77	31.34	62.88	83.5
4-5 cm	94.03	5.97	28.98	65.05	83.2
5-6 cm	94.49	5.51	28.09	66.40	83.6
6-7 cm	95.58	4.42	28.48	67.10	83.4
7-8 cm	95.39	4.61	26.99	68.40	83.3
8-9 cm	95.83	4.17	25.06	70.78	82.8
9-10 cm	95.34	4.66	26.15	69.19	82.4
11-12 cm	91.50	8.50	28.77	62.73	80.4
13-14 cm	89.31	10.69	26.19	63.13	78.7
15-16 cm	93.56	6.44	27.93	65.63	79.1
17-18 cm	95.86	4.14	22.87	72.99	79.1
19-20 cm	94.91	5.09	24.62	70.29	79.8
21-22 cm	97.84	2.16	24.00	73.84	79.3
23-24 cm	97.86	2.14	31.39	66.48	77.1
25-26 cm	97.23	2.77	25.58	71.65	78.7
27-28 cm	97.02	2.98	32.28	64.74	76.5
29-30 cm	94.03	5.97	27.63	66.40	76.7
31-32 cm	94.15	5.85	25.95	68.20	76.8
33-34 cm	88.42	11.58	28.14	60.27	75.6
35-36 cm	87.76	12.24	28.20	59.57	74.8
37-38 cm	94.38	5.62	25.92	68.45	77.6
39-40 cm	95.47	4.53	24.27	71.20	78.4
41-42 cm	97.34	2.66	20.23	77.11	79.2
43-44 cm	97.55	2.45	21.13	76.43	78.8
45-46 cm	94.58	5.42	24.59	69.98	78.9

Lavaca Bay Sample C6WL1

(Latitude: 28d 35.636') (Longitude: 96d 35.263')

Core Depth	% Mud	% Sand	% Silt	% Clay	% Porosity
0-1 cm	99.30	0.70	22.62	76.68	87.8
1-2 cm	99.56	0.44	22.20	77.36	85.9
2-3 cm	99.47	0.53	21.72	77.75	85.2
3-4 cm	99.66	0.34	22.37	77.28	85.3
4-5 cm	99.72	0.28	20.24	79.48	85.3
5-6 cm	99.70	0.30	21.80	77.89	84.9
6-7 cm	99.72	0.28	20.24	79.48	85.2
7-8 cm	99.53	0.47	20.22	79.31	85.3
8-9 cm	98.80	1.20	23.39	75.41	85.2
9-10 cm	98.75	1.25	25.46	73.29	85.2
11-12 cm	98.05	1.95	21.57	76.48	85.4
13-14 cm	96.48	3.52	25.91	70.56	84.9
15-16 cm	96.70	3.30	25.95	70.75	84.2
17-18 cm	83.71	16.29	22.12	61.60	83.6
19-20 cm	94.53	5.47	22.14	72.39	83.1
21-22 cm	95.54	4.46	20.83	74.70	82.5
23-24 cm	98.13	1.87	16.52	81.60	83.4
25-26 cm	98.27	1.73	16.03	82.25	83.0
27-28 cm	97.98	2.02	15.96	82.03	82.3
29-30 cm	97.55	2.45	16.94	80.62	81.5
31-32 cm	99.15	0.85	19.24	79.91	81.3
33-34 cm	98.73	1.27	24.28	74.46	81.0
35-36 cm	97.12	2.88	26.93	70.20	79.6
37-38 cm	95.37	4.63	25.35	70.02	79.5
39-40 cm	96.73	3.27	21.78	74.95	80.2
41-42 cm	94.99	5.01	27.59	67.40	79.5
43-44 cm	97.99	2.01	25.24	72.75	79.9
45-46 cm	98.17	1.83	30.46	67.72	78.8
47-48 cm	98.66	1.34	25.77	72.89	80.5
49-50 cm	99.25	0.75	19.17	80.08	81.3

Lavaca Bay Sample C7SL1

(Latitude: 28d 34.478') (Longitude: 96d 32.968')

Core Depth	% Mud	% Sand	% Silt	% Clay	% Porosity
0-1 cm	81.19	18.81	27.22	53.97	86.7
1-2 cm	83.58	16.42	26.73	56.85	84.9
2-3 cm	75.11	24.89	24.49	50.62	83.0
3-4 cm	76.30	23.70	22.03	54.27	82.7
4-5 cm	74.07	25.93	25.20	48.87	81.5
5-6 cm	69.75	30.25	22.83	46.92	80.3
6-7 cm	71.34	28.66	24.20	47.14	80.6
7-8 cm	73.25	26.75	23.48	49.77	81.1
8-9 cm	73.28	26.72	22.22	51.06	80.7
9-10 cm	71.27	28.73	23.47	47.80	79.6
11-12 cm	74.87	25.13	20.37	54.49	79.9
13-14 cm	75.98	24.02	20.34	55.64	79.5
15-16 cm	72.06	27.94	20.33	51.73	77.0
17-18 cm	70.64	29.36	19.74	50.90	77.5
19-20 cm	70.01	29.99	17.84	52.16	77.0
21-22 cm	70.08	29.92	15.43	54.65	77.0
23-24 cm	71.99	28.01	15.63	56.36	78.0
25-26 cm	73.46	26.54	16.70	56.77	77.7
27-28 cm	71.59	28.41	14.48	57.11	76.3
29-30 cm	70.00	30.00	13.51	56.50	76.1
31-32 cm	68.71	31.29	16.28	52.44	74.0
33-34 cm	70.91	29.09	16.91	54.00	75.4
35-36 cm	58.23	41.77	12.44	45.79	72.6

Lavaca Bay Sample C8CB1

(Latitude: 28d 37.307') (Longitude: 96d 32.373')

Core Depth	% Mud	% Sand	% Silt	% Clay	% Porosity
0-1 cm	97.05	2.95	20.21	76.83	88.7
1-2 cm	96.41	3.59	24.59	71.82	86.2
2-3 cm	95.00	5.00	27.43	67.56	84.2
3-4 cm	91.68	8.32	24.83	66.86	83.7
4-5 cm	92.65	7.35	23.90	68.75	83.1
5-6 cm	93.48	6.52	24.93	68.55	83.2
6-7 cm	93.93	6.07	25.45	68.48	82.6
7-8 cm	94.58	5.42	23.75	70.84	82.6
8-9 cm	94.04	5.96	23.59	70.45	82.0
9-10 cm	93.91	6.09	21.51	72.40	81.8
11-12 cm	93.42	6.58	23.45	69.97	81.4
13-14 cm	84.73	15.27	21.00	63.73	79.0
15-16 cm	90.88	9.12	25.58	65.31	79.0
17-18 cm	93.19	6.81	25.58	67.60	79.0
19-20 cm	94.03	5.97	24.01	70.02	80.2
21-22 cm	88.02	11.98	25.83	62.18	78.2
23-24 cm	83.31	16.69	25.50	57.81	76.8
25-26 cm	88.61	11.39	25.66	62.95	78.6
27-28 cm	81.77	18.23	23.45	58.32	75.9
29-30 cm	80.81	19.19	24.95	55.86	74.7
31-32 cm	78.82	21.18	22.72	56.10	73.6
33-34 cm	80.38	19.62	24.96	55.43	74.2
35-36 cm	76.51	23.49	22.45	54.06	72.5
37-38 cm	77.67	22.33	14.03	63.64	72.2
39-40 cm	75.68	24.32	20.91	54.78	71.8
41-42 cm	71.92	28.08	18.29	53.63	70.4
43-44 cm	73.70	26.30	22.28	51.42	71.2
45-46 cm	68.38	31.62	20.13	48.24	68.9
47-48 cm	73.38	26.62	19.79	53.59	71.3
49-50 cm	75.20	24.80	21.10	54.10	70.2

Lavaca Bay Sample C9SL2

(Latitude: 28d 35.446') (Longitude: 96d 30.116')

Core Depth	% Mud	% Sand	% Silt	% Clay	% Porosity
0-1 cm	79.61	20.39	24.99	54.61	82.8
1-2 cm	84.00	16.00	30.50	53.50	81.2
2-3 cm	83.96	16.04	28.14	55.82	81.2
3-4 cm	84.65	15.35	29.06	55.59	80.9
4-5 cm	86.60	13.40	29.37	57.22	80.7
5-6 cm	87.48	12.52	28.68	58.80	80.2
6-7 cm	85.52	14.48	28.50	57.03	79.7
7-8 cm	85.52	14.48	30.08	55.45	79.7
8-9 cm	84.73	15.27	29.65	55.08	78.4
9-10 cm	84.62	15.38	31.39	53.23	78.3
11-12 cm	86.05	13.95	31.00	55.05	78.7
13-14 cm	81.01	18.99	30.62	50.38	77.3
15-16 cm	79.96	20.04	29.23	50.72	75.9
17-18 cm	77.58	22.42	29.32	48.26	73.9
19-20 cm	81.92	18.08	28.60	53.32	73.5
21-22 cm	83.01	16.99	30.31	52.70	71.5
23-24 cm	81.06	18.94	28.97	52.09	70.1
25-26 cm	71.44	28.56	29.06	42.38	70.0
27-28 cm	75.64	24.36	28.48	47.17	70.4
29-30 cm	78.54	21.46	28.45	50.09	70.3
31-32 cm	77.30	22.70	25.66	51.64	71.2
33-34 cm	77.85	22.15	25.29	52.56	74.3
35-36 cm	74.41	25.59	22.63	51.78	74.1
37-38 cm	66.74	33.26	20.41	46.33	69.7
39-40 cm	68.27	31.73	18.00	50.27	67.5
41-42 cm	59.07	40.93	16.36	42.71	61.8
43-44 cm	57.32	42.68	13.55	43.76	65.3
45-46 cm	51.15	48.85	14.39	36.76	60.7
47-48 cm	47.44	52.56	13.99	33.44	57.5
49-50 cm	39.07	60.93	11.56	27.51	56.1

Keller Bay Sample C10KLB1

(Latitude: 28d 36.007') (Longitude: 96d 27.355')

Core Depth	% Mud	% Sand	% Silt	% Clay	% Porosity
0-1 cm	90.58	9.42	50.17	40.41	80.1
1-2 cm	90.45	9.55	55.16	35.29	76.6
2-3 cm	88.11	11.89	61.42	26.69	71.9
3-4 cm	89.48	10.52	59.82	29.65	70.3
4-5 cm	90.58	9.42	57.74	32.84	70.3
5-6 cm	89.78	10.22	54.19	35.59	70.9
6-7 cm	90.70	9.30	53.19	37.50	71.3
7-8 cm	91.07	8.93	48.48	42.59	71.0
8-9 cm	90.74	9.26	52.17	38.56	72.0
9-10 cm	91.63	8.37	51.98	39.64	70.4
11-12 cm	86.33	13.67	47.75	38.59	67.7
13-14 cm	91.33	8.67	46.04	45.28	68.3
15-16 cm	90.91	9.09	52.45	38.46	67.2
17-18 cm	89.47	10.53	54.03	35.45	66.7
19-20 cm	87.98	12.02	56.57	31.41	61.9
21-22 cm	84.28	15.72	57.37	26.91	58.8
23-24 cm	79.29	20.71	56.31	22.98	57.6
25-26 cm	83.95	16.05	58.39	25.56	56.0
27-28 cm	84.45	15.55	57.65	26.80	54.8
29-30 cm	81.54	18.46	54.74	26.80	53.2
31-32 cm	84.17	15.83	60.19	23.98	70.6
33-34 cm	81.68	18.32	56.72	24.96	22.0
35-36 cm	81.46	18.54	58.96	22.51	53.7
37-38 cm	80.70	19.30	58.57	22.14	53.2
39-40 cm	73.80	26.20	55.91	17.89	50.6
41-42 cm	76.28	23.72	58.13	18.16	52.7
43-44 cm	73.48	26.52	56.26	17.22	50.8
45-46 cm	75.32	24.68	57.75	17.57	49.5
47-48 cm	73.50	26.50	56.44	17.05	49.1
49-50 cm	73.77	26.23	57.73	16.04	51.5

Keller Bay Sample C11KLB2

(Latitude: 28d 36.007') (Longitude: 96d 27.355')

Core Depth	% Mud	% Sand	% Silt	% Clay	% Porosity
0-1 cm	83.85	16.15	27.78	56.06	87.3
1-2 cm	87.02	12.98	33.77	53.26	86.3
2-3 cm	90.25	9.75	43.94	46.31	85.6
3-4 cm	87.04	12.96	29.25	57.79	85.2
4-5 cm	84.70	15.30	28.06	56.64	83.7
5-6 cm	84.62	15.38	28.30	56.32	82.6
6-7 cm	83.32	16.68	24.72	58.60	82.3
7-8 cm	83.84	16.16	24.68	59.16	82.0
8-9 cm	83.62	16.38	26.91	56.71	80.6
9-10 cm	80.43	19.57	26.79	53.63	80.1
11-12 cm	79.80	20.20	30.73	49.07	77.6
13-14 cm	81.05	18.95	30.32	50.72	76.4
15-16 cm	83.65	16.35	30.78	52.87	75.8
17-18 cm	86.36	13.64	28.14	58.22	75.4
19-20 cm	89.04	10.96	28.42	60.62	75.9
21-22 cm	85.25	14.75	42.79	42.46	69.6
23-24 cm	66.45	33.55	33.16	33.29	66.8
25-26 cm	64.89	35.11	29.09	35.80	68.3
27-28 cm	61.68	38.32	29.09	32.60	67.0
29-30 cm	61.97	38.03	27.49	34.48	65.4
31-32 cm	67.05	32.95	28.23	38.82	64.3
33-34 cm	68.59	31.41	28.39	40.20	64.3
35-36 cm	68.58	31.42	28.59	39.99	63.9
37-38 cm	70.59	29.41	29.01	41.58	66.6
39-40 cm	75.20	24.80	33.31	41.89	68.5
41-42 cm	70.63	29.37	31.47	39.15	68.4
43-44 cm	71.39	28.61	34.89	36.50	68.7
45-46 cm	59.21	40.79	31.41	27.80	64.7
47-48 cm	75.76	24.24	36.13	39.62	70.5
49-50 cm	73.93	26.07	30.78	43.15	73.1

Post Hurricane Lavaca Bay Sample C12NL4

(Latitude: 28d 40.524') (Longitude: 96d 36.929')

Core Depth	% Mud	% Sand	% Silt	% Clay	% Porosity
0-1 cm	74.56	25.44	32.26	42.30	79.2
1-2 cm	83.68	16.32	27.79	55.89	79.7
2-3 cm	87.38	12.62	23.16	64.22	83.4
3-4 cm	86.68	13.32	25.86	60.82	80.5
4-5 cm	85.87	14.13	-9.04	94.91	79.8
5-6 cm	84.58	15.42	27.16	57.43	79.7
6-7 cm	82.47	17.53	22.10	60.37	78.8
7-8 cm	79.04	20.96	21.69	57.35	79.3
8-9 cm	82.55	17.45	20.86	61.68	78.8
9-10 cm	82.47	17.53	20.61	61.87	79.3
11-12 cm	76.86	23.14	21.20	55.66	77.2
13-14 cm	62.17	37.83	14.50	47.67	75.9
15-16 cm	77.86	22.14	19.39	58.48	76.2
17-18 cm	89.48	10.52	16.59	72.89	79.3
19-20 cm	91.78	8.22	24.32	67.46	78.8
21-22 cm	92.48	7.52	20.75	71.73	78.2
23-24 cm	87.27	12.73	16.25	71.02	78.6
25-26 cm	82.10	17.90	18.98	63.13	78.1
27-28 cm	73.30	26.70	21.58	51.72	75.1
29-30 cm	69.15	30.85	17.95	51.21	76.4
31-32 cm	62.15	37.85	15.80	46.35	74.6
33-34 cm	44.79	55.21	12.42	32.37	64.3
35-36 cm	42.72	57.28	12.10	30.62	62.7
37-38 cm	42.47	57.53	12.88	29.60	65.8
39-40 cm	42.31	57.69	14.95	27.36	64.4
41-42 cm	48.91	51.09	17.76	31.15	66.9
43-44 cm	27.03	72.97	9.04	17.98	56.6
45-46 cm	26.36	73.64	9.08	17.28	60.6
47-48 cm	45.84	54.16	13.89	31.95	69.4
49-50 cm	46.41	53.59	14.24	32.17	69.0
54-55 cm	54.10	45.90	13.84	40.27	71.5
59-60 cm	77.81	22.19	16.96	60.85	74.7
64-65 cm	75.72	24.28	72.32	3.40	75.3
69-70 cm	87.06	12.94	11.75	75.30	77.1
74-75 cm	91.66	8.34	15.84	75.82	78.1
79-80 cm	93.63	6.37	11.66	81.97	78.5
84-85 cm	87.10	12.90	11.56	75.55	76.8
89-90 cm	94.14	5.86	15.66	78.47	76.5

Post Hurricane Lavaca Bay Sample C13CB2

(Latitude: 28d 37.307') (Longitude: 96d 32.373')

Core Depth	% Mud	% Sand	% Silt	% Clay	% Porosity
0-1 cm	97.67	2.33	30.51	67.16	85.9
1-2 cm	96.71	3.29	33.87	62.84	80.4
2-3 cm	95.02	4.98	39.33	55.69	82.8
3-4 cm	94.35	5.65	35.74	58.60	85.6
4-5 cm	96.59	3.41	31.47	65.12	84.0
5-6 cm	96.52	3.48	33.19	63.33	86.4
6-7 cm	93.83	6.17	35.03	58.80	83.3
7-8 cm	93.90	6.10	29.27	64.64	84.4
8-9 cm	92.96	7.04	26.16	66.80	82.2
9-10 cm	91.52	8.48	30.86	60.66	81.1
11-12 cm	92.17	7.83	31.09	61.09	78.3
13-14 cm	84.30	15.70	25.78	58.52	78.3
15-16 cm	79.47	20.53	26.47	53.00	76.9
17-18 cm	84.95	15.05	24.42	60.53	76.6
19-20 cm	76.21	23.79	21.85	54.36	75.2
21-22 cm	83.50	16.50	29.21	54.30	76.2
23-24 cm	85.04	14.96	28.60	56.44	75.5
25-26 cm	83.34	16.66	28.38	54.97	74.7
27-28 cm	86.30	13.70	30.46	55.84	71.7
29-30 cm	79.56	20.44	27.19	52.36	73.6
31-32 cm	87.01	12.99	26.80	60.21	73.6
33-34 cm	87.31	12.69	27.40	59.91	75.7
35-36 cm	91.39	8.61	30.06	61.33	74.2
37-38 cm	92.78	7.22	32.54	60.24	79.0
39-40 cm	92.42	7.58	24.09	68.33	79.9
41-42 cm	86.21	13.79	22.40	63.81	76.3
43-44 cm	67.20	32.80	29.71	37.49	63.7
45-46 cm	72.71	27.29	28.96	43.75	70.3
47-48 cm	57.67	42.33	23.55	34.12	65.3

Post Hurricane Keller Bay Sample C14KLB3

(Latitude: 28d 36.007') (Longitude: 96d 27.355')

Core Depth	% Mud	% Sand	% Silt	% Clay	% Porosity
0-1 cm	83.98	16.02	25.07	58.91	83.4
1-2 cm	90.42	9.58	49.72	40.69	81.1
2-3 cm	84.04	15.96	28.22	55.83	82.8
3-4 cm	84.89	15.11	26.14	58.75	82.5
4-5 cm	84.46	15.54	34.49	49.96	81.1
5-6 cm	82.38	17.62	31.28	51.10	80.4
6-7 cm	82.73	17.27	28.22	54.52	81.1
7-8 cm	81.42	18.58	27.75	53.67	79.0
8-9 cm	80.90	19.10	30.76	50.14	78.6
9-10 cm	83.04	16.96	28.80	54.24	80.2
11-12 cm	78.53	21.47	24.08	54.45	74.5
13-14 cm	81.72	18.28	27.11	54.60	78.0
15-16 cm	80.67	19.33	27.09	53.58	75.6
17-18 cm	82.75	17.25	25.34	57.40	74.7
19-20 cm	87.60	12.40	24.78	62.81	74.7
21-22 cm	84.66	15.34	25.37	59.28	76.2
23-24 cm	77.64	22.36	27.61	50.03	65.7
25-26 cm	66.93	33.07	30.95	35.99	65.9
27-28 cm	67.77	32.23	28.61	39.16	71.9
29-30 cm	62.34	37.66	25.44	36.90	63.9
31-32 cm	67.49	32.51	31.58	35.91	64.9
33-34 cm	67.65	32.35	29.05	38.61	57.4
35-36 cm	52.44	47.56	22.39	30.05	63.0
37-38 cm	61.95	38.05	22.92	39.03	64.2
39-40 cm	59.28	40.72	28.26	31.02	59.1
41-42 cm	65.96	34.04	29.13	36.83	59.7
43-44 cm	52.64	47.36	22.38	30.25	62.2
45-46 cm	60.92	39.08	25.69	35.23	61.6

Post Hurricane Lavaca Bay Sample C15SL3

(Latitude: 28d 35.446') (Longitude: 96d 30.116')

Core Depth	% Mud	% Sand	% Silt	% Clay	% Porosity
0-1 cm	79.43	20.57	23.52	55.91	79.2
1-2 cm	83.26	16.74	25.36	57.90	75.9
2-3 cm	82.51	17.49	29.45	53.07	80.0
3-4 cm	82.88	17.12	28.20	54.68	78.9
4-5 cm	80.43	19.57	27.18	53.25	79.9
5-6 cm	87.81	12.19	25.84	61.98	84.4
6-7 cm	92.09	7.91	25.47	66.63	82.7
7-8 cm	78.42	21.58	28.16	50.26	76.1
8-9 cm	75.74	24.26	52.66	23.07	72.9
9-10 cm	84.18	15.82	24.39	59.79	74.7
11-12 cm	84.28	15.72	30.51	53.77	77.2
13-14 cm	82.83	17.17	29.25	53.58	77.1
15-16 cm	83.69	16.31	19.95	103.64	76.9
17-18 cm	80.58	19.42	26.46	54.12	76.9
19-20 cm	83.27	16.73	29.85	53.42	79.4
21-22 cm	86.43	13.57	32.65	53.78	79.5
23-24 cm	76.08	23.92	31.90	44.18	76.0
25-26 cm	85.72	14.28	32.76	52.95	77.6
27-28 cm	88.25	11.75	32.89	55.36	77.9
29-30 cm	85.59	14.41	31.57	54.02	78.6
31-32 cm	92.83	7.17	30.31	62.53	78.2
33-34 cm	93.60	6.40	30.71	62.89	81.4
35-36 cm	77.58	22.42	26.08	51.50	77.5
37-38 cm	80.79	19.21	27.80	52.99	73.7
39-40 cm	71.48	28.52	25.79	45.69	71.8

Surficial Sediment Grab Samples

Core Number	Latitude	Longitude	% Mud	% Sand	% Silt	% Clay
G1	28d 39.302'	96d 36.236'	31.68	68.32	13.80	17.89
G2	28d 40.973'	96d 37.602'	64.80	35.20	22.94	41.86
G3	28d 42.303'	96d 35.821'	59.03	40.97	24.85	34.18
G4	28d 38.861'	96d 35.169'	82.10	17.90	23.58	58.52
G5	28d 37.201'	96d 36.440'	53.75	46.25	30.21	23.55
G6	28d 36.027'	96d 32.308'	5.35	94.65	1.24	4.11
G7	28d 36.529'	96d 36.882'	95.99	4.01	35.34	60.65
G8	28d 40.794'	96d 34.932'	22.29	77.71	11.88	10.41
G9	28d 37.584'	96d 35.232'	87.45	12.55	35.40	52.05
G10	28d 36.786'	96d 36.822'	52.88	47.12	26.57	26.32
G11	28d 35.292'	96d 32.526'	97.38	2.62	24.08	73.31
G12	28d 36.780'	96d 36.810'	52.38	47.62	41.70	10.68
G13	28d 40.788'	96d 34.938'	61.11	38.89	33.49	27.62
G14	28d 37.572'	96d 30.264'	87.72	12.28	64.44	23.28
G15C1	28d 40.524'	96d 36.930'	90.15	9.85	25.20	64.94
G15C2	28d 41.772'	96d 38.064'	74.20	25.80	28.56	45.65
G15C3	28d 42.294'	96d 36.150'	46.72	53.28	17.21	29.51
G15C4	28d 37.950'	96d 36.336'	53.49	46.51	22.02	31.48
G15C5	28d 36.954'	96d 34.860'	92.26	7.74	30.56	61.70
G15C6	28d 35.634'	96d 35.262'	99.30	0.70	22.62	76.68
G15C7	28d 34.476'	96d 32.970'	81.19	18.81	27.22	53.97
G15C8	28d 37.308'	96d 32.376'	97.05	2.95	20.21	76.83
G15C9	28d 35.448'	96d 30.114'	79.61	20.39	24.99	54.61
G15C10	28d 37.566'	96d 27.882'	90.58	9.42	50.17	40.41
G15C11	28d 36.006'	96d 27.354'	83.85	16.15	27.78	56.06
G16	28d 41.923'	96d 36.760'	55.07	44.93	15.13	39.94
G17	28d 41.280'	96d 36.321'	44.38	55.62	14.74	29.64
G18	28d 40.903'	96d 37.683'	99.37	0.63	18.30	81.06
G19	28d 40.458'	96d 35.771'	74.41	25.59	22.57	51.84
G20	28d 39.990'	96d 35.300'	95.49	4.51	24.58	70.92
G21	28d 39.490'	96d 36.915'	97.87	2.13	27.45	70.43
G22	28d 38.922'	96d 34.974'	98.06	1.94	22.60	75.46
G23	28d 37.287'	96d 36.235'	6.35	93.65	1.83	4.52
G24	28d 36.046'	96d 36.349'	78.27	21.73	27.46	50.81
G25	28d 36.875'	96d 34.687'	54.64	45.36	24.87	29.77
G26	28d 35.104'	96d 33.714'	87.33	12.67	29.09	58.25
G27	28d 36.515'	96d 32.985'	42.29	57.71	19.05	23.23
G28	28d 37.695'	96d 33.214'	89.80	10.20	29.20	60.60
G29	28d 37.900'	96d 31.284'	11.53	88.47	5.21	6.32
G30	28d 37.504'	96d 30.325'	8.84	91.16	2.19	6.65
G31	28d 36.342'	96d 31.298'	71.47	28.53	28.31	43.16
G32	28d 36.039'	96d 32.154'	47.37	52.63	15.59	31.78
G33	28d 34.799'	96d 31.041'	94.08	5.92	28.61	65.47

Surficial Sediment Grab Samples Continued

Core Number	Latitude	Longitude	% Mud	% Sand	% Silt	% Clay
G34	28d 33.679'	96d 31.745'	99.36	0.64	13.47	85.89
G35	28d 34.083'	96d 30.262'	35.43	64.57	9.50	25.93
G36	28d 34.823'	96d 29.483'	64.43	35.57	23.92	40.52
G37	28d 36.088'	96d 29.454'	64.43	35.57	23.92	40.52
G38	28d 36.517'	96d 28.370'	37.64	62.36	14.62	23.02
G39	28d 36.806'	96d 26.928'	47.61	52.39	17.63	29.98
G40	28d 35.636'	96d 27.859'	93.27	6.73	25.26	68.01

APPENDIX B

GEOCHEMISTRY DATA

The maximum depths of ^{137}Cs were measured on Canberra 2000 mm^2 planar coaxial detectors for 1-2 days per sample.

Core Number	Max. ^{137}Cs Depth
C1NL1	24 cm
C2NL2	24 cm
C3NL3	30 cm
C4BL1	Not Measured
C5CL1	36 cm
C6WL1	Below Core Depth
C7SL1	26 cm
C8CB1	Below Core Depth
C9SL2	40 cm
C10KLB1	46 cm
C11KLB2	38 cm

Samples were prepared for Alpha counting by Santschi method. The supported activities were determined by the mean activity of ^{210}Pb in the core below where excess activity exists.

Core Number	Depth Interval	Uncorrected ^{210}Pb Activity	Excess ^{210}Pb Corrected Activity	Error
C1NL1	0-1cm	2.69	1.81	0.44
	4-5cm	2.47	1.55	0.47
	9-10cm	1.98	1.07	0.39
	15-16cm	2.38	1.47	0.48
	19-20cm	1.65	0.74	0.35
	25-26cm	1.06	0.14	0.26
C2NL2	0-1cm	2.14	1.25	0.36
	4-5cm	1.82	0.91	0.38
	9-10cm	1.98	1.07	0.42
	15-16cm	1.48	0.57	0.26

Core Number	Depth Interval	Uncorrected ^{210}Pb Activity	Excess ^{210}Pb Corrected Activity	Error
	19-20cm	1.09	0.18	0.20
	25-26cm	1.15	0.23	0.19
	29-30cm	1.06	0.14	0.20
	35-36cm	1.03	0.11	0.22
C3NL3	0-1cm	1.42	0.59	0.26
	4-5cm	1.36	0.52	0.24
	9-10cm	1.27	0.43	0.19
	15-16cm	1.12	0.28	0.23
	19-20cm	1.14	0.30	0.25
	25-26cm	0.99	0.14	0.25
	29-30cm	1.08	0.23	0.25
C4BL1	NONE	NONE	NONE	NONE
C5CB1	0-1cm	2.37	1.59	0.47
	4-5cm	2.84	2.04	0.49
	9-10cm	3.19	2.40	0.56
	15-16cm	2.18	1.37	0.40
	19-20cm	1.38	0.58	0.28
	25-26cm	1.34	0.54	0.22
	29-30cm	1.38	0.58	0.26
	35-36cm	1.21	0.41	0.21
	39-40cm	1.23	0.42	0.30
	45-46cm	1.17	0.37	0.20
C6WL1	0-1cm	2.93	2.16	0.55
	4-5cm	2.91	2.12	0.60
	9-10cm	3.13	2.33	0.68
	15-16cm	2.67	1.87	0.51
	19-20cm	2.49	1.69	0.45
	25-26cm	1.99	1.19	0.49
	29-30cm	1.53	0.72	0.25
	35-36cm	1.80	1.01	0.34
	39-40cm	1.61	0.81	0.25
	45-46cm	1.45	0.65	0.30
	49-50cm	1.30	0.49	0.20
C7SL1	0-1cm	2.71	1.94	0.52
	4-5cm	1.97	1.16	0.32
	9-10cm	1.97	1.17	0.27
	15-16cm	1.62	0.81	0.24

Core Number	Depth Interval	Uncorrected ^{210}Pb Activity	Excess ^{210}Pb Corrected Activity	Error
	19-20cm	1.51	0.70	0.17
	25-26cm	1.26	0.45	0.24
	29-30cm	1.17	0.36	0.23
C8CB1	0-1cm	3.12	2.36	0.56
	4-5cm	3.15	2.36	0.54
	9-10cm	3.21	2.42	0.52
	15-16cm	2.24	1.43	0.34
	19-20cm	2.30	1.49	0.42
	25-26cm	2.19	1.39	0.38
	29-30cm	1.53	0.72	0.33
	35-36cm	1.43	0.63	0.26
	39-40cm	1.37	0.56	0.29
	45-46cm	1.11	0.31	0.22
C9SL2	0-1cm	2.71	1.95	0.56
	4-5cm	2.19	1.39	0.44
	9-10cm	1.90	1.10	0.33
	15-16cm	1.72	0.92	0.19
	19-20cm	1.59	0.79	0.33
	25-26cm	1.52	0.71	0.24
	29-30cm	1.37	0.56	0.26
	35-36cm	1.37	0.57	0.29
C10KLB1	0-1cm	3.00	2.28	0.57
	4-5cm	2.49	1.73	0.36
	9-10cm	1.95	1.19	0.31
	15-16cm	1.55	0.79	0.27
	19-20cm	1.41	0.64	0.23
	25-26cm	1.15	0.38	0.20
	29-30cm	0.95	0.18	0.15
C11KLB2	0-1cm	3.60	2.71	0.69
	4-5cm	3.13	2.20	0.41
	9-10cm	3.16	2.22	0.41
	15-16cm	1.53	0.58	0.20
	19-20cm	1.71	0.76	0.21
	25-26cm	1.18	0.23	0.26
	29-30cm	1.05	0.10	0.21

APPENDIX C

SEDIMENTOLOGICAL / GEOCHEMICALPROFILES

Grainsize (%), ^{210}Pb (dmp/g), and porosity (%) profiles verses depth (cm). Sedimentation rates were calculated by a linear fit regression equation where the excess ^{210}Pb activity had no uniform activity. The maximum 137Cs depth is marked by a broad horizontal line. X-radiograph shows the internal sedimentological structures, as well as the dense distribution. Density was interpreted as; light = sand, dark = mud.

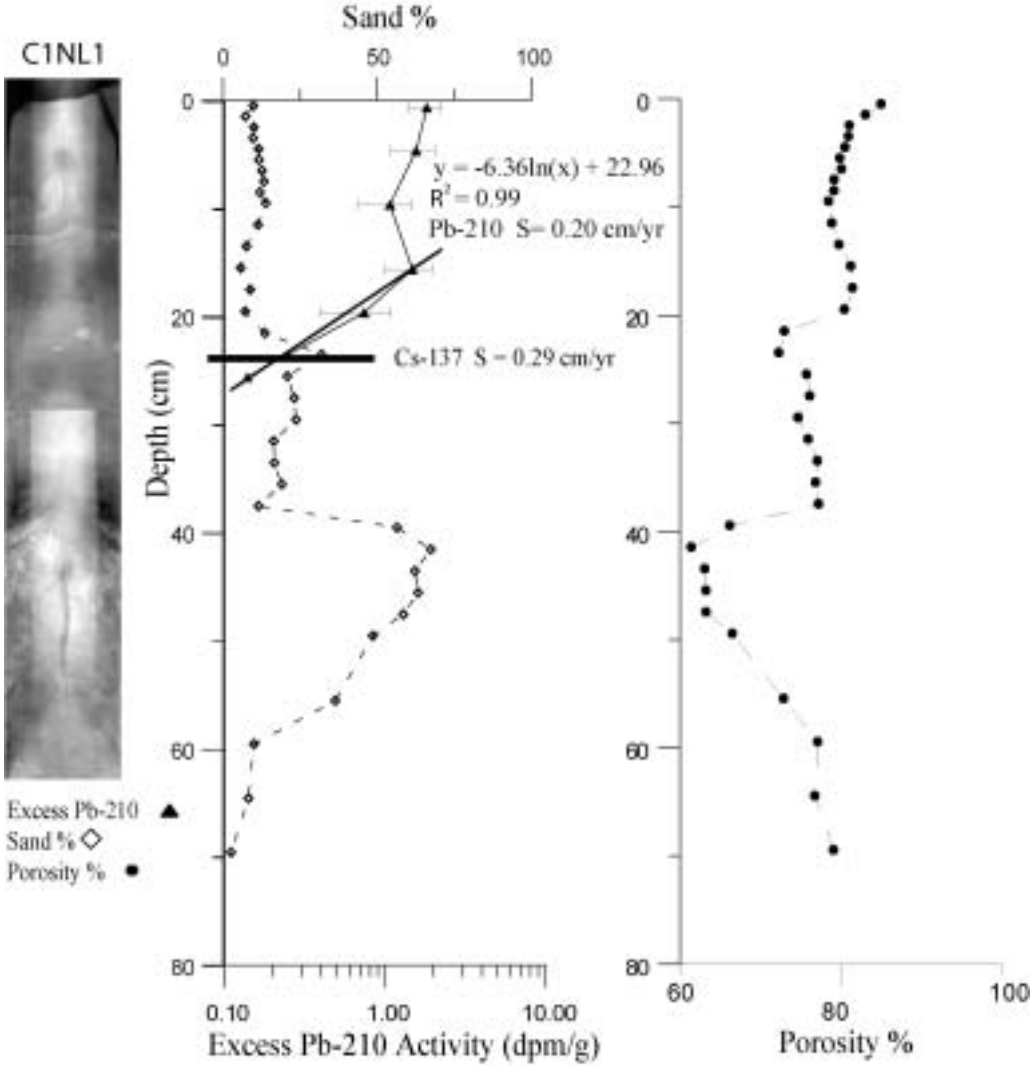

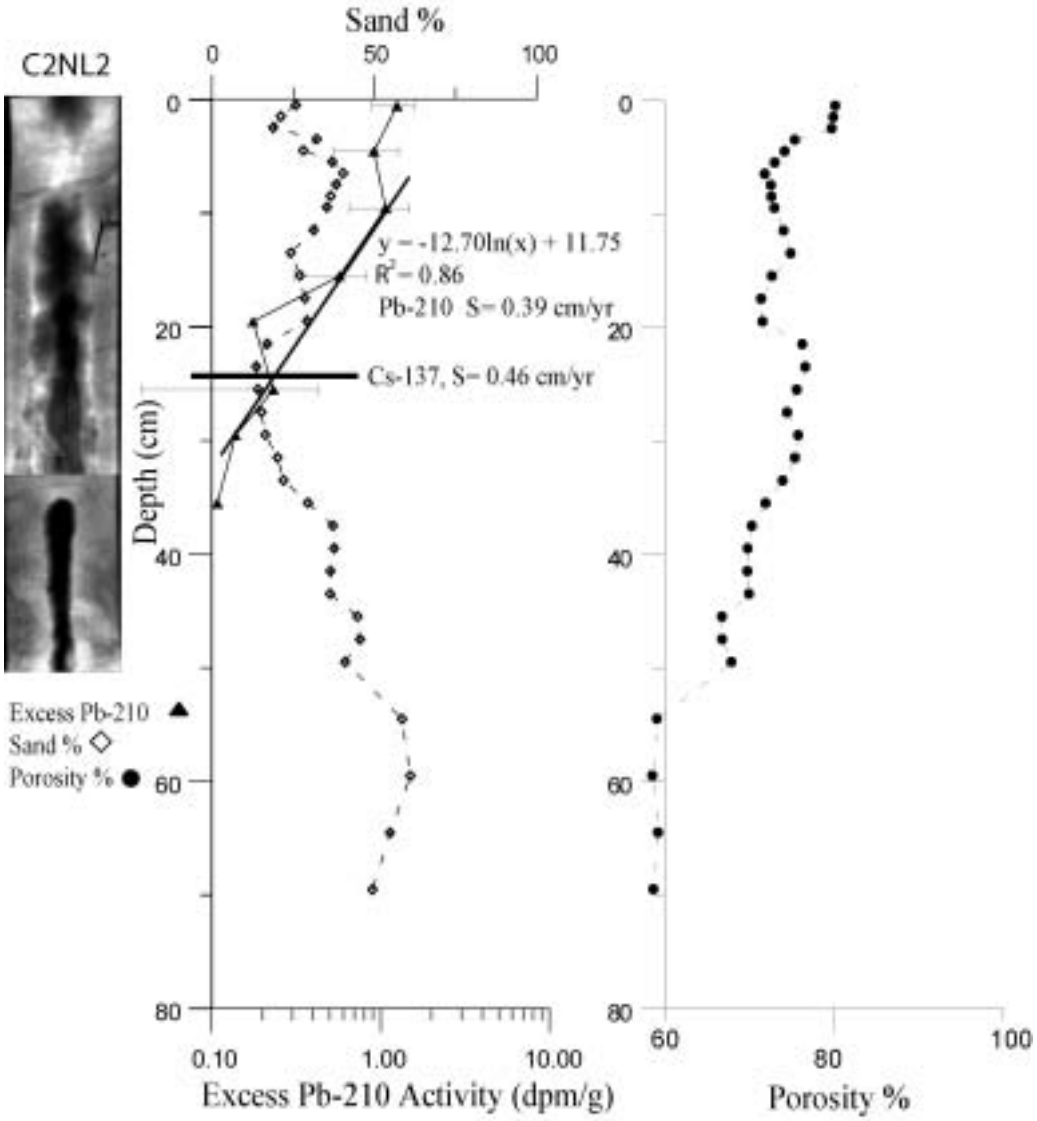
C2NL2
Sand %
0
50
100
0
20
40
60
80
Depth (cm)
y = -12.70ln(x) + 11.75
R² = 0.86
Pb-210 S= 0.39 cm/yr
Cs-137, S= 0.46 cm/yr
Excess Pb-210
Sand %
Porosity %
0.10
1.00
10.00
Excess Pb-210 Activity (dpm/g)
60
80
100
Porosity %

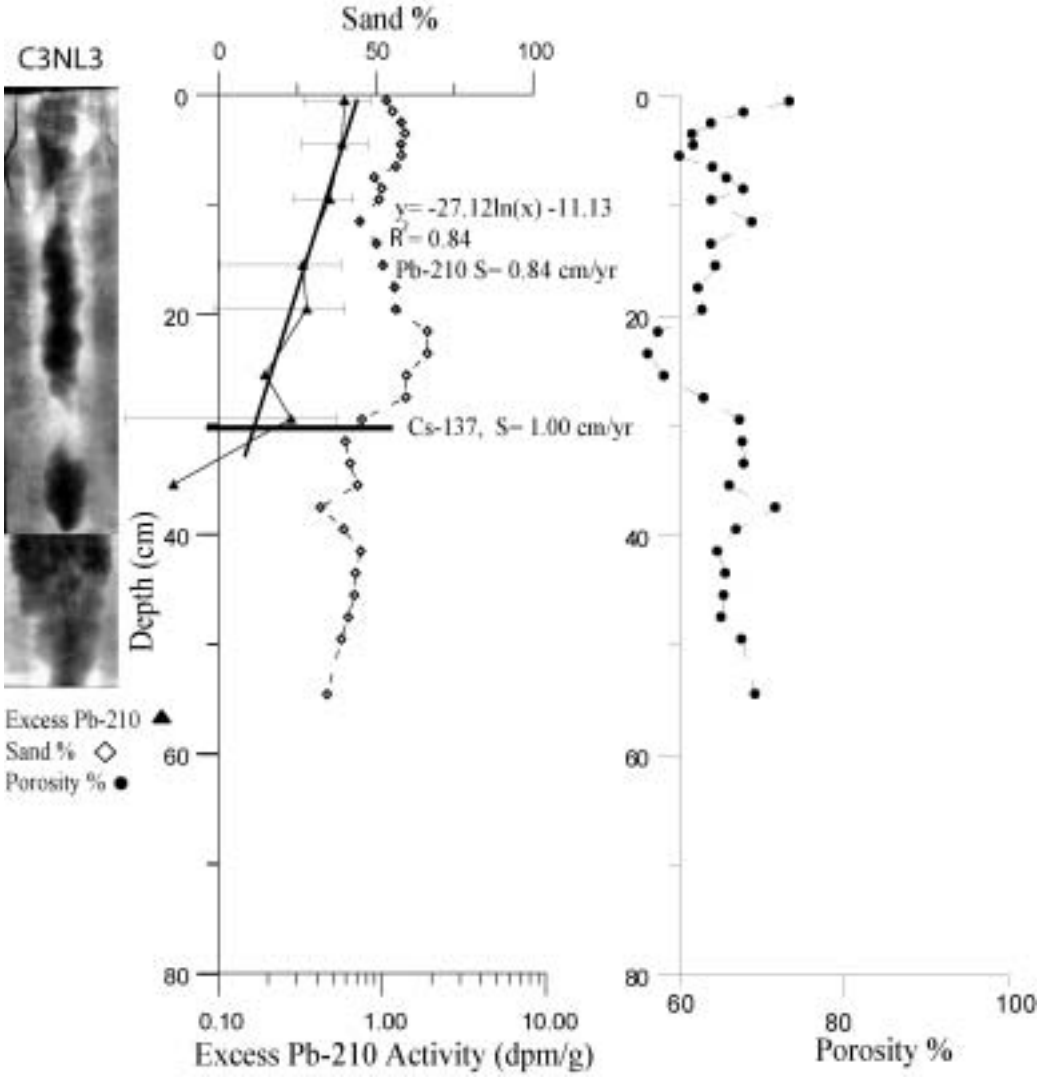
C3NL3
Sand %
0
50
100
y= -27.12ln(x) -11.13
R² = 0.84
Pb-210 S= 0.84 cm/yr
Cs-137, S= 1.00 cm/yr
Depth (cm)
0
20
40
60
80
Excess Pb-210
Sand %
Porosity %
0.10
1.00
10.00
Excess Pb-210 Activity (dpm/g)
60
80
100
Porosity %

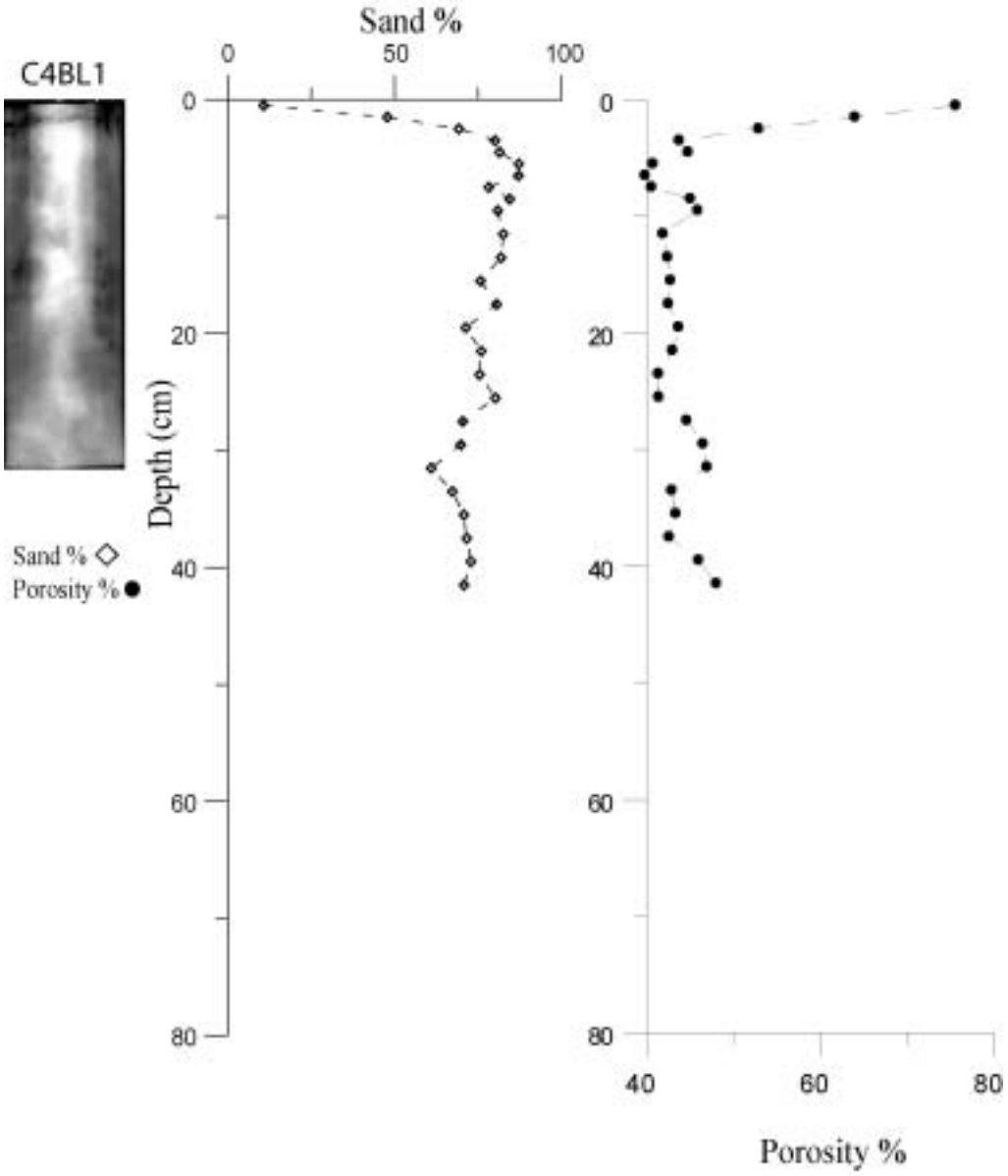
C4BL1
Sand %
0
50
100
0
20
40
60
80
Depth (cm)
Sand % ◇
Porosity % ●
0
20
40
60
80
40
60
80
Porosity %

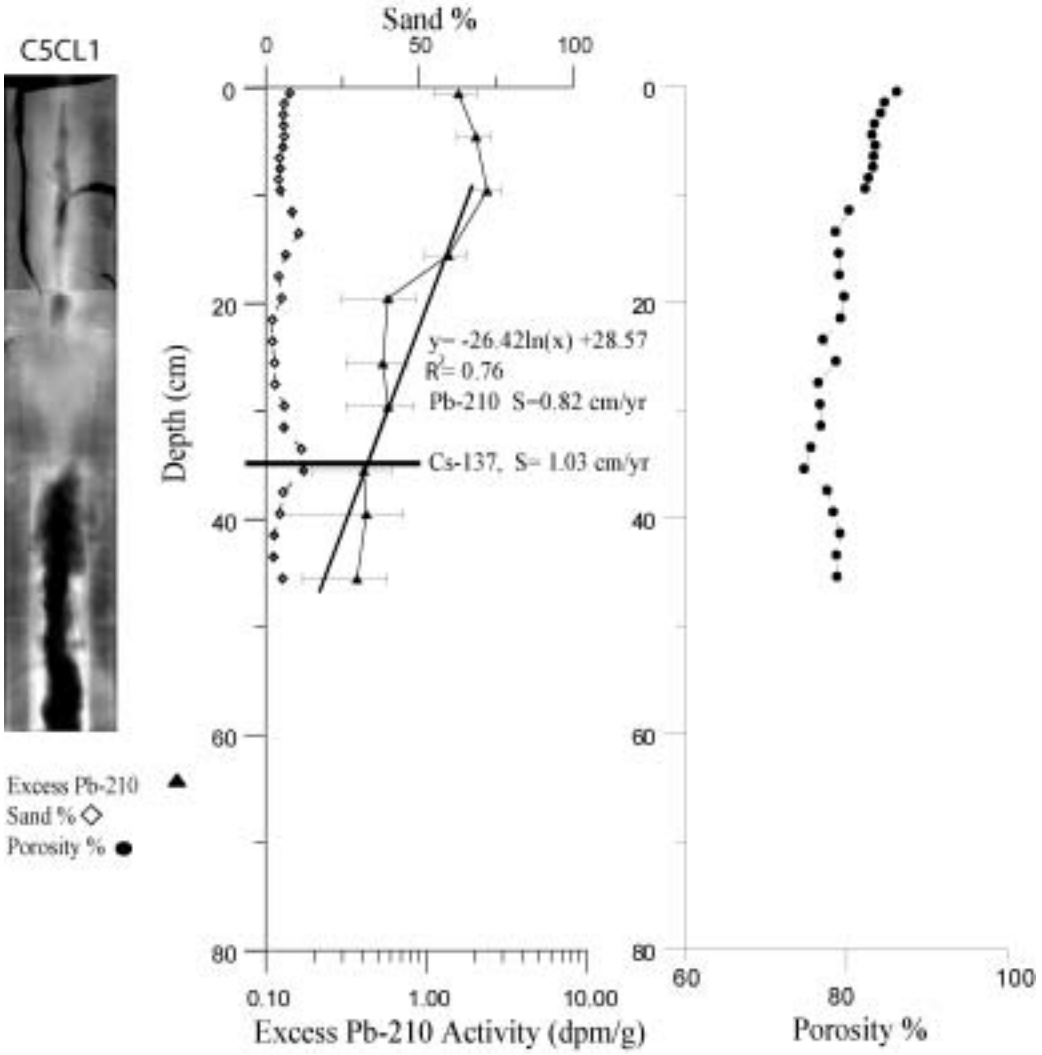
C5CL1
Sand %
0
50
100
0
20
40
60
80
Depth (cm)
y= -26.42ln(x) +28.57
R²= 0.76
Pb-210 S=0.82 cm/yr
Cs-137, S= 1.03 cm/yr
Excess Pb-210 ▲
Sand % ◇
Porosity % ●
0.10
1.00
10.00
Excess Pb-210 Activity (dpm/g)
60
80
100
Porosity %

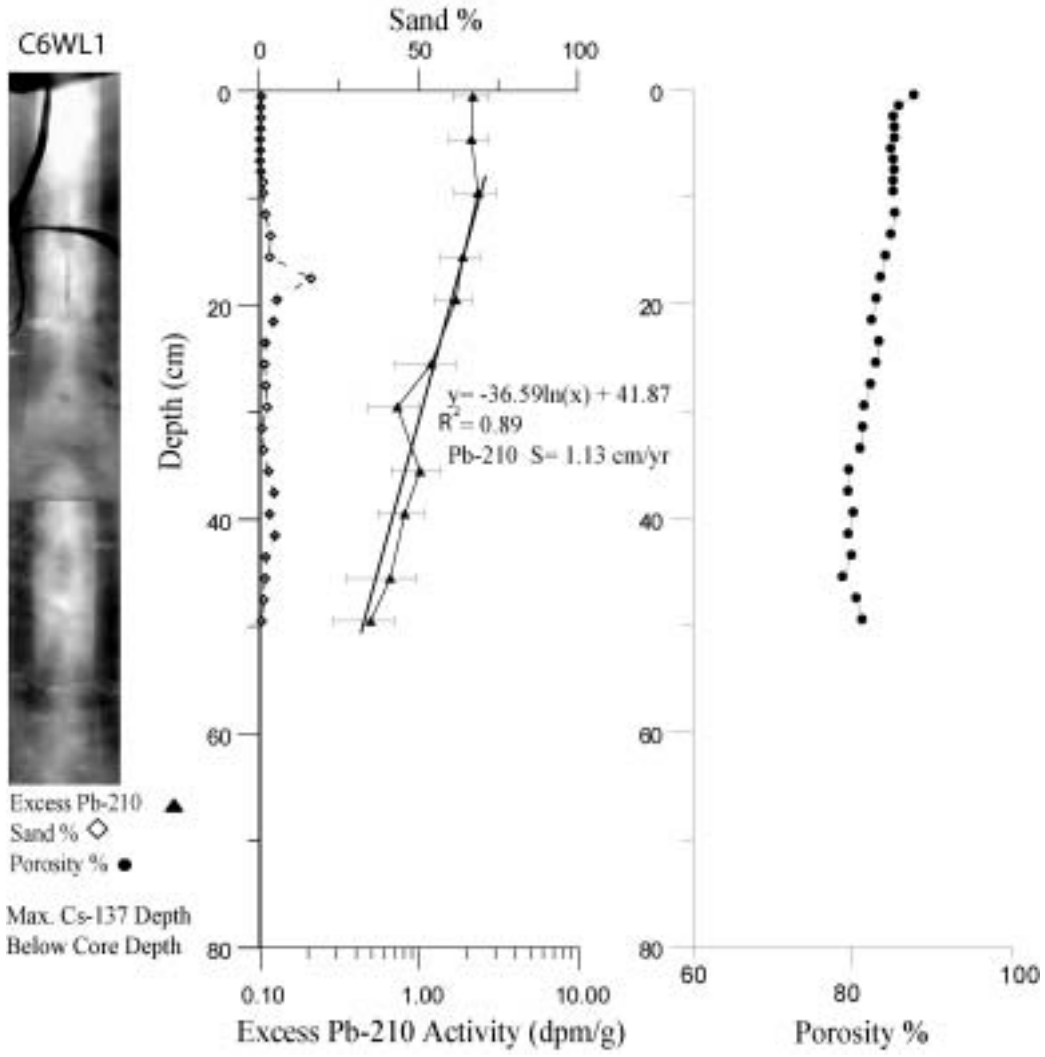
C6WL1
Sand %
0
50
100
0
20
40
60
80
Depth (cm)
y= -36.59ln(x) + 41.87
R2 = 0.89
Pb-210 S= 1.13 cm/yr
Excess Pb-210
Sand %
Porosity %
Max. Cs-137 Depth
Below Core Depth
0.10
1.00
10.00
Excess Pb-210 Activity (dpm/g)
60
80
100
Porosity %

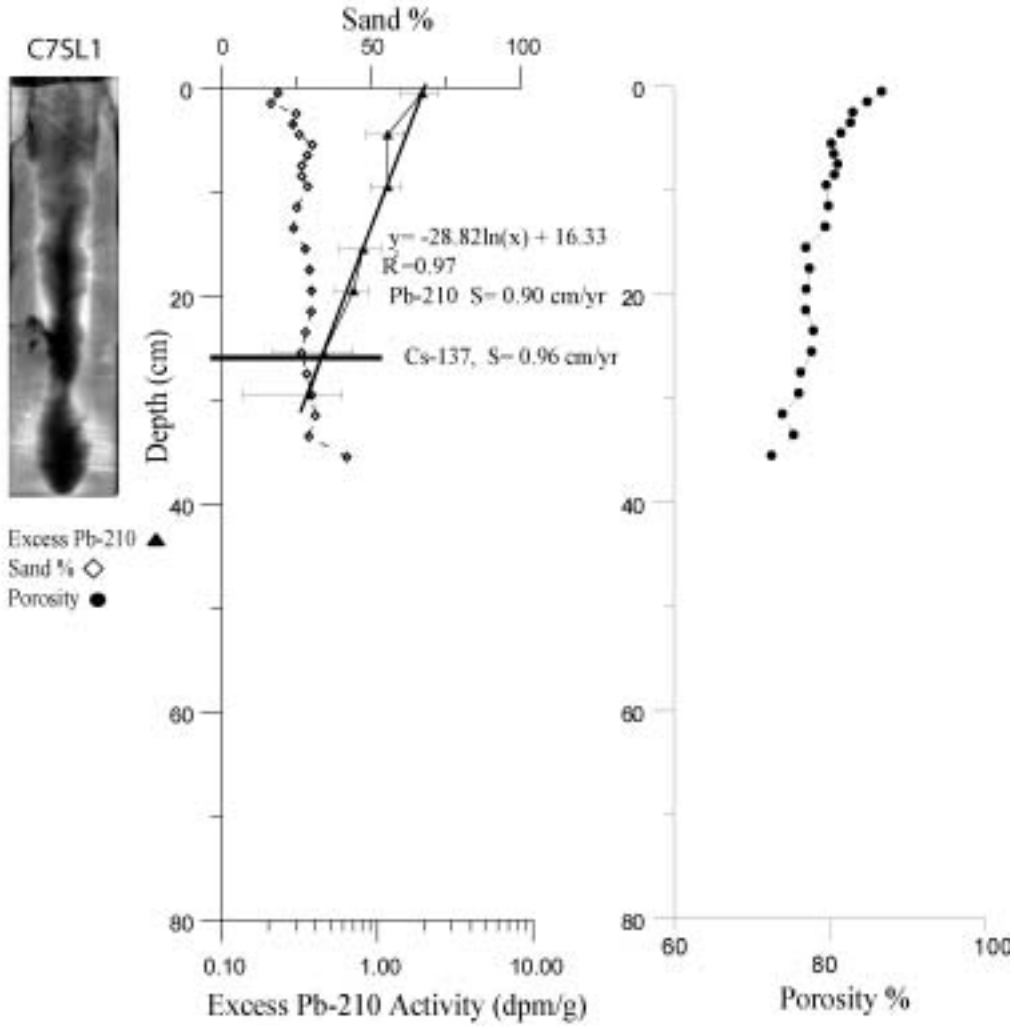
C7SL1
Sand %
0
50
100
0
20
40
60
80
Depth (cm)
y= -28.82ln(x) + 16.33
R²=0.97
Pb-210 S= 0.90 cm/yr
Cs-137, S= 0.96 cm/yr
Excess Pb-210 ▲
Sand % ◇
Porosity ●
0.10
1.00
10.00
Excess Pb-210 Activity (dpm/g)
60
80
100
Porosity %

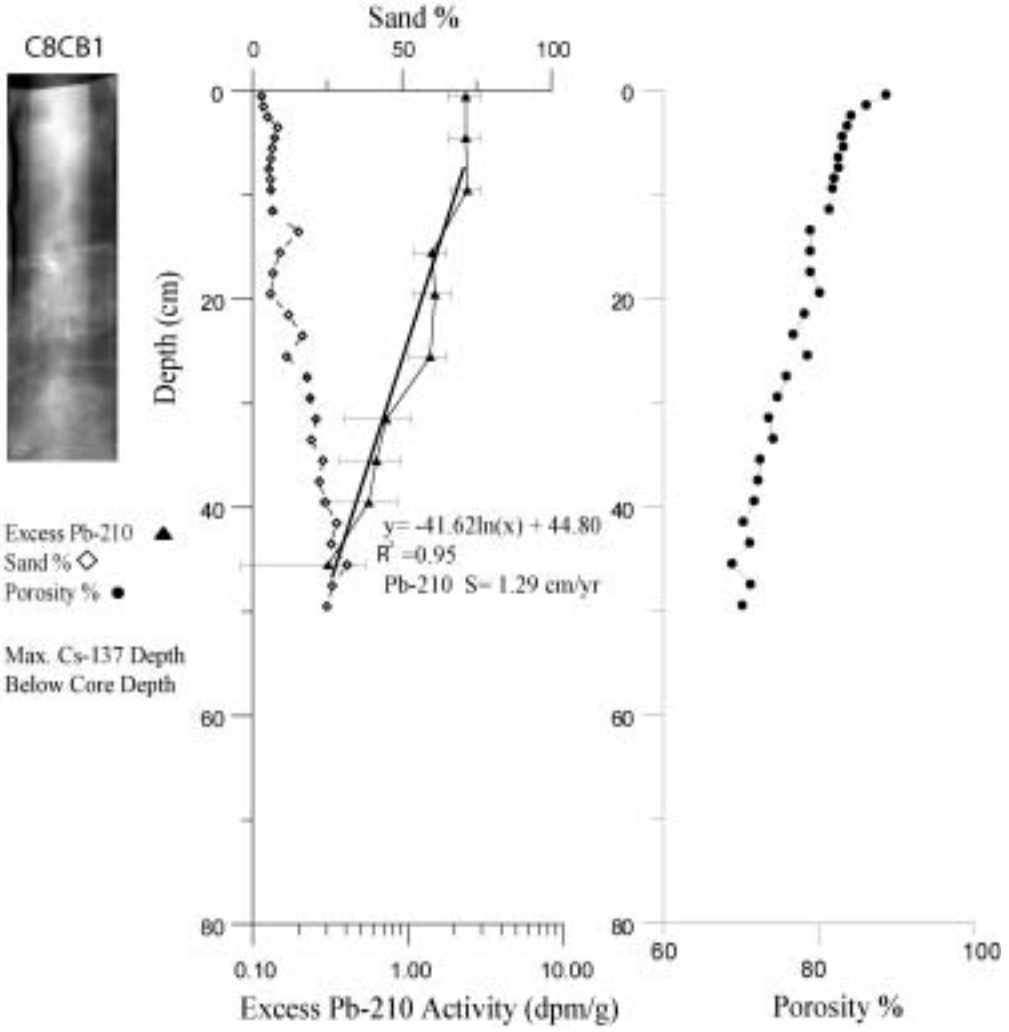
C8CB1
Sand %
0
50
100
Depth (cm)
0
20
40
60
80
Excess Pb-210
Sand %
Porosity %
Max. Cs-137 Depth
Below Core Depth
y= -41.62ln(x) + 44.80
R² =0.95
Pb-210 S= 1.29 cm/yr
0.10
1.00
10.00
Excess Pb-210 Activity (dpm/g)
60
80
100
Porosity %

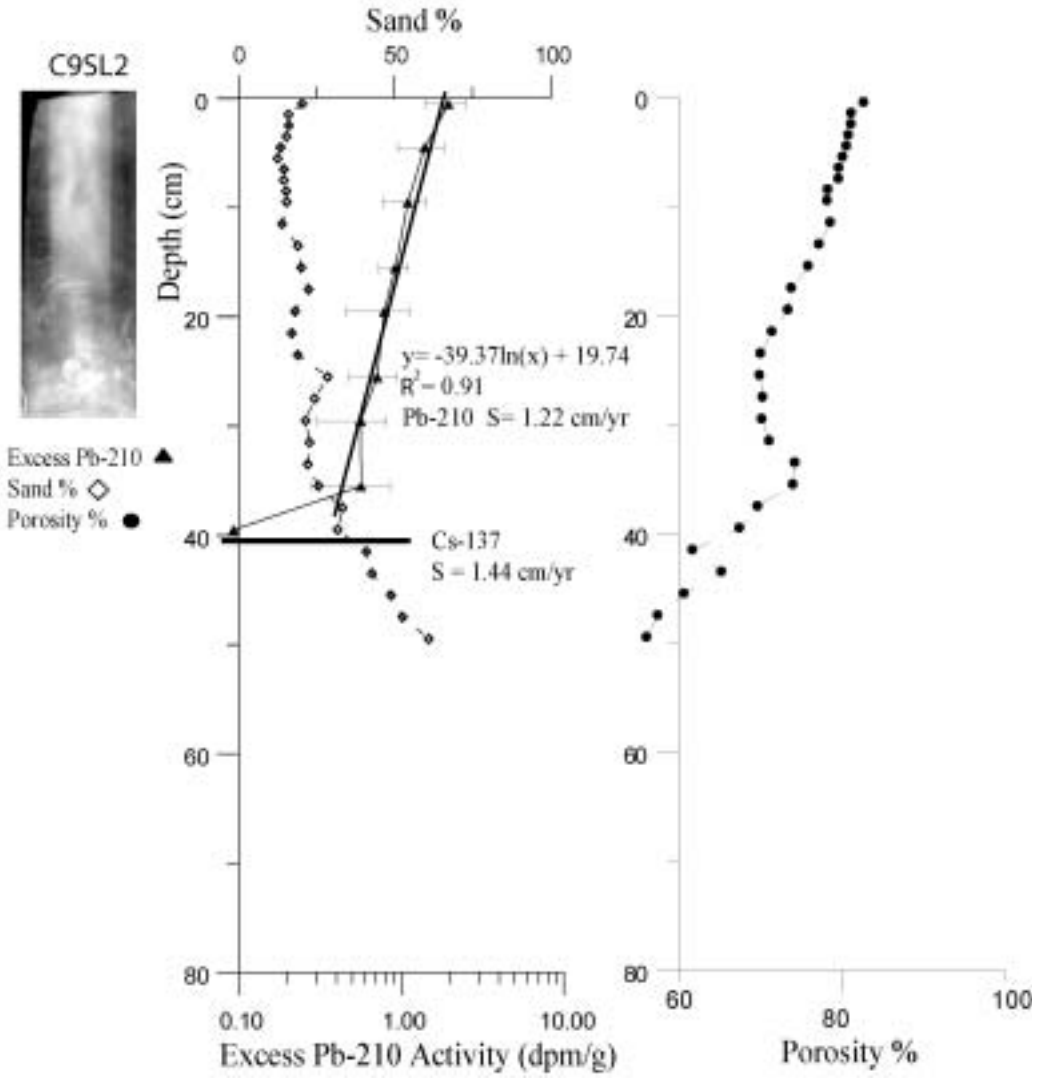
C9SL2
Sand %
0
50
100
Depth (cm)
0
20
40
60
80
y= -39.37ln(x) + 19.74
R² = 0.91
Pb-210 S= 1.22 cm/yr
Cs-137
S = 1.44 cm/yr
Excess Pb-210
Sand %
Porosity %
0.10
1.00
10.00
Excess Pb-210 Activity (dpm/g)
60
80
100
Porosity %

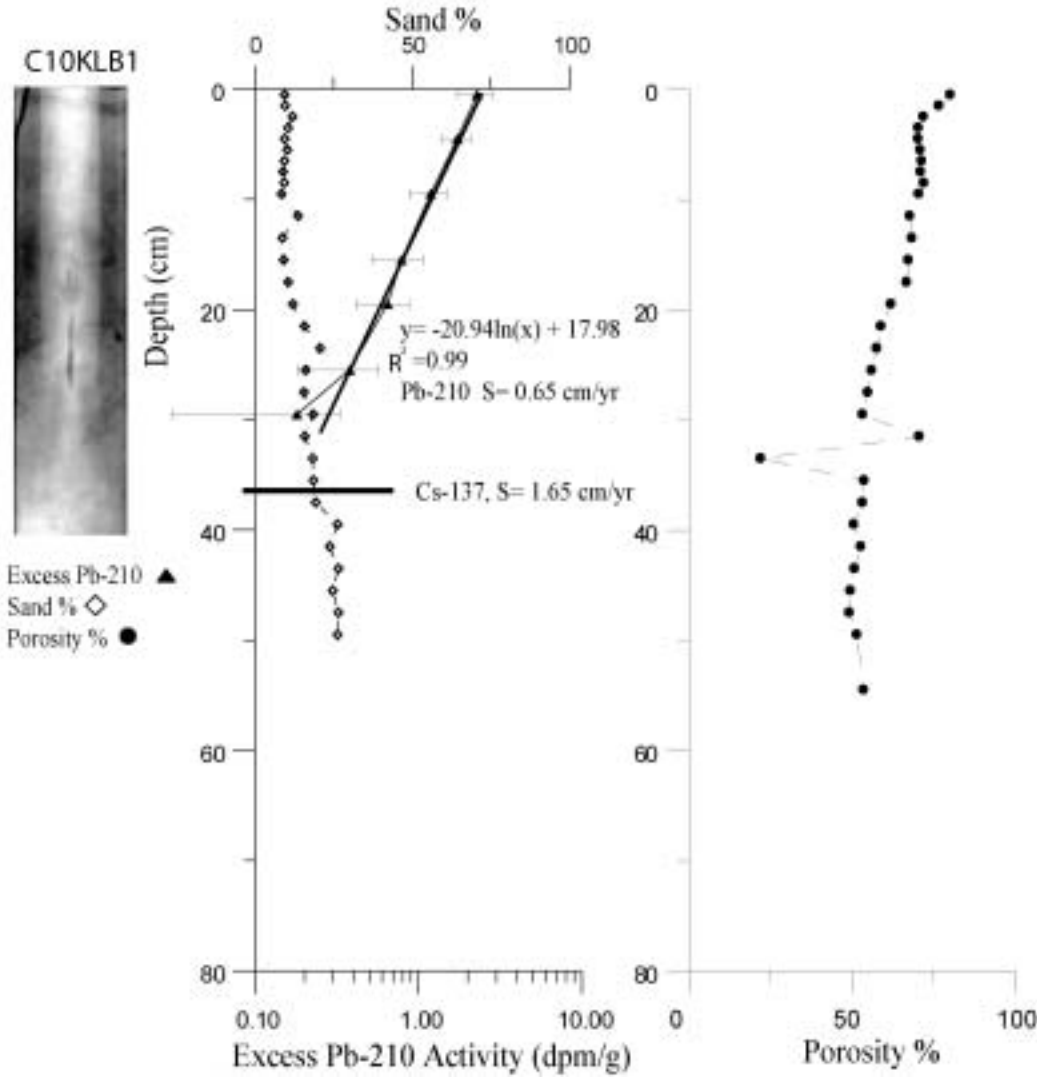
C10KLB1
Sand %
0
50
100
Depth (cm)
0
20
40
60
80
y= -20.94ln(x) + 17.98
R² =0.99
Pb-210 S= 0.65 cm/yr
Cs-137, S= 1.65 cm/yr
Excess Pb-210 ▲
Sand % ◇
Porosity % ●
0.10
1.00
10.00
Excess Pb-210 Activity (dpm/g)
0
50
100
Porosity %

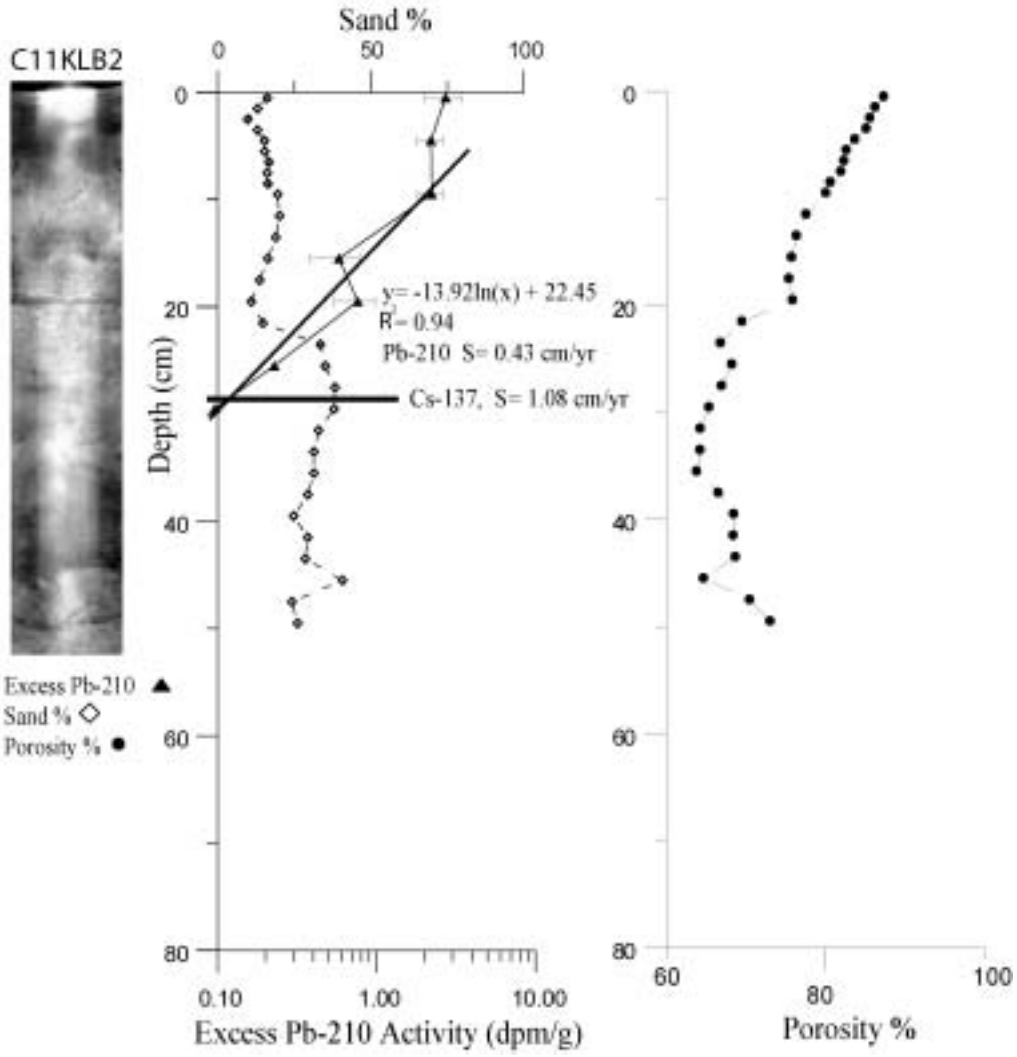
C11KLB2
Sand %
0
50
100
0
20
40
60
80
Depth (cm)
y= -13.92ln(x) + 22.45
R²= 0.94
Pb-210 S= 0.43 cm/yr
Cs-137, S= 1.08 cm/yr
Excess Pb-210 ▲
Sand % ◇
Porosity % ●
0.10
1.00
10.00
Excess Pb-210 Activity (dpm/g)
60
80
100
Porosity %

VITA

The author, Jason Lee Bronikowski, began his studies at Posen Consolidated High School of Michigan and graduated in 1997. In the fall of 1997 he attended Alpena Community College for 2 semesters, and finished up his Bachelor of Science in Geology and a minor in Mathematics at Lake Superior State University of Michigan in the spring of 2001. With the completion of this thesis the author will receive a Master of Science from Texas A&M University in the field of Oceanography. The author can be contacted at 211 Liberty Avenue, Apt. No. 132, Lafayette, Louisiana 70508.